SIMULATION OF SURFACE GENERATED IN FINE GRINDING—A PROBABILISTIC APPROACH

by

PRASANTA KUMAR BASURAY

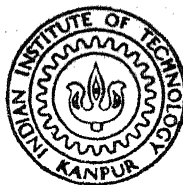DEPARTMENT OF MECHANICAL ENGINEERING

INDIAN INSTITUTE OF TECHNOLOGY KANPUR

AUGUST 1977

SIMULATION OF SURFACE GENERATED IN FINE GRINDING—A PROBABILISTIC APPROACH

A Thesis Submitted
In Partial Fulfilment of the Requirements
for the Degree of
DOCTOR OF PHILOSOPHY

by

PRASANTA KUMAR BASURAY

to the

DEPARTMENT OF MECHANICAL ENGINEERING

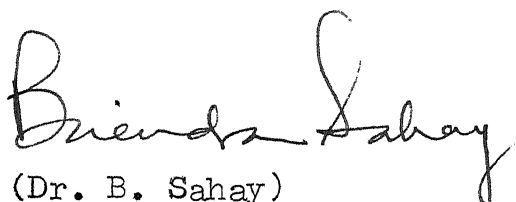INDIAN INSTITUTE OF TECHNOLOGY KANPUR

AUGUST 1977

ME - 1977 - D - BAS - SIM
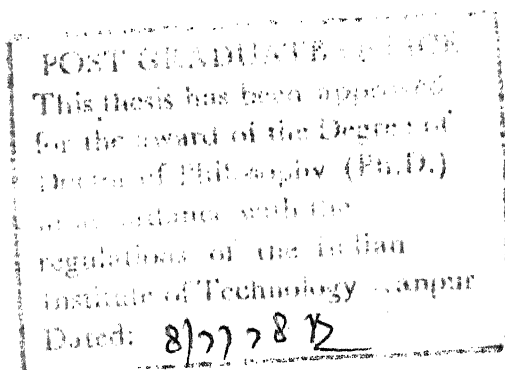
DEDICATED TO MY

RESPECTED PARENTS

CERTIFICATE

Certified that the work entitled "SIMULATION OF SURFACE GENERATED IN FINE GRINDING - A PROBABILISTIC APPROACH" by Mr. Prasanta Kumar Basuray has been carried out under our supervision and has not been submitted elsewhere for a degree.

(Dr. B. Sahay)
Assistant Professor
Dept. of Mechanical Engg.
Indian Institute of Technology
Kanpur

(Dr. G.K. Lal)
Assistant Professor
Dept. of Mechanical Engg.
Indian Institute of Technology
Kanpur

ACKNOWLEDGEMENT

TABLE OF CONTENTS

LIST OF FIGURES

NOMENCLATURE

A	Constant
A1	Radius of locus of ith grain tip in workpiece
A2	Radius of locus of jth grain tip in workpiece
a	A given number $\ll 1$
a_1, b_1, b_2	Unbiased estimator
$\begin{bmatrix} a_{ij} \end{bmatrix}$	Coefficient matrix of normal equations
B	Bartlett's test statistic
BB	Section along transverse direction
B (i,j)	Intersection point of paths traced by ith and jth grain in any column
b	Average width of chip
C	Nominal grain density
C_1, C_3	Average number of active grin density responsible for surface generation
c_1	Number of level of factor d
c_2	Variable
$\begin{bmatrix} c_{ij} \end{bmatrix}$	Inverse of coefficient matrix $\begin{bmatrix} a_{ij} \end{bmatrix}^{-1}$
D	Wheel diameter
D_e	Equivalent wheel diameter
D_w	Workpiece diameter
d	Wheel depth of cut
d_e	Effective profile depth
d_o	Elastic grain deflection for outermost grain

$\overline{d}$ Mean value of depth of cut, d_i for $i = 1, \ldots,$ N_2 observations

e Mean square error

$E[\ ]$ Expected value of variable $[\ ]$

F'_P Tangential force per unit grinding width

F-ratio $\dfrac{\text{Mean square for any source of variation}}{\text{Mean square for within}}$

$\cdot\ \cdot\cdot$ Random variable

$F_{\cdot\cdot}(..)$ Distribution function of random variable $(..)$

$f_{\cdot\cdot}(..)$ Probability density function of random variable $(..)$

$f_{i'}$ Degrees of freedom for i'th repeated trial, $i' = 1, \ldots, N_1$

fc Cut-off frequency (0.5 c/$\triangle$)

fq Frequency in cycles per interval (c/$\triangle$)

$\cdot$ Source of variation (e,g,d,v, etc.)

$f_{\cdot}$ Degrees of freedom associated with source of variation $(\cdot)$

f Total number of degrees of freedom for N_1 repeated trials

$G_z(fq)$ Power spectral density function

$\widetilde{G}_z(fq)$ Raw estimate of power spectral density at any frequency, fq

$\widetilde{G}_{k_1} =$
$\widetilde{G}\left(\dfrac{k_1\ fc}{m_1}\right)$ Raw estimate of power spectral density at harmonic k_1 corresponding to frequency, $\dfrac{k_1\ fc}{m_1}$

$\widehat{G}(k_l)$ Smoothed power spectral density after hamming (and after being compensated for prewhitening, if applied)

$\widehat{G}(fq, \xi)$ Smoothed spectral density of the actual work-piece profile at frequency, fq, for grinding condition, ξ .

$\widehat{G}(fq, \xi, k)$ Smoothed spectral density of the theoretical profile at frequency, fq, with radial distribution parameter, k, for grinding condition ξ

g Nominal grain diameter

$g_z(z)$ Probability density function of radial position of grain types.

h_l Radial depth for coarsest grain spacings

h_u Radial depth for finest grain spacings

h Idealised mean peak to valley height

$\bar{h}$ Centre line average (CLA) value of surface roughness

k Radial distribution parameter

k_{iju} Value of k obtained in uth observation in any trial having treatment combination of ith level of factor, d and jth level of factor, v, for $u = 1, \ldots, n_1; \ i = 1, \ldots, c_1; \ j = 1, \ldots, r_1$

$\bar{k}_{ij}$ Mean value of k obtained in repeated i'th trial for $i' = 1, \ldots, N_1$

k_i Estimated values of k for depth of cut, d_i, and table speed, v_i, for ith observation,

$\hat{k}_i$ Estimated regression of k_i on d_i and v_i

$\hat{\bar{k}}$ Mean of $\hat{k}_i$, $i = 1, \ldots, N_2$

$\bar{k}$ Mean of estimated values of k_i, $i = 1, \ldots, N_2$

L   Maximum width of groove cut by any grain; observation length

l_c Chip length

l_o, $l_{o''}$ Arbitrary initial value

l_r Minimum record length . (simulated width)

M   Total number of grains in column

M'   Total number of grain lying below radial depth h_u

M"   Total number of grains lying below d_e for an average width of cut, b

m   mth sample point

m_1 Maximum number of correlation lag

N_c Total number of columns

N_S Sample size

N_1 Number of repeated trials

N_2 Total number of observations

N_3 (i)   Number of grains responsible for longitudinal surface generation along a section passing through ith column position, $i = 1, \ldots, N_c$

N_4 $(y_{n'})$ Number of grains responsible for transverse surface generation in any section at a distance $y_{n'}$, $n' = 1, \ldots, N_5$ (number of sections)

$\bar{N}_3$ Mean number of grains responsible for longitudi-

$\overline{N}_4$ Mean number of columns which will mutually interfere to produce transverse surface

p Axial pitch

$\overline{p}$ Average value of pitch

p_{o1} Transition probability matrix of going from state 0 to 1

$p(x_o, y_o)$ Coordinate of any point p in (x, y) plane

Q Square identity

q Speed ratio ($\frac{V}{v}$)

R Radius of grinding wheel

R^i Radial position of ith grain tip on wheel surface from grinding wheel centre

R_u, $R_{u_{i-1}}$, R_{u_i}, R_{u_j} Uniformly distributed random numbers lying between 0 and 1

$R_z(0)$ Autocorrelation at zero displacement

$R_z(\tau)$ Autocorrelation function of any sample record $z(1)$ at displacement τ

r $\dfrac{\text{Mean scratch width}}{\text{Mean scratch depth}}$

$R_r = R_z(r \triangle 1)$ Estimate of autocorrelation function at lag r, r = 0, 1, ..., m_1

S_g Grain size

$SS.$ Sum of square for source of variation

S Within

$S_{k/d,v}^2$ Unbiased estimates of variance of k in any cutting condition

s_{rep}^2 (k) Variance of reproducibility of parameter, k

$s_{i'}^2$ (k) Variance of k in i'th repeated trial,

$$i' = 1, \ldots, N_1$$

s_f Feed per grain

Tr Treatment combination

$$T_{ij.} = \sum_{u=1}^{n_1} k_{iju}$$

$$T_{i..} = \sum_{j=1}^{r_1} \sum_{u=1}^{n_1} k_{iju}$$

$$T_{.j.} = \sum_{i=1}^{c_1} \sum_{u=1}^{r_1} k_{iju}$$

$$T \quad \text{Grand Total} = \sum_{i=1}^{c_1} \sum_{j=1}^{r_1} \sum_{u=1}^{n_1} k_{iju}$$

T' Time

t Maximum value of undeformed chip thickness

t_i Undeformed chip thickness for any ith grain

$t_{\alpha_c/2}$ (ν) Percentage point of t distribution with ν degrees of freedom for $\alpha_c/2$ % significance level

U Specific energy

u (p) Uniform random variable

u (l) Arbitrary sample record of length l transformed to zero mean value

$(l_{n'})$ Height of sample record u(l) at sample point $l_{n'}$

$\overline{U^2}$ Sample mean square

V Wheel speed

v Table speed

$v1, v2$ Volume of chip

$\overline{v}$ Mean value of table speed v_i for $i = 1, \ldots, N_2$
            observations

w $x_{j+1} - x_j$

(x, y, z) Right handed coordinate system fixed at the
            leading edge of the workpiece

y_j^{ti} Distance of ith grain tip position measured
            along periphery from $(i - 1)$ grain position

z_j^{ti}, z_j^{ti} Distance of ith grain tip position measured
            radially inward from the outermost circle pass-
            ing through the lowermost grain tip.

$z^{t} =$ $z'' + d_e$ (z'' lies between 0 to d_e)

$z_k (y_o)$ Longitudinal profile height in kth column at a
            distance y_o from reference coordinate systems

$z_k^i (y_o)$ Transformed position of ith grain tip at a dis-
            tance y_o in (y, z) plane passing through kth
            column position

$z (x_o)$ Surface profile height at a distance x_o in
            (x, z) plane

$x_{i,r}, z_{i,r}$ Coordinates of intersection point of ith and
            rth grooves

$y (i, j),$ Coordinates of intersection point B (i, j)

$z(1)$ Arbitrary sample record of length 1

$z(1, fq, \triangle fq)$ Portion of $z(1)$ in the frequency range

from fq to $fq + \triangle fq$

α Simulated width

α_c Confidence level

$\alpha_1, \beta_1, \beta_2$ Variable coefficients of k

$\triangle x$ Amount of increment in axial direction

$\triangle y$ Interval of lowest position of grain tips along

the cutting direction

$\triangle y'$ Interval of successive appearance of grain for a

fixed point on workpiece in any column

$\triangle z'$ Interval of radial positions of successive

grains in any column

$\triangle 1, \triangle 1''$ Sampling intervals

$\triangle fq$ Frequency interval

$\epsilon(fq)$ Uncorrelated error

η_i True regression of k_i on d_i and v_i

$\emptyset(.)$ Response function of parameter $(.)$

λ Average linear grain spacing in peripheral **direction** (for a nominal grain density C)

λ_1 Average linear grain spacing after being

transformed to workpiece

λ_2 Average value of linear grain spacing for

active grain density C_3

μ Micron (10^{-4} cm)

μ_z Mean value of the sample record, $z(1)$

ρ Grain tip radius

ζ Cutting condition (kinematic and operating parameters)

σ^2 Variance

$\sigma^2_{b_i}$ Variance of coefficients b_i

τ Displacement lag

ψ^2 Mean square value of the sample record

$\psi^2_z \left[\overline{fq}, fq + \triangle \overline{fq} \right]$ Mean square value of the power spectral density from fq to fq + $\triangle$fq

SIMULATION OF SURFACE GENERATED IN

FINE GRINDING - A PROBABILISTIC APPROACH

A Thesis Submitted
In Partial Fulfilment of the Requirements
for the Degree of
DOCTOR OF PHILOSOPHY

by

PRASANTA KUMAR BASURAY

to the

DEPARTMENT OF MECHANICAL ENGINEERING
INDIAN INSTITUTE OF TECHNOLOGY, KANPUR

AUGUST, 1977

SYNOPSIS

The thesis entitled "SIMULATION OF SURFACE
GENERATED IN FINE GRINDING - A PROBABILISTIC APPROACH"
deals with the generation of theoretical surface profile
simulating the actual workpiece surface profile obtained
under single pass plunge-cut grinding conditions through
estimation of probabilistic parameters to describe the
cutting surface. A theoretical model is proposed to
describe the probability density functions of the random
positions of grains on the wheel surface based on the
interference of grooves produced by different grains,
effective profile depth, and the elastic grain deflection.
The workpiece surface being the sample realisation of
random grinding process, power spectral density of the

simulated and experimental profiles are compared which
provides information about the real system in terms of
radial distribution parameter and effective profile depth
for various cutting conditions. The surface roughness
and active grain density are also calculated as outputs
of the grinding system.

Chapter I introduces the earlier developments
of both the deterministic and probabilistic analyses of
the grinding process and outlines the need for the pre-
sent investigation.

The model based on the probability density func-
tion of the random position of grains on the wheel sur-
face, and the generation of the theoretical profiles in
the longitudinal as well as in the transverse direction,
for various grinding conditions, based on the interference
of cuts made by random grain tips is described in
Chapter II.

Chapter III provides the statistical analysis
to obtain the functional dependence of radial distribu-
tion parameter and effective profile depth on the table
speed and wheel depth of cut, by comparing the power
spectra of the simulated and experimental profiles using
a systematic variation of the table speed and depth of
cut through a 2 x 2 factorial experiment.

Numerical techniques to evaluate the power
spectral density and generation of surface profile with
all random possibilities of interaction of grooves is
discussed in Chapter IV. Digitization and handling of
random data using standard methods are also described
in this chapter.

Chapter V presents an approximate analysis to
obtain the surface roughness and variation of active
grain density with undeformed chip-thickness.

Experimental details and results are summarised
in Chapter VI. It is shown that the effective profile
depth is independent of depth of cut and table speed, and
that the radial distribution parameter is linearly rela-
ted to table speed and depth of cut. Results indicate
that the power spectra of the simulated profiles obtained
using the proposed model are in close agreement with the
experimental profiles, and shows the dependence of sur-
face roughness on the cutting conditions.

CHAPTER I

INTRODUCTION

1.1 Introduction

In recent years, grinding has received more
attention because of the ever increasing higher trend
towards precision in the processing of varied and stronger
materials which are difficult to machine. Increased inte-
rest in the mechanics of grinding as a metal cutting
process has contributed significantly in understanding its
fundamental parameters. Though, the grinding process, in
many ways, is similar to milling, it is unique since the
material removal is carried out by small closely spaced
and randomly placed grains of hard abrasive materials.

The art of using abrasives is very old and is
being successfully practiced since the pre-historic times.
Archaeological evidences confirm that early man in the
paleolithic age, from 25,000 B.C. to 15,000 B.C., was well
versed in the use of abrasives in fashioning and sharpen-
ing of bones and horns [1]. Many synthetic grains such
as Aluminium Oxide (produced by fusing Bauxite in a
special electric furnace [2]), White Aluminium Oxide (a
more refined form of Aluminium Oxide), or Silicon Carbide
have replaced the use of natural abrasives such as emery,

and corrundum. Aluminium Oxide is recommended for grinding metals of high tensile strength due to its toughness. White Aluminium Oxide has the characteristics of high friability and first rate cool-cutting properties [3, 4]. Silicon Carbide, the first synthetic abrasive discovered by Archeson around 1895 [5], was at one time the hardest manufactured abrasive but it is very brittle [6, 7, 8]. More research is continuing into the development of new types of abrasives.

Abrasive grains are held together by bonding materials. Majority of the wheels are made with vitrified bonds. Resenoid bonded wheels are extensively used on special swing frame, floor stand, and high speed portable grinders for the grinding of steel, malleable and iron castings where quick removal of metal is the primary consideration.

Grinding wheels are made in a variety of grain size, grade and structure. The important properties of an abrasive grain (or grit) are hardness [9], body strength, or toughness (inversely proportional to friability), and attrition resistance [10, 11]. Hardness values are expressed by Wooddell scale [12] which are directly comparable with cohesive energy density [13]. Grade is the degree of hardness of the wheel. It varies according to the tenacity with which the bond holds the abrasive grits

together and does not represent the hardness of the abrasive material itself. The grain size is designated in terms of openings per linear length in the screen to size the grain. The sizes usually range from 10 to 120; 10 being very coarse and 120 being very fine. The structure of the grinding wheel denotes the spacing of grain and controls the density of the wheel. The grinding wheel is not a dense mass of abrasives and bond. It has intergranular space distributed throughout its structure which helps to clear the wheel face of metal and remove the chips cut by abrasive grains.

The grinding process differs fundamentally from other cutting methods in the following [14 - 16]:

(i)   the space distribution of the cutting edges on the cutting surface of a grinding wheel is of random nature;

(ii)   the shapes, sizes, and orientation of cutting edges vary over a wide range;

(iii)   the radius of curvature of cutting edge of a grain determines chip thickness;

(iv)   grains, held elastically by bond bridges are displaced in tangential and normal directions during grinding;

(v) the types of wear of the cutting edges are quite different from those of other cutting tools,

(vi) the chip thickness is very small with wide variations in shape and size;

(vii) the temperature of cutting edges are extremely high.

Because of the large number of parameters involved, an enormous number of trials will be required to determine experimentally the relative importance of each parameter influencing the grinding process. Efforts have been made to obtain a relevant basic parameter to combine several effects produced by a large number of parameters. The various proposals related to basic grinding parameters are split into two groups; one based on geometric relations (speed, depth of cut, cutting edge spacings, etc), and the other based on concepts such as specific energy, specific contact pressure etc. [17 - 23] . It is generally agreed that the basic parameter should be decided in such a manner that it refers explicitly to those values which can be evaluated with reasonable accuracy. The parameter undeformed chip thickness, t, is generally accepted as the basic parameter.

Some typical kinematic arrangements used in grinding such as (a) internal grinding, (b) horizontal spindle surface grinding, (c) external cylindrical grinding, and (d) abrasive cut-off are shown schematically in Figure 1.1.

1.2 The Role of Chip-thickness

The important factor in deriving the expression for undeformed chip-thickness, t, is the number of cutting elements per unit area of wheel surface, C, that are present in a layer whose thickness is related to that of thickest chip produced [24-27]. The deeper the grain lies above the outermost wheel surface, the greater is the probability that a grain will not contact the workpiece surface because a more protruding grain immediately ahead of it has already removed the material. The other parameter, affecting t is the ratio of mean scratch width to scratch depth, r, [28]. The chip size determines the area of contact between chip and the grain and the force on the entire grain. The specific energy, U [29] is given by

$$U = \frac{F'_p V}{vd} \qquad (1.1)$$

where F'_p is tangential force per unit grinding width, V and v are the wheel and table speeds respectively and

d is wheel depth of cut. Figure 1.2 shows a plot of U versus t on a log-log scale [24]. In plotting this curve the values of t were computed using equation (1.10) in which C was assumed to have a constant value depending on the grain size.

1.3 Mechanics of Grinding

As the average linear grain spacing, λ, between two grains on the wheel surface in the same peripheral plane passing through their tips can not be measured directly, equation for t can be obtained from volume continuity [28]. In surface grinding, represented schematically in Figure 1.3 a, the actual shape of the chip produced is shown in Figure 1.3 b. An idealised chip shape (Figure 1.3 c) can be assumed to ensure volume continuity. Since the chip length, l_c, is much greater than t and s_f where s_f is feed per grain, given by

$$s_f = \lambda v/V \tag{1.2}$$

v_1, the volume of the chip shown in Figure 1.3 c is given approximately by

$$v_1 = \frac{1}{2} l_c t b \tag{1.3}$$

where b is the average width of the chip. The volume

removal rate by the number of cuts made per unit time,

$$v_2 = \frac{v}{V} \frac{b}{b} \frac{d}{C} = \frac{v}{V} \frac{d}{C} \qquad (1.4)$$

where C is the number of active grains per unit area on the wheel surface. From equations (1.3) and (1.4) we get,

$$t = \frac{2}{V} \frac{v}{C} \frac{d}{l_c} \frac{}{b} \qquad (1.5)$$

Ignoring the local wheel deflections,

$$l_c \simeq \sqrt{D_e d} \qquad (1.6)$$

where D_e is the equivalent wheel diameter given by

$$D_e = \frac{D D_w}{D \pm D_w} \qquad (1.7)$$

In equation (1.7), D is the wheel diameter, D_w is the work-piece diameter, positive sign is for external and negative sign is for internal grinding. For plunge cut surface grinding, D_w is infinite. Therefore,

$$D_e \approx D \qquad (1.8)$$

Hence,

$$t = \frac{2}{V} \frac{v}{C} \frac{}{b} \sqrt{\frac{d}{D}} \qquad (1.9)$$

Assuming [22, 24, 29],

$$t = \sqrt{\frac{4\ v}{V\ C\ r}\ \sqrt{\frac{d}{D}}} \qquad (1.10)$$

Expressing C in terms of average linear grain spacing,

$$C = \frac{1}{\lambda\ b} \qquad (1.11)$$

t, can be obtained from equation (1.9) as

$$t = 2\ \lambda\ (v/V)\ \sqrt{\frac{d}{D}} \qquad (1.12)$$

In the above analysis, the path traced by an individual grain has been assumed to be circular instead of trochoidal. This assumption seems to be justified in view of the speed ratio, $q = V/v$, being very high. In equation (1.10), the unknown parameters are C and r.

1.4 Determination of C and r

The number of cutting edges per unit length or unit area, the distance between cutting edges, and the distribution of cutting edges in the direction normal to the wheel surface quantitatively characterise the cutting surface. C was originally determined by rolling a dressed wheel over a soot-coated plate and counting the number of contacts indicated on an enlargement using the plate as negative [24, 25]. This method gives a very high value of C as vibrations, local wheel and work deflections, etc., are not included. Several other methods have been used to evaluate C. It has been suggested [30, 31] to observe

the wear flats produced on the grains and to get the C
value by dividing the number of wear flats by the viewing
area, or by counting the number of chips produced after
separating the chips from the debris collected [32]. The
latter method is based on the assumption that each cutting
element produces only one chip. In another method [33],
C was evaluated from the length and spacing of the scrat-
ches produced during grinding on a lapped inclined surface.
A plot of C versus z' (Figure 1.4) has been obtained, where
z' is the distance measured radially inward from the outer-
most grain on the wheel face. From Figure 1.4, z' is taken
equal to t, and the value of C is obtained. The equation
(1.10) is solved iteratively till the assumed and calcu-
lated values of t match.

It has been observed [34] that when the value
of U is evaluated for any value of t obtained in con-
junction with Figure 1.4, the plot of U versus t
(Figure 1.5) has a very steep slope, which suggests that
there is practically no difference in t for the finest
and coarsest grinding. The difficulty is believed to lie
in the fact that the curves of Figure 1.4 have been extra-
polated in obtaining Figure 1.5. Therefore, it has been
suggested [29] that the curves of Figure 1.4 will not
continue upward indefinitely as shown by dotted curve in

Figure 1.6 but they should level off beyond some value of z' (or t) as shown by dashed curve. Thus, in the practical range of values of t, C will be approximately constant. Attempts have also been made to find the relationship between the size distribution of abrasive particles removed from grinding wheel by dressing and the number of active grains per unit area of the wheel for different grain sizes and wheel grades [35].

The quantity, r, was originally obtained from a taper section [24]. It depends on the shape of a typical grit which has been the subject of much uncertainty. Earlier, it had been a widely held belief that abrasive grits generally have a large negative rake angle [36]. However, this concept cannot explain a number of important features of the grinding process such as the existence of large specific energy for metal removal. The action of a single abrasive grain were simulated by many researchers using spherical and conical tools [37-43]. However, the manner in which tools having these idealised shapes form a groove or remove a chip is still not clear. These workers [37-43] suggest that grinding mechanism can be broadly divided in two categories, fine and rough grinding. Hence, if grinding is viewed as a scraping process, two typical grit geometries can be assumed. At large wheel depths, the grit may be assumed to be conical

whereas for small wheel depths, a spherical shape may be a better approximation [44]. Tests conducted with single grains [45, 46] indicate that in fine grinding, the average grit shape may be approximated by a sphere. Based on this, the grinding mechanism is assumed to be of extrusion type rather than concentrated shearing mechanism involved in normal metal cutting operation [47]. It has been shown that scratches produced in overcut fly-milling is closely approximated by an arc of a circle [48], and the radius of curvature is independent of grain type and grinding conditions in fine grinding but varies with the grain size (Figure 1.7). The equation for undeformed chip thickness can be rederived as [48]

$$t = \frac{v}{V\,C\sqrt{D}\,\sqrt{2\rho - d}} \qquad (1.13)$$

where ρ is the grain tip radius as shown in Figure 1.8. Single grain abrasive studies suggest that the best estimate for the average transverse grain shape is a cone with radius ρ at the tip, thus for material removal, the conical shape is assumed but for surface finish analysis, the spherical shape is assumed [49].

1.5 Grinding as a Random Process

In most of the material removal processes, a single point or multipoint cutting tool with well defined

cutting edge geometry is used. For grinding process, unfortunately the cutting edges are not well defined or equispaced, rather they are placed randomly on the grinding wheel. Thus they produce a surface whose behaviour can not be predicted exactly in a deterministic manner. Due to this randomness of cutting particles on the grinding wheel surface, it is natural to strive for a stochastic model of the grinding wheel and the grinding process.

1.6 Stochastic Model

In most of the engineering problems involving randomness, the first step is to consider randomness in the analysis and ultimately to construct a reasonable stochastic model representing such randomness which gives the output characteristics closest to desired output. It has to be reasonable in the sense that it can be handled analytically without too much cost of computation and should also be consistent with the quality and quantity of information pertinent to the particular random phenomenon of interest. An overly sophisticated and complex model that cannot be verified by means of existing data and possibly by way of sound engineering judgement could simply complicate rather than solve the problem at hand [50]. Stochastic modelling of physical system can be achieved through Monte-Carlo Simulation method or Markov-Chain method.

Monte-Carlo method [51] is based on random numbers generated for a known or assumed probability density function of any variable. Depending upon the dynamics of the process, the random response of the system is evaluated and compared with desired output of the system.

Markov process [52] is best visualized as a process where the stochastic dependence of the future is independent of the past information given the present state precisely. If the state of space is discrete or contains finite or countably infinite number of states, the process is known as Markov-Chain.

1.7 Previous Models

Surface roughness of the workpiece is one of the most important output parameters in precision machining. The grinding process can therefore be analysed in terms of the surface roughness produced on workpieces. Yang and Shaw [53] have derived an expression for centre line average (CLA) value of the surface roughness for surface grinding, assuming that all the grains are at the same radial position on the grinding wheel generating chips of equal size. The mean peak to valley height has been evaluated by assuming either the grain population density to vary parabolically with the distance from the

outermost grain on the wheel face [54] , or the grains
to be uniformly spaced [33]. The surface roughness values,
thus, obtained [53, 54, 33] were either too low or high as
compared with the actual measurements. This was primarily
because these analyses were based on the assumption of
some form of population density function of grain position
with radial distance without considering the dynamic effect
of table speed, v, wheel depth of cut, d, and elastic
grain deflection. The grains responsible for surface
generation are distributed within an effective profile
depth, d_e, which is defined as the radial zone on the wheel
surface within which the grains contribute cutting [55].
Comparison of surface roughness in terms of CLA value or
mean peak to valley height is not likely to give a good
representation of the surface generated, since the sur-
face profile itself is not considered. In this respect,
autocorrelation and Fourier spectrum analyses are likely
to lead to a much better representation of the generated
surface profile. This can be obtained through a random
model.

1.8 Random Models

A simple random model was proposed by Baul [56]
where the asperities and valleys of abrasive surface have
been simulated by rods of varying heights having a

truncated normal distribution. The sample distributions
of the distances between active asperities, defined as
grit pitch, and the depth of penetration were then obtain-
ed. The cutting performance in belt grinding was studied
theoretically [57] by analysing the profile using Markov-
Chain theory. The theoretical distribution for distan-
ces between two active grains was obtained by observing
the lands and voids of the representative profile of the
abrasive surface through the transition probability matrix
p_{o_1} of going from state o to 1. When the profile height
measured at constant intervals along some fixed length
exceeded a fixed height, it was defined as state 1 and
when it failed to exceed, was state o.

The grinding process was simulated by Yoshikawa
and Sata [58] using the Monte-Carlo method. The transfer
function of the process was obtained using the simulated
profile as the input and the experimental profile as the
output. Figure 1.9 shows that the transfer function of
the process, thus obtained, is very much amplified at
lower frequencies and almost unity at higher frequencies.
The reasons attributed for the distortion of transfer
function at low frequency and the assumption that the
radial distribution of grain tips is proportional to the
depth from the outermost grain on the wheel face needs
justification.

Peklenik [59] investigated the grinding process as a linear system with random input and output. The elementary cutting profile of the grinding wheel was taken to be a stationary stochastic process described in terms of averages and auto-correlation functions. These characteristics were obtained for representative grinding wheels and were functions of physical and geometrical behaviour, and the dressing conditions. The frequency transfer function of the surface roughness and the wear of grinding wheel provide an insight into the tranformation of the disperson spectra in the grinding process. Information on the shape of transfer function make it possible to determine the cutting action of the elementary cutting profile in terms of the distribution of the instantaneous chip size.

Autoregressive moving average model was developed by Deutsch and Wu [60] to represent grinding wheel profiles for different combinations of sampling parameters including the sample interval, the number of observations, and the length of record. The choice of sample interval determines the appropriate model form, the model order and the estimated parameters. The use of larger number of observations is necessary only to increase the confidence associated with the estimated parameters.

Another simulated model was proposed by Law and Wu [61] by systematically varying the table speed, wheel depth of cut, and grain apex angle. In this analysis, the dynamic influence of table speed, depth of cut over a preselected region and elastic grain deflections were predicted through the radial distribution parameter. It was proposed that the radial distribution parameter has two range of values, one less than 8 for fine dressing and the other greater than 8 for coarse dressing. This was explained in terms of change in the grain apex angle due to dressing conditions.

In all the previous analyses [55-60], the transverse shape of the grain was assumed to be triangular with negligible thickness along peripheral direction. A single grain may have many tiny cutting points on the surface and during interaction with the workpiece may cause material removal. The transverse shape of the groove (Figure 1.10) can, however, be approximated by a circular arc [48]. Further, in most of the earlier studies [57 - 60], it was assumed that there is no overlapping of cuts. For continuous feed, successive tips lying in different radial levels may produce cut at a particular point whenever there is grain-workpiece interaction. The generated profile height at that point will be the lowest height left after removal of material by cutting grains.

1.9 Present Model

In the present model, the grinding process is
simulated to study the surface generated under different
cutting conditions. The dynamic influence of table speed,
and wheel depth of cut on grain distribution is analysed
through the radial distribution parameter. The probabi-
lity density functions of position of grain tips on the
wheel surface are obtained on the basis of interference
of grooves produced in transverse direction and the grain
elastic deflection in radial direction. The regression
equation of radial distribution parameter with depth of
cut and wheel speed is obtained by comparing the power
spectra of the experimental profile with the theoretical
profile generated using Monte-Carlo simulation. The study
is confined to single pass surface grinding under plunge-
cut conditions. The transverse shape of the grooves
produced by individual grains are assumed to be circular
in section without side pile-up. Further, the grains are
assumed to move in a circular arc which is approximately
true since the wheel speed is much higher than the table
speed. The wear of the grains are assumed to be negligible
for a single pass. Only the grains distributed randomly
along the radial direction within the effective profile
depth, d_e, from the outermost wheel surface are considered

to be contributing to the surface generation and not those lying beyond d_e. Considering successive cuts by grains along the cutting direction, longitudinal surface profile can be obtained from the grain-workpiece interference pattern. Transverse surface roughness and generated profile can be obtained theoretically by considering the interaction of grooves produced at different points where the groove mid-points are separated by a random distance called axial pitch.

Once the radial distribution parameter under various cutting conditions is known, an approximate analysis can afford a simpler way to obtain the undeformed chip thickness and the surface roughness.

(a)

(b)

(c)
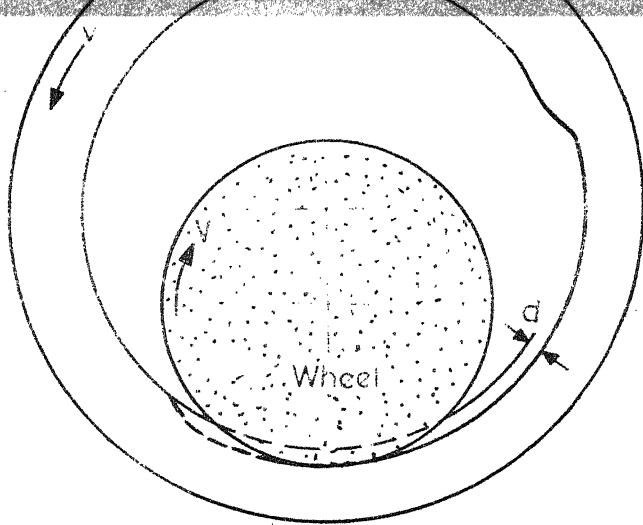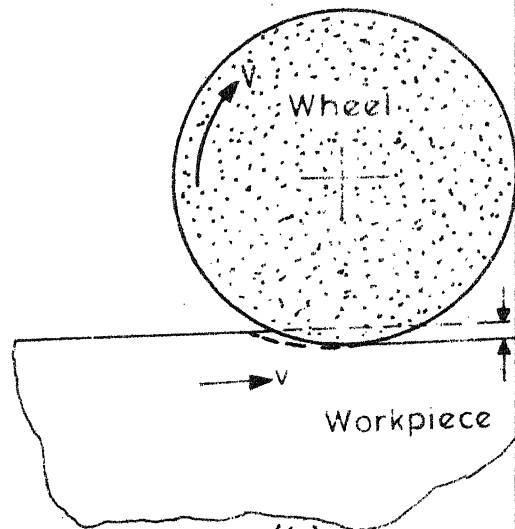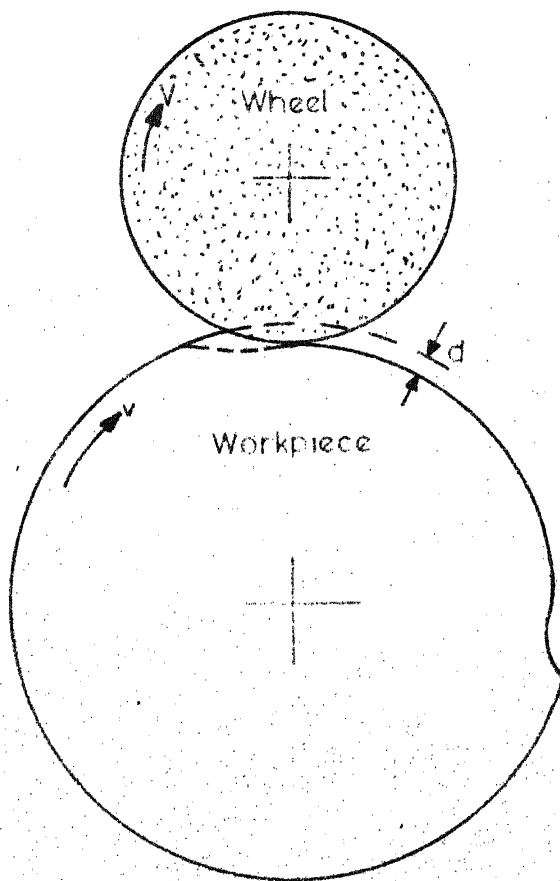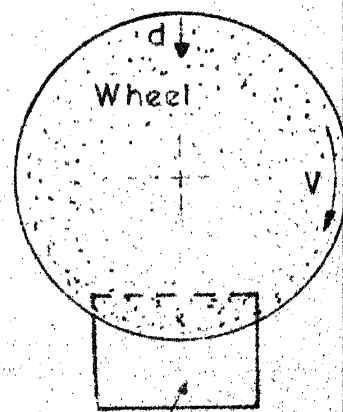
(d)

FIGURE 1.1 KINEMATIC ARRANGEMENTS IN GRINDING
    (a) INTERNAL GRINDING   (b) HORIZONTAL SPINDLE SURFACE
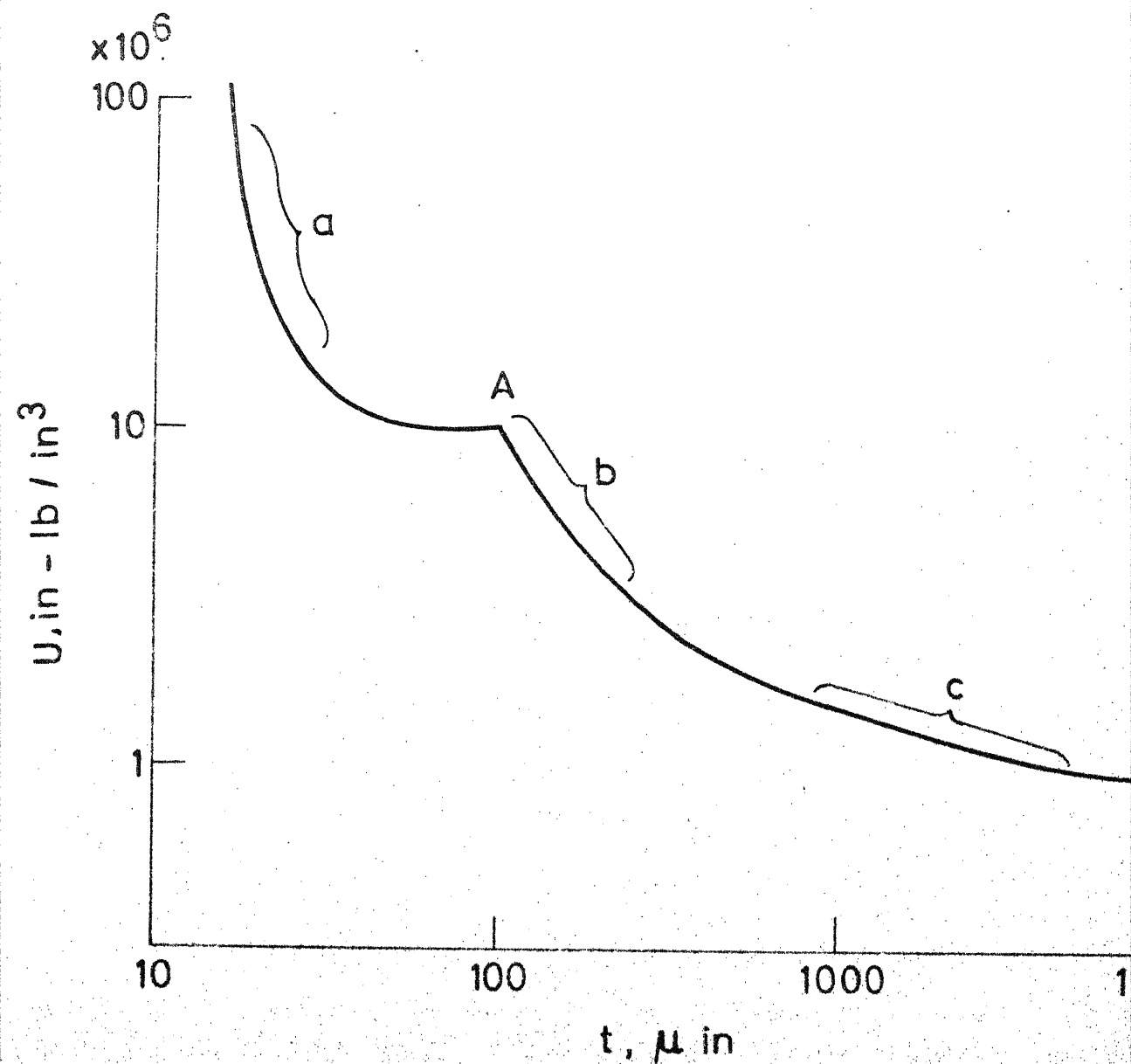
FIGURE 1.2 VARIATION OF SPECIFIC ENERGY, U WITH UNDEFORMED
CHIP THICKNESS, t, FOR :
(a) INTERNAL GRINDING;
(b) FINE SURFACE AND CYLINDRICAL GRINDING;
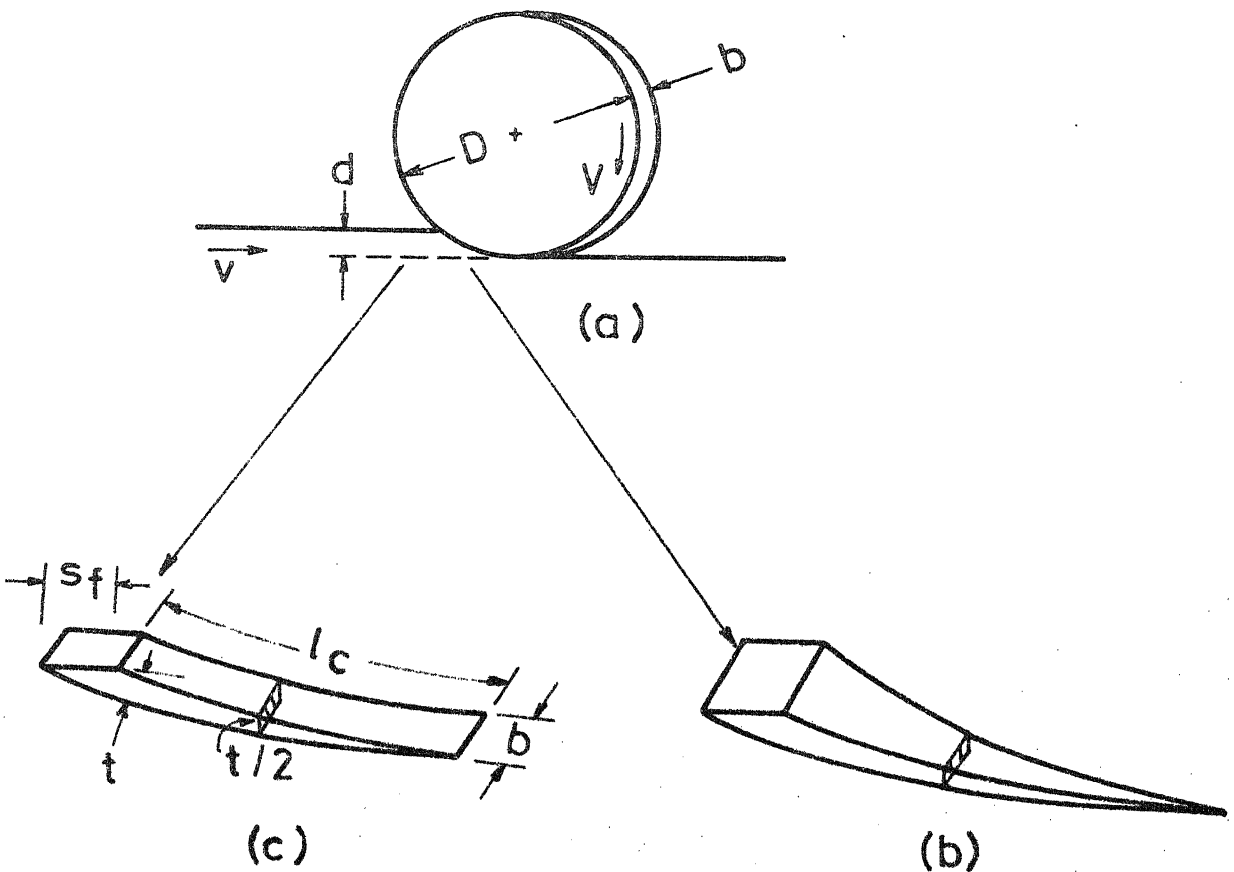
FIGURE 1.3 INDIVIDUAL CHIP PRODUCED IN SURFACE GRINDING :

(a) SCHEMATIC VIEW OF THE PROCESS;

(b) ACTUAL SHAPE OF THE CHIP PRODUCED;

(c) IDEALISED CHIP USED TO ENSURE VOLUME
     CONTINUITY. [AFTER LAL AND SHAW [28]]
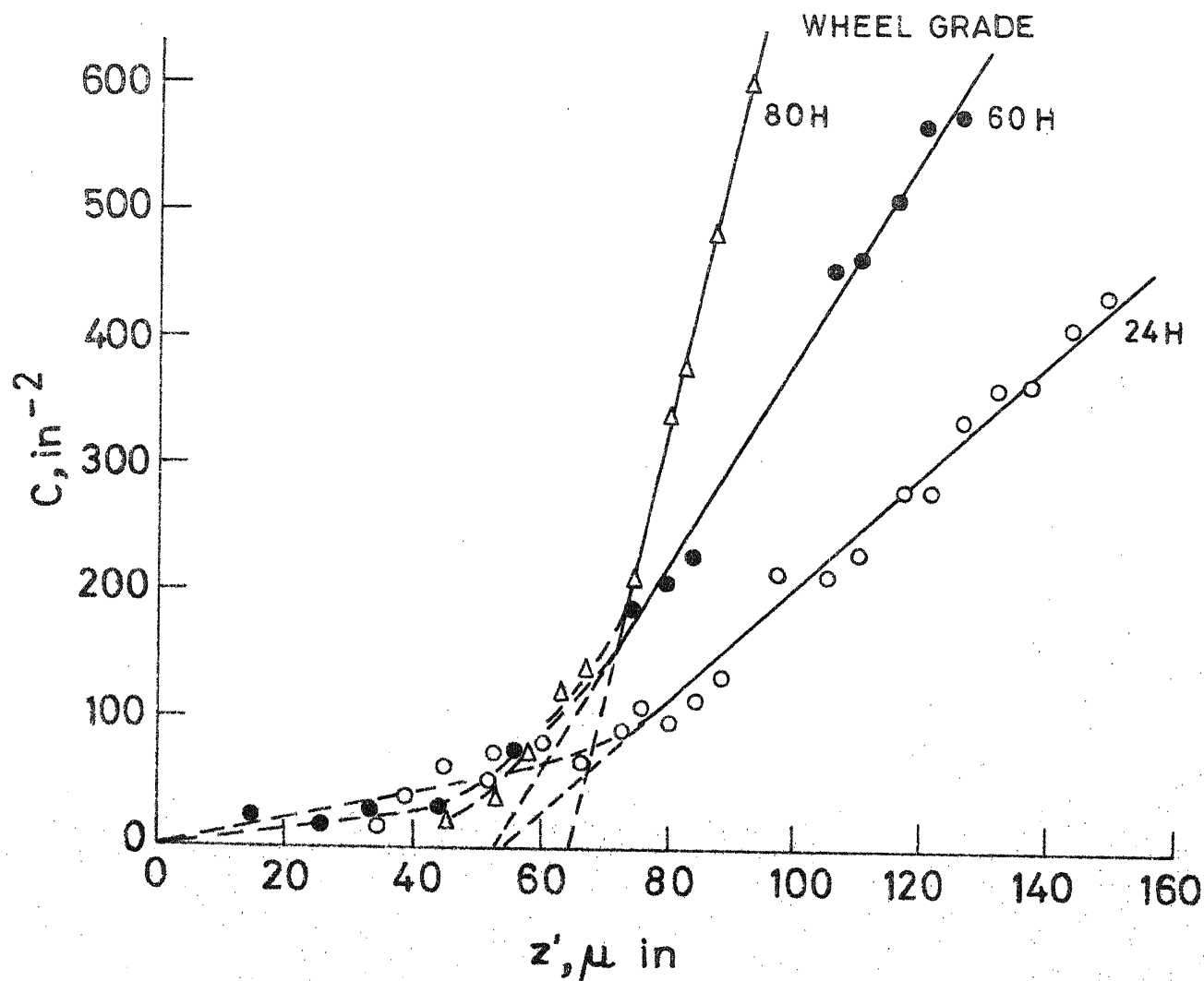
FIGURE 1.4 VARIATION OF EFFECTIVE NUMBER OF CUTTING POINTS
PER UNIT AREA, C, ON THE WHEEL SURFACE WITH
RADIAL DISTANCE FROM OUTERMOST GRAIN, Z'. [AFTER
NAKAYAMA AND SHAW [33]]
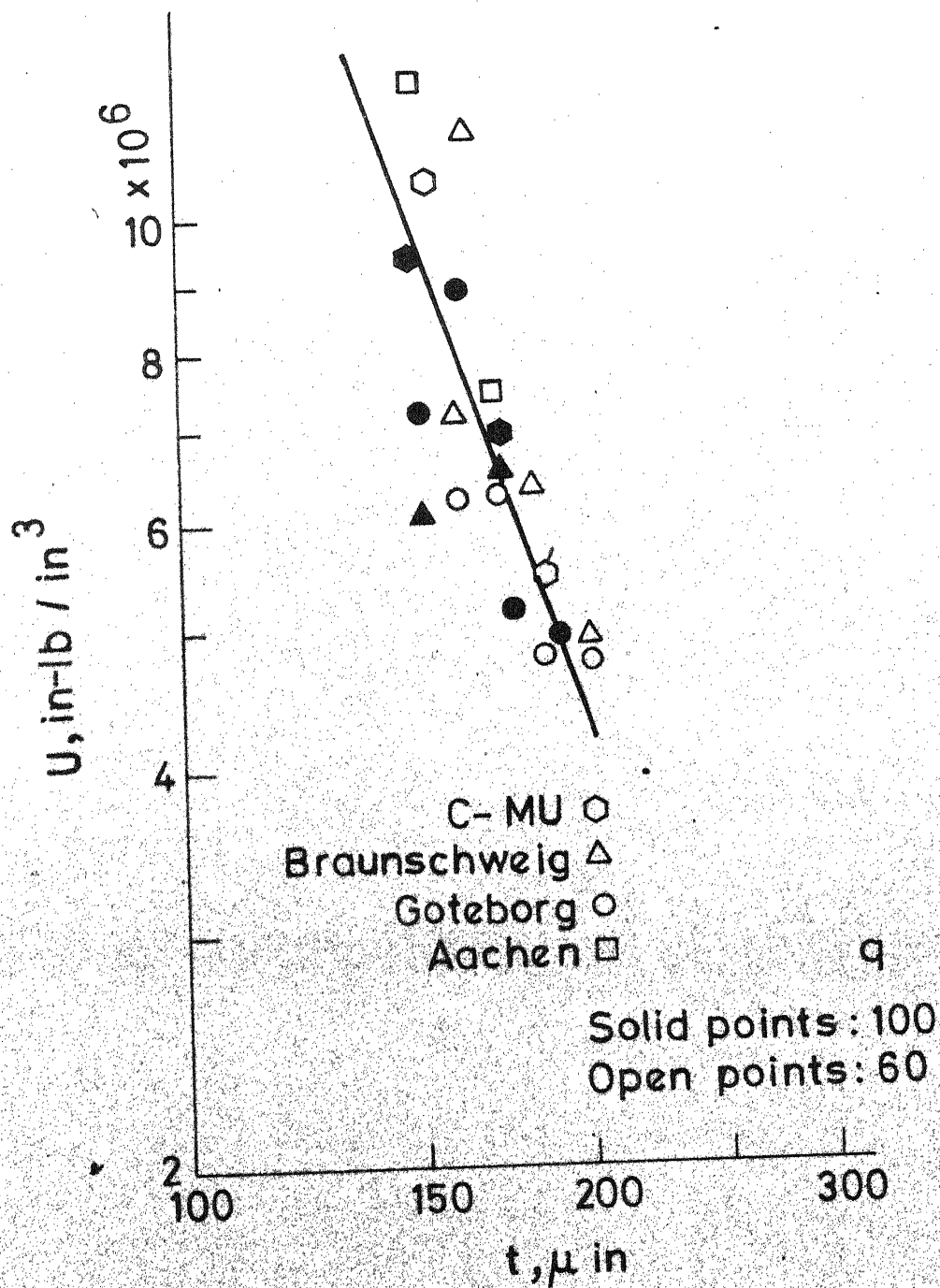
FIGURE 1.5 VARIATION OF SPECIFIC ENERGY, U, WITH
UNDEFORMED CHIPTHICKNESS : WHEEL : 60L;
q : 60 AND 100; V : 6300 AND 12,000 fpm;
v : 0.03 AND 0.12 ipm [After Breaker,
Sauer, et al [34]]
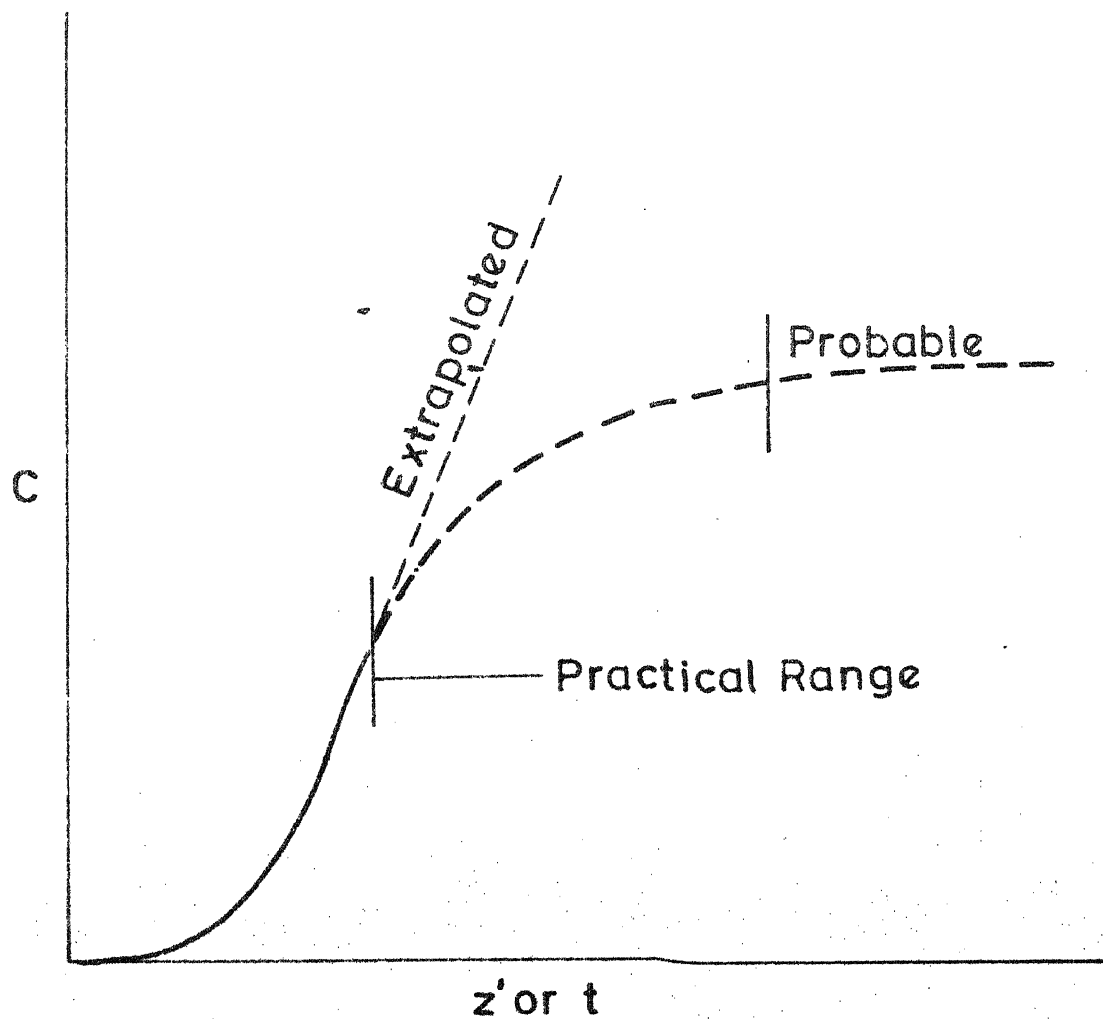
FIGURE 1.6 COMPARISON OF EXTRAPOLATED AND PROBABLE
            CURVES OF C VERSUS t [AFTER SHAW [29]]

$\rho = 0.5g$

$\rho = 0.053g^{0.53}$

× C-34

● 75 A

○ AZ-40

■ SS
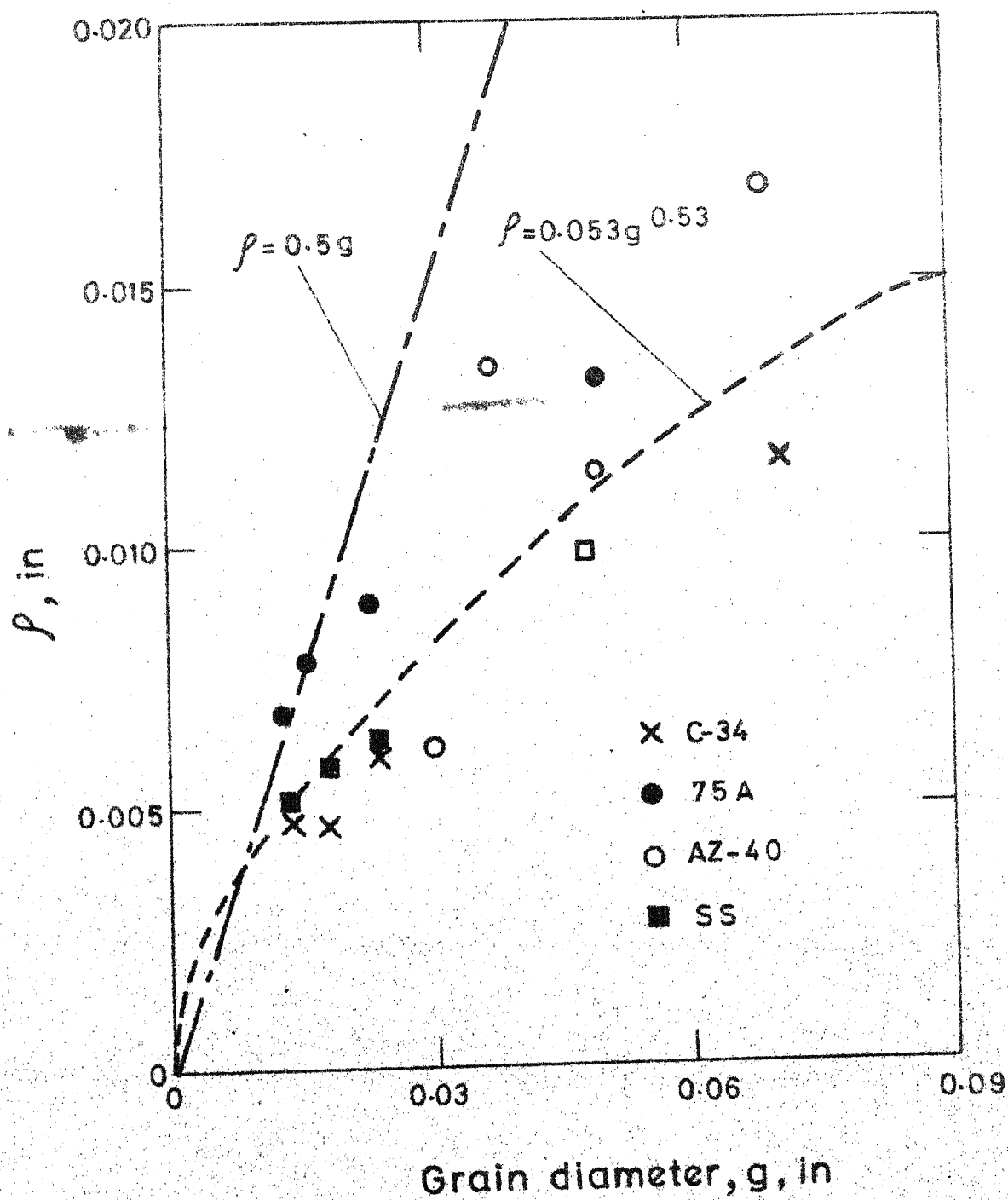
Grain diameter, g, in

FIGURE 1.7 VARIATION OF EFFECTIVE GRAIN TIP RADIUS, ρ
WITH NOMINAL GRAIN DIAMETER, g FOR VARIOUS
GRAIN TYPES [AFTER LAL AND SHAW [28]]
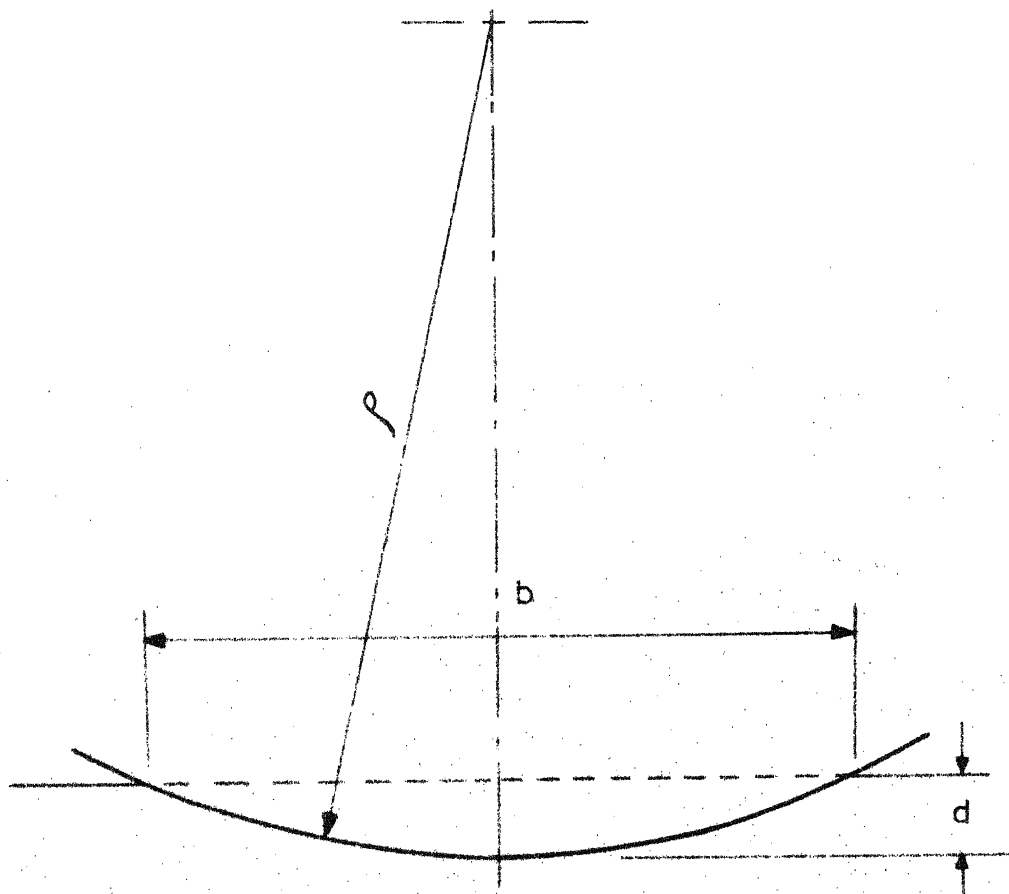
FIGURE 1.8   TRANSVERSE VIEW OF GRAIN TIP [AFTER LAL AND SHAW [28]]
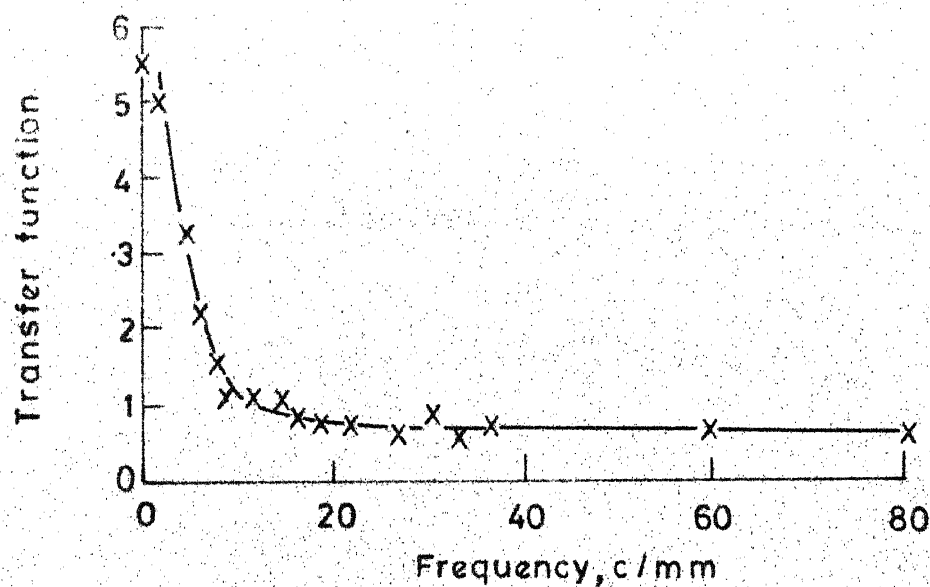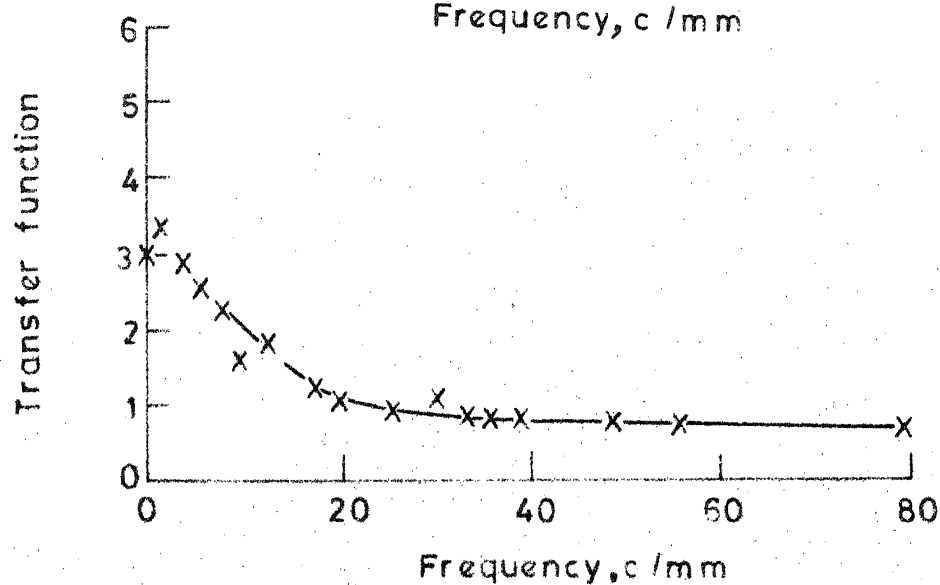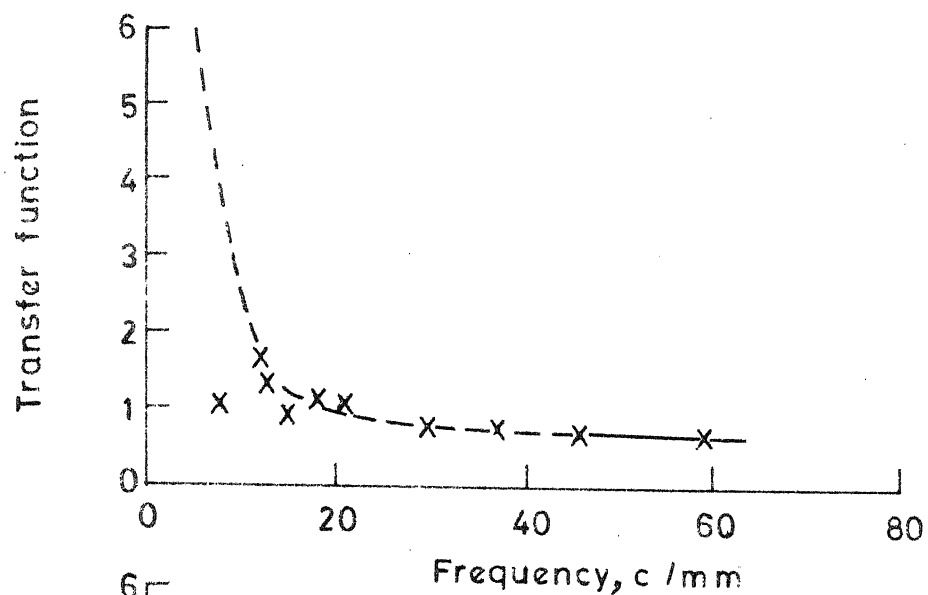
FIGURE 1.9 SOME EXAMPLE OF TRANSFER FUNCTION (ABSOLUTE VALUE) OF THE PROCESS WHOSE INPUT IS SIMULATED PROFILES AND OUTPUT IS EXPERIMENTAL PROFILE [AFTER YOSHIKAWA AND SATA [58]]

(a)

$\rho = 0.0126$ in
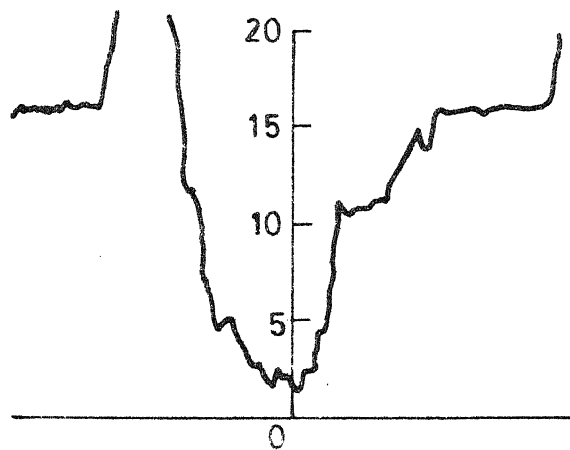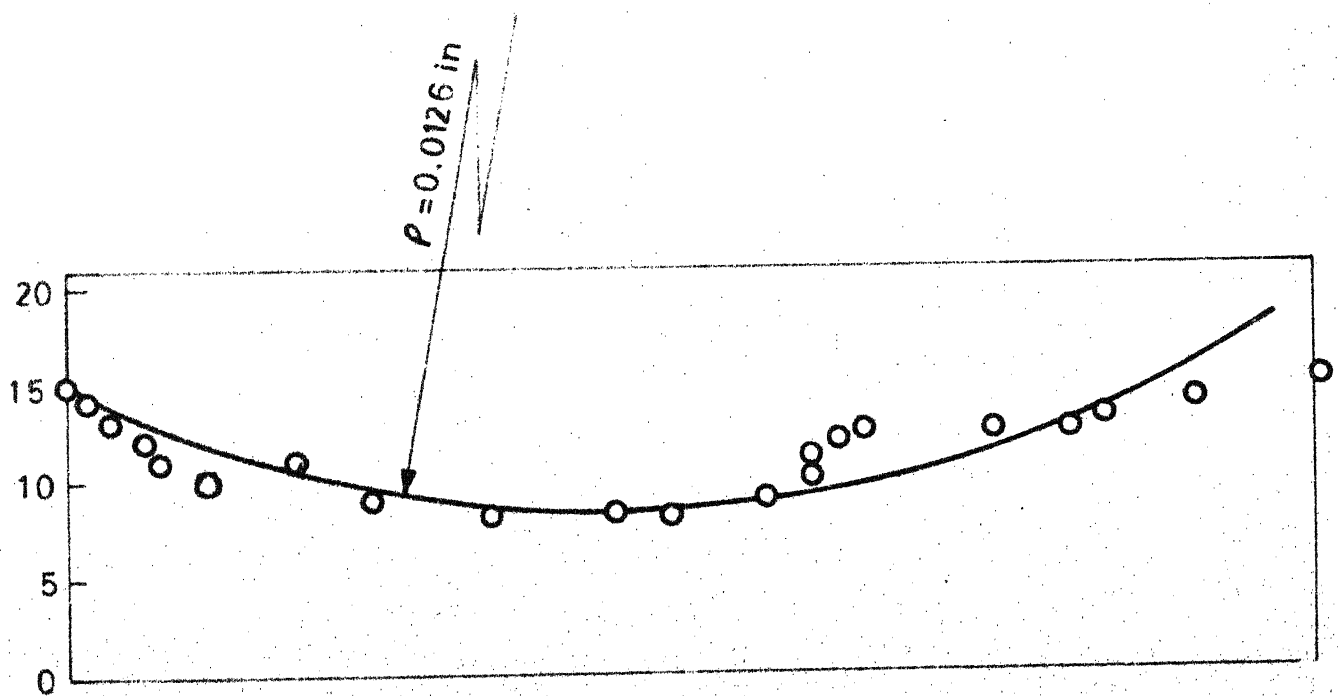
(b)

FIGURE 1.10 (a) GRAIN: C-34; WHEEL SPEED: 22,000 fpm; TABLE SPEED: 120 fpm; MATERIAL: AISI 1020; SCALE: HOR: 1 DIV.=2000 μin, VERT: 1 DIV = 100 μin.

(b) TRANSVERSE SHAPE OF OVERCUT FLY MILLING GROOVES WITH CIRCULAR ARC PASSING THROUGH pOINTS FROM TALYSURF TRACE AISI 1020 STEEL [AFTER LAL AND SHAW [48]]

PROBABILISTIC MODEL AND SIMULATION

2.1   Introduction

The cutting surface of the grinding wheel can
be thought of as a number of infinitesimally small
cutting points distributed randomly over the surface. If
the material is removed from a smooth surface, the result-
ing surface will have a random profile characterising the
grinding wheel surface. If the probability distribution
function of the random cutting points on the wheel surface
is mathematically known, the output surface profile can
be generated knowing the input surface profile and input
grinding conditions. Thus, the process can be modelled
with grinding wheel surface characteristics as the black
box having inputs such as grinding conditions and input
surface profile of the workpiece and output as simulated
profile of the surface.

2.2   The Axial Pitch

The developed surface of the grinding wheel will
appear as shown in Figure 2.1 a, where the various columns
have been shown to be passing through the grain tips. The
distance between the coloumns, defined as axial pitch, p,
is a random variable. The tip position of ith grain in

jth column is shown in Figure 2.1 b, where $y_j^{'i}$ is the distance of ith grain tip measured along the periphery and $z_j^{'i}$ is the distance measured radially inward from the circle passing through the outermost grain tip. For any simulated width, λ, of the grinding wheel, the number of columns, N_c, will be approximately given by

$$N_c \simeq \frac{\alpha}{\bar{p}} \tag{2.1}$$

where $\bar{p}$ is the average value of the axial pitch. Let L be the maximum width of cut produced by grain during interference with workpiece and $f_p(p)$ be the probability density function of the random variable p. The influential width of groove is produced by any grain during interference and therefore, the pitch, p, will lie between O and L. Hence, the average value of pitch, $\bar{p}$, can be evaluated from

$$\bar{p} = E[p] = \int_0^L p \, f_p(p) \, dp \tag{2.2}$$

2.3 Probability Density Function

2.3.1 Axial Pitch

In Figure 2.2 a, (x, y, z) is a right handed coordinate system fixed at the leading edge of the workpiece. At any section BB along the transverse direction,

grooves produced by any grain on j and j+1th columns
(Figure 2.2b). As the grains pass independently of each
other through the workpiece, x_j and x_{j+1} are independent
random variables. The population under consideration for
the independent section 0, L along axial direction has
a distribution function $F_X(x)$ and density function
$f_X(x)$ (Figure 2.3 a) given by

$$f_X(x) = \frac{1}{L} \qquad (0 \leqslant x \leqslant L)$$

$$= 0 \qquad (x < 0; \quad x > L) \qquad (2.3)$$

$$F_X(x) = 0 \qquad (x < 0)$$

$$= \frac{x}{L} \qquad (0 \leqslant x \leqslant L) \qquad (2.4)$$

$$= 1 \qquad (x > L)$$

Assuming the surface generated by successive interference
of grooves produced, p, to be given by

$$p = \left| x_{j+1} - x_j \right| \qquad (2.5)$$

Using the transformation

$$w = x_{j+1} - x_j \qquad (2.6)$$

the probability density function of w is obtained
[62] as

$$f_W(w) = \int_0^L f_{X_2}(w - x_1) f_{X_1}(-x_1) \, d x_1 \qquad (2.7)$$

which is of triangular form (Figure 2.3 b). As the random variable x_{j+1} and x_j are uniformly distributed between 0 and L, and $f_W(w)$ is an even function

$$f_p(p) = 2 f_W(w) U(p) \qquad (2.8)$$

as shown in Figure 2.3 c, where $U(p)$ is a random variable uniformly distributed between 0 and 1. Using equations (2.7) and (2.8), we get

$$f_p(p) = \frac{2}{L^2}(L - p) \qquad (2.9)$$

Therefore, from equation (2.2), we get

$$\bar{p} = \frac{1}{3} L \qquad (2.10)$$

Assuming the groove shape to be a circular arc of radius ρ (Figure 2.2), the maximum width of cut, L, will be given by

$$L = 2\sqrt{(2 \rho d_e - d_e^2)} \qquad (2.11)$$

where d_e is the effective profile depth. Neglecting the higher order terms in the above equation,

$$L \simeq 2\sqrt{2 \rho d_e} \qquad (2.12)$$

For grain size greater than 36, it has been shown [28] that grain tip radius can be approximated by

$$\rho \simeq g/2 \qquad (2.13)$$

where g is the nominal grain diameter and is approximated by

$$g \approx \frac{0.6}{S_g} \quad (\text{inch}) \tag{2.14}$$

where S_g represents the grain size. Therefore,

$$\bar{p} = \frac{2}{3} \sqrt{g\, d_e} \tag{2.15}$$

and

$$N_c = \frac{3}{2} \frac{\alpha}{\sqrt{g\, d_e}} \tag{2.16}$$

2.3.2 Grain Positions

In any column passing through the tips of grains, the position of grain tip will be random because of the random occurrence of grain on the wheel surface. It has been shown [54, 57] that the random variable $\Delta y'$, representing the interval of successive appearance of grains for a fixed point on the workpiece, has an exponential probability density function, $f_Y(\Delta y')$, given by

$$f_Y(\Delta y') = \frac{1}{\lambda} e^{-\Delta y'/\lambda} \tag{2.17}$$

where,

$$\Delta y' = y'^i_j - y'^{i-1}_j \tag{2.18}$$

and

$$\lambda = \frac{\pi D}{M} \tag{2.19}$$

In equation (2.19), M is the total number of grains in any column. Therefore, M is obtained by dividing the total number of grains existing on the wheel surface by

the number of columns, N_c. Hence, M can be approximated by

$$M \approx \frac{\pi D \cdot C}{N_c} \qquad (2.20)$$

where C is the nominal grain density. From equations (2.19) and (2.20), we get

$$\mathcal{A} = \frac{N_c}{\pi C} = \frac{3}{2 \, G\sqrt{g \, d_e}} \qquad (2.21)$$

The radial positions of grain tips (z') are random. From the nature of the curve shown in Figures 1.4 and 1.6, the radial position of grain tips can be obtained [29, 33]. Different curves are obtained for different wheels. These curves are generally extrapolated in the finer region where the values of t are very small. Various probability density function, $f_Z(z')$, of the random variable, z' , have been used in the past [53, 54, 58, 61] . From the nature of the curve shown in Figure 1.4, the general form of the probability density function appears to be of the form

$$f_Z (z') = A \, z'^k \qquad (2.22)$$

where A and k are constants depending upon the cutting conditions and grinding wheel. Most of the forms of $f_Z (z')$, used earlier [54, 58, 61] can be obtained from the above equation assuming particular values of A and k.

Under dynamic conditions, the outermost grain gets elastically deflected inwards [61] . The radial distribution of grain tip positions is thus modified. It is the conditional distribution of grain tip positions in the radial direction (after the grains get elastically deflected) which defines the radial positions of grain tips on the wheel surface. The probability density function $f_Z'(z)$ and the corresponding distribution function $F_Z'(z)$ are shown in Figure 2.4 a and 2.4 b, respectively. If d_o is the amount of deflection undergone by lowermost grain (Figure 2.4 c), then the grains will be lying between d_o and $d_o + t$ along the radial direction of wheel surface.

In Figure 2.5, ith grain lies at an average linear distance, λ, measured along the wheel periphery behind (i - 1)th grain and the radial distance between the two concentric circles passing through the tips of ith and (i - 1)th grain is $\Delta z'$. The maximum depth of cut by ith grain, t_i, is

$$t_i = 2\lambda \frac{v}{V} \sqrt{\frac{d}{D}} - \Delta z' \qquad (2.23)$$

$$= t - \Delta z' \qquad (2.24)$$

The condition for the ith grain to be an active cutting point (at least to contact the workpiece) is that the numerical value of t_i should be positive [63] , i.e., $\Delta z'$

must lie between 0 and t. It has been found [33, 61], that the value of d_e is approximately equal to the maximum value of t in the fine grinding range. Therefore, for any grains lying between d_o and $d_o + d_e$, the probability density function of radial position of grain tips will be given by

$$g_Z(z') = f_Z(z' \mid d_o < z' \leqslant d_o + d_e)$$

$$= \frac{f_Z(z')}{\displaystyle\int_{d_o}^{d_o + d_e} f_Z(z')\, d z'} \qquad (2.25)$$

which on simplification becomes

$$g_Z(z') = \frac{(k+1)(z')^k}{(d_o + d_e)^{k+1} - d_o^{k+1}} \qquad (2.26)$$

In equation (2.22) and (2.25), the parameter k is a function of the cutting conditions. This has been generally defined as the radial distribution parameter. The magnitude of elastic grain deflection, d_o, is generally of the same order as d_e [64]. Hence, d_o can be taken to be approximately equal to d_e. Now using the transformation (Figure 2.4 a)

$$z' = z'' + d_e \qquad (2.27)$$

we get

$$f_z(\overset{''}{z}) = \frac{(k+1)\,(\overset{''}{z} + d_e)^k}{d_e^{\,k+1}\,\left[2^{k+1} - 1\right]} \;;\quad 0 < \overset{''}{z} \leqslant d_e$$

$$(2.28)$$

The probability density functions of random positions of grain tips on wheel surface in any column are expressed by equations (2.17) and (2.28).

2.4 Simulation of Surface Profile

2.4.1 Transformation of Grain Tips to Workpiece

The theoretical surface profile can now be generated using computer simulation techniques. The coordinates of the random positions of grain tips can be generated using the probability density functions in equations (2.17) and (2.28). The surface is produced due to individual interaction of grains and workpiece. Since the speed ratio is high, the path traced by an individual grain will be assumed to be circular as discussed in Chapter I. It will be further assumed that the material is removed either in the form of a chip or through plastic deformations without side pile-up, whenever grain-workpiece interference occurs. Depending upon the interference, the grain tip positions can be transformed to the workpiece co-ordinate. The locus of the transformed points on the workpiece during grinding will be a circular arc and hence

the tip point of the grain after being transformed to the workpiece will be the lowest point of the circular arc. These kinematic transformations can be represented by

$$y^i = y'^i/q \qquad (2.29 a)$$

and

$$z^i = z''^i \qquad (2.29 b)$$

The locus thus formed will be a circular arc of radius R^i, where

$$R^i = R - z^i \qquad (2.30)$$

having its centre at $(y'^i/q, R)$; R being the radius of the grinding wheel. The schematic arrangement is shown in Figure 2.6. From equations (2.17) and (2.29 a), the probability density function, $f_Y (\Delta y)$, of the interval, Δy, of the lowest positions of tips in the groove along the direction of cutting will be

$$f_Y (\Delta y) = \frac{1}{\lambda_1} e^{-\Delta y/\lambda_1} \qquad (2.31)$$

where

$$\lambda_1 = \lambda/q \qquad (2.32)$$

Using equations (2.28) and (2.29 b), the probability density function of the lowest position of ith grain tip in the groove along the vertical direction will be

$$f_Z (z^i) = f_Z(z''^i) \qquad (2.33)$$

Hence the lowest positions of tips in the groove with respect to the (x, y, z) coordinate system are

$$x_j^i = x_j^{i+1} = \ldots = x_j^M = x_{j-1}^i + L \left(1 - \sqrt{1 - R_{u_j}}\right);$$

$$(2.34)$$

$$y_j^i = y_j^{i-1} - \Lambda_1 \log (R_{u_{i-1}}) \qquad (2.35)$$

and

$$z_j^i = d_e \left[(2^{k+1} - 1) R_{u_i} + 1\right]^{1/(k+1)} - d_e$$

$$(2.36)$$

where,

$i = 1, \ldots, M$

$j = 1, \ldots, N_c$

and $R_{u_{i-1}}$, R_{u_i} and R_{u_j} denote the random numbers uniformly distributed between 0 and 1. The transformations of probability density functions to random variates are given in Appendix A.

2.4.2 Longitudinal Profile

Once the lowest position of grain tips in the groove and its locus is obtained, the longitudinal surface profile generated by grains in any column can be obtained in the following manner:

(a) The path traced by the preceeding grain may be overlapped by the succeeding grain as shown in Figure 2.7 a. In this case, the surface produced

will correspond to the path traced by the succeeding grain and the active grain responsible for surface generation is the succeeding grain.

(b) The path traced by ith, i + 1 th and i + 2 th grains are shown in Figure 2.7 b. It may happen that the path traced by i + 1 th grain is overlapped by path traced by i + 2 th grain. Though in this case, all these grains are removing material, actual grains responsible for surface generation will be ith grain and i + 2 th grain.

(c) It may happen that the paths traced by ith, i + 1 th and i + 2 th grains are such that none is overlapped completely (Figure 2.7 c). In this case, all these grains will remove material and will be responsible for surface generation.

This complex behaviour of the grooves produced in longitudinal direction by different grains is due to the random grain-workpiece interference. As a result, the number of active grains removing material or producing chip and the actual number of grains responsible for surface generation under any cutting condition will be random. Combining the cases a, b and c, a general algorithm to generate the longitudinal surface profile can be developed in terms of the coordinates of the intersection points of the paths produced by the grains.

If B (i, j) represents the intersection of the paths traced by ith and jth grain in any column, then height of the intersection point z (i, j) will be given by

$$z~(i,~j)~=~z^i + \frac{(~y~(i,~j)~-~y^i)^2}{2~(R~-~z^i)} \qquad (2.37)$$

where

$$y~(i,~j)~=~y^i + 0.5 \left[\frac{(z^j~-~z^i)~2~R}{(y^j~-~y^i)} + (y^j~-~y^i) \right]$$

$$(2.38)$$

Here y (i, j) and z (i, j) are the coordinates of the intersection point B (i, j) with respect to (x, y, z) coordinate system. The derivations of the above equations are given in Appendix B. From Figure 2.7, it is observed that

for case (a) : $z~(i,~i + 1) > d_e$,

for case (b) : $d_e > z~(i,~i + 1) > z~(i,~i + 2)$,

and

for case (c) : $d_e > z~(i,~i + 2) > z~(i,~i + 1)$.

Extending the above algorithm for M number of grains in N_c number of columns, the longitudinal surface profile generated by the grinding wheel in different columns can be obtained. The computer flow chart for numerical computation of longitudinal surface profile height is given in Chapter IV. The number of active

grains responsible for surface generation in each column can also be obtained using the same algorithm.

2.4.3 Transverse Profile

Once the longitudinal profile along different columns are generated, the vertical heights of the surface profile at different column positions along the transverse direction can now be obtained. These vertical heights will correspond to the mid points of the circular shaped grooves. Superimposing the groove shape by a circular arc of grain tip radius, ρ, and considering the intersections of different grooves, the transverse profile can be generated. There are different possibilities of intersections of grooves. The groove with its mid-point at $j + 1$ th column may be overlapped completely by groove with its mid-point at jth column, (Figure 2.8 a), or is overlapped by grooves with its mid-points at jth and $j + 2$ th column, (Figure 2.8 b), or none of the grooves are completely overlapped and have intersections with each other (Figure 2.8 c). The transverse profile, thus generated in each case, is shown by hatched lines in Figures 2.8 a, 2.8 b and 2.8 c.

At any point $p (x_o, y_o)$ where x_o is the axial position along transverse direction and y_o is the longitudinal position along cutting direction with respect to

the fixed coordinate system (x, y, z), the resultant
height of the surface profile, z (x_o), can be obtained
from the following algorithms

$$z (x_o) = \text{Min} \left\{ (z_k (y_o) + (x_o - x_k)^2/g \right\} ;$$
$$k = 1, \ldots, N_c, \qquad (2.39)$$

where,

$$z_k (y_o) = \text{Min} \left\{ d_e, z_k^i (y_o) \right\} \quad i = 1, \ldots, M, \qquad (2.40)$$

and

$$z_k^i (y_o) = \frac{(y_o - y_k^i)^2}{2 (R - z_k^i)} + z_k^i \qquad (2.41)$$

In order to calculate the number of columns
responsible for surface generation, a similar procedure
as for determining the number of grains responsible for
generating the longitudinal profile, is applied. First,
the intersection point of ith groove with rth groove
is obtained whose coordinates are given by

$$x_{i,r} = x_i + \frac{1}{2} \left[\frac{(z_r (y_o) - z_i (y_o))g}{(x_r - x_i)} + (x_r - x_i) \right] \qquad (2.42)$$

$$z_{i,r} = z_i (y_o) + \frac{(x_{i,r} - x_i)^2}{g} \qquad (2.43)$$

where $z_i (y_o)$ denotes the longitudinal profile height
in ith column at the transverse section at a distance y_o

from the reference coordinate system (x, y, z). Here.
$x_{i,r}$, $z_{i,r}$ are the coordinates of the intersection points
of ith and rth grooves with respect to fixed coordinate
system (x, y, z). If $z_{i,k}$ is the minimum of all the
$z_{i,r}$, r varying from i + 1 to N_c, then the transverse
profiles will be produced by the intersection of ith and
kth grooves.

At any transverse section at a distance y_o
from the reference coordinate axes, the increment $\triangle x$
in the axial direction, is given by

$$\triangle x = x_m - x_{m-1} ; \quad m = 1, \ldots, N_s \qquad (2.44)$$

where N_s is the total number of sample points. The
transverse profile height at N_s number of sample points,
can be obtained using equations (2.39), (2.40), (2.41),
and (2.43). The transverse surface profile can thus be
generated by joining these points. Computer flow chart
for generating the transverse profile height at different
sample points is given in Chapter IV.
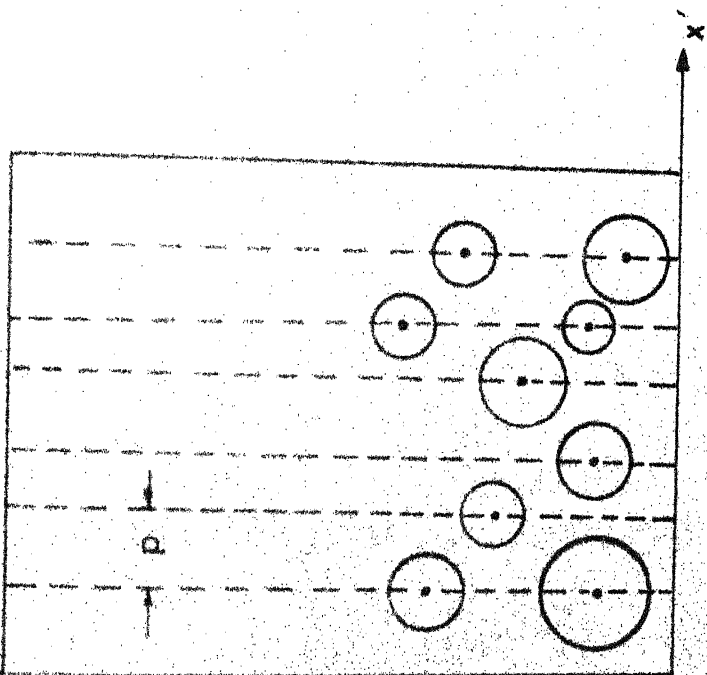
(a)
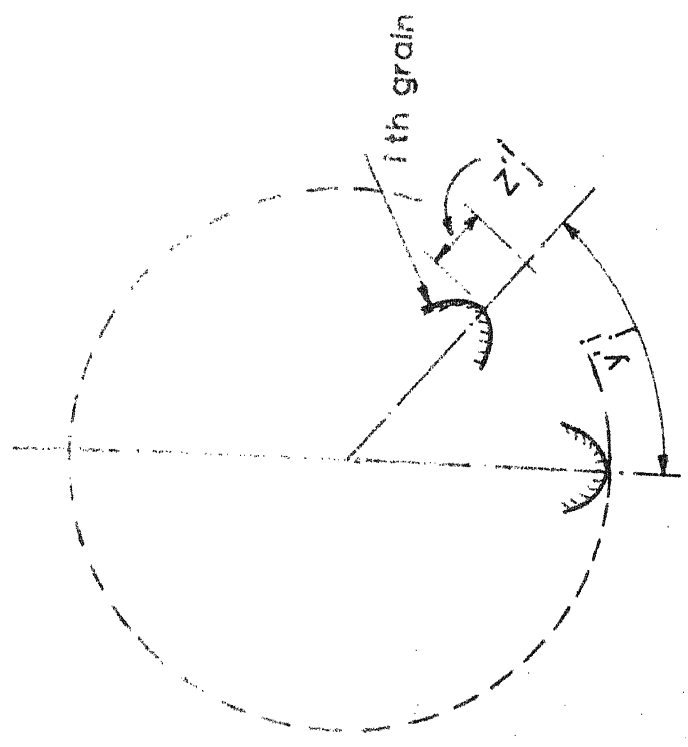
(b)

FIGURE 2.1 (a) DEVELOPED SURFACE OF THE GRINDING WHEEL ON $x'-y'$ PLANE;

(b) REPRESENTATION OF ith GRAIN IN jth COLUMN

a_p

(b)

(a)
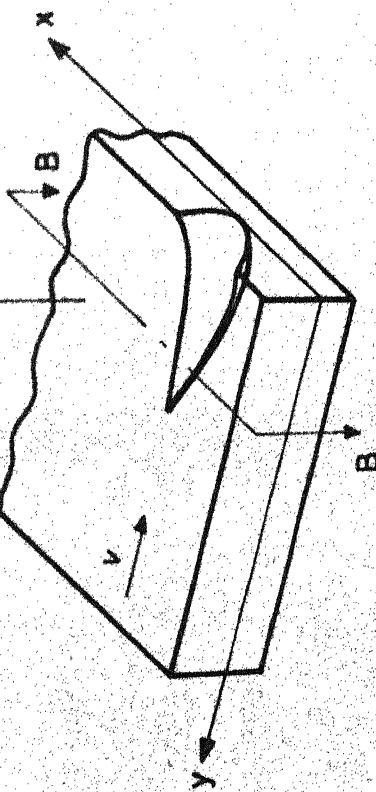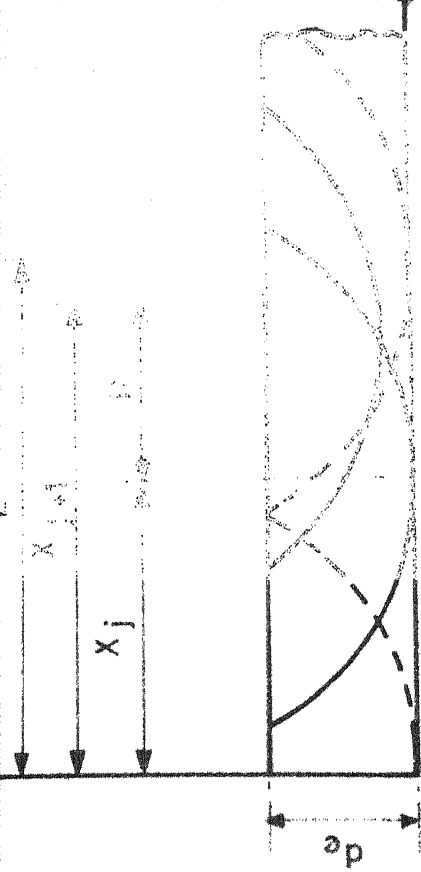
FIGURE 2.2: (a) SCHEMATIC VIEW OF THE WORK PIECE WITH CO-ORDINATE
SYSTEM (x,y,z);

(b) SECTIONAL VIEW BB OF THE WORK PIECE SHOWING MAXIMUM
WIDTH OF CUT L AND AXIAL PITCH p
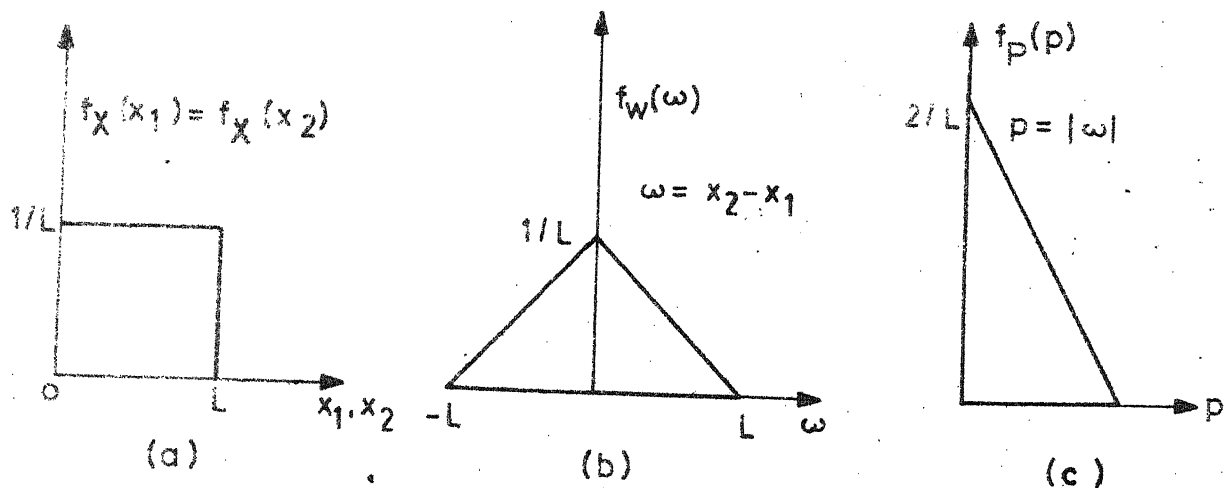
FIGURE 2.3 GRAPHICAL REPRESENTATION OF PROBABILITY DENSITY FUNCTION
OF RANDOM VARIABLE : (a) x; (b) w; (c) p
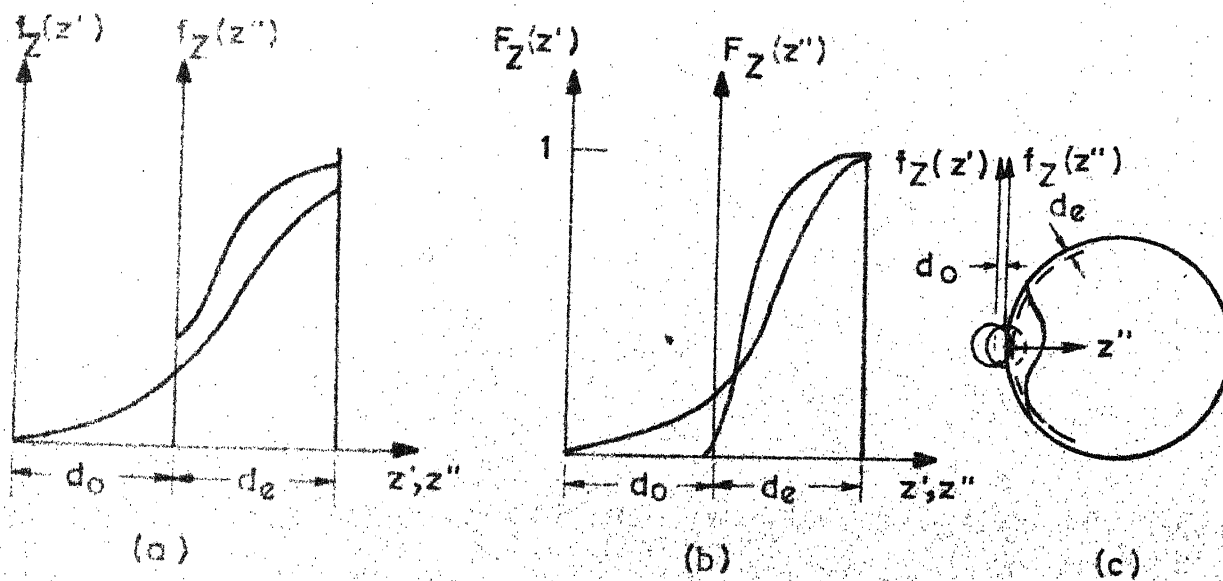
FIGURE 2.4 GRAPHICAL REPRESENTATION OF :
(a) PROBABILITY DENSITY FUNCTION OF z', z'';
(b) DISTRIBUTION FUNCTION OF z', z'';
(c) ENLARGED VIEW OF GRAIN DEFLECTION.
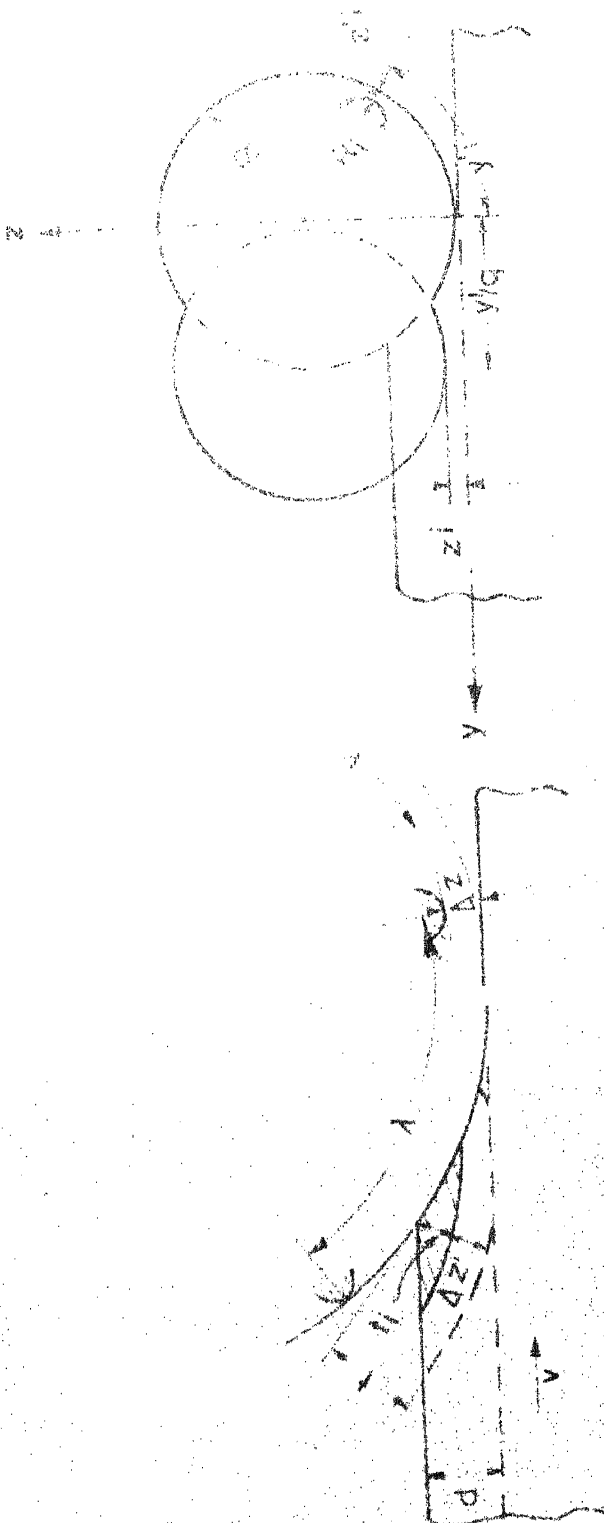
FIGURE 2.5 SCHEMATIC VIEW OF GRINDING SHOWING GRAIN DEPTH OF CUT

FIGURE 2.6 SCHEMATIC ARRANGEMENT SHOWING TRANSLATION OF GRAIN AND THE WORKPIECE
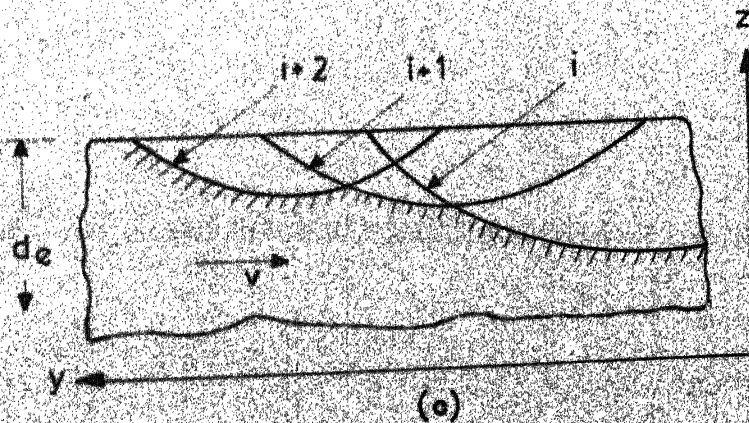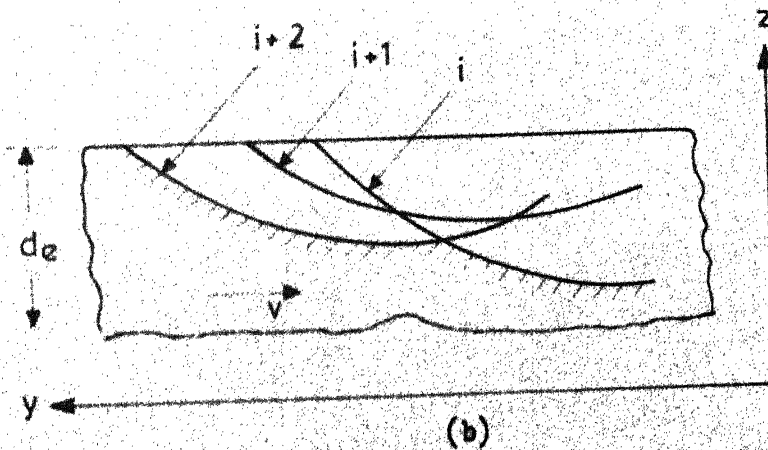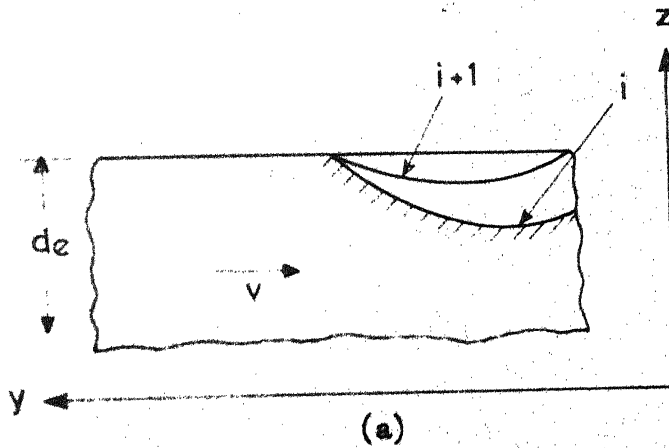
FIGURE 2.7   GENERATION OF LONGITUDINAL PROFILE :
(a) OVERLAPPING OF PRECEEDING AND SUCCEEDING GRAIN PATH;
(b) OVERLAPPING OF INTERMEDIATE GRAIN PATH;
(c) NO OVERLAPPING.
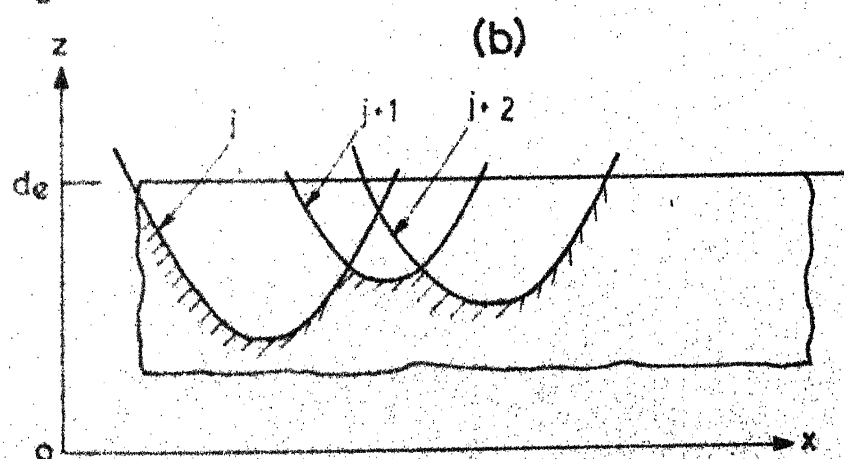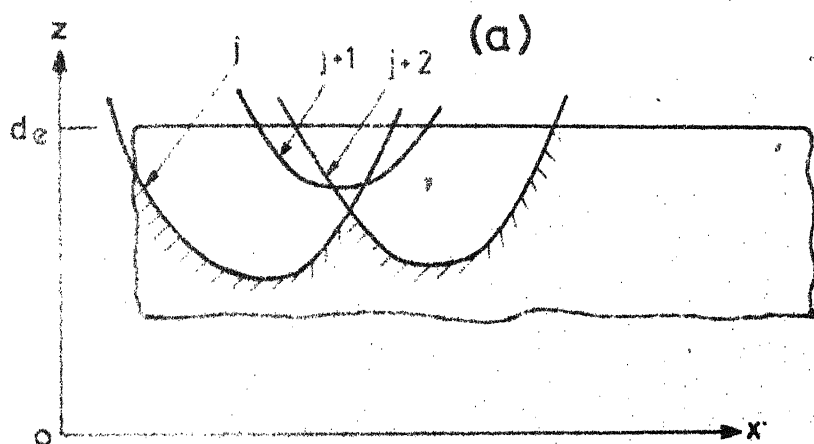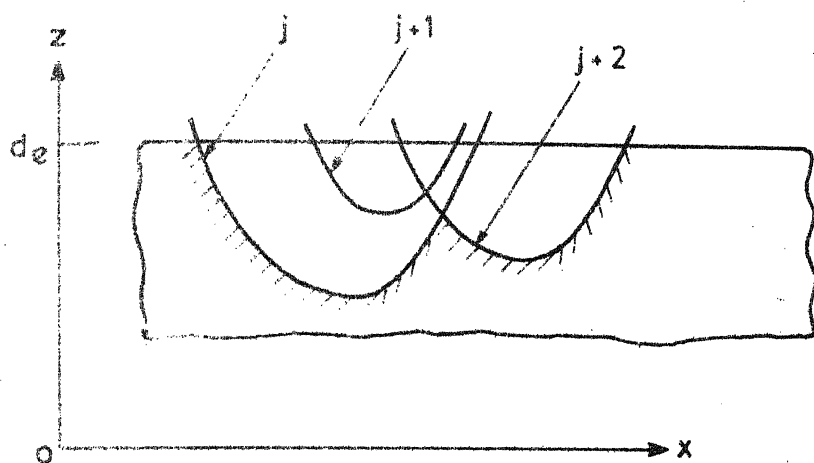
FIGURE 2.8   GENERATION OF TRANSVERSE PROFILE :

(a) OVERLAPPING OF PRECEEDING GROOVE BY
     SUCCEEDING GROOVE;

(b) OVERLAPPING OF INTERMEDIATE GROOVE;

(c) NO OVERLAPPING

CHAPTER III

REGRESSION AND SPECTRAL ANALYSIS

3.1 Introduction

In the previous chapter, it has been shown that the statistics of the surface profile can be theoretically determined by knowing the values of radial distribution parameter, k, and effective profile depth, d_e. Since these parameters are dependent on variables such as table speed, v and wheel depth of cut, d, the functional relationship can be obtained using the well established methods of Design of Experiment and Least Square Estimates.

Design of Experiment is a powerful tool for obtaining the functional estimate of the output parameters such as k and d_e which can be represented as a function of the input parameters such as v and d. The least square estimates of the output parameter can be evaluated at the minimum of the sum of squares of the difference of the power spectral density of the simulated and experimental profile. The workpiece profile is the sample realisation of the stochastic grinding process and its statistic is characterised by its spectral density or autocorrelation function. The effect of v and d on radial distribution parameter, k, and d_e can be estimated using analysis of variance. Applying regression analysis, they can be evaluated as a function of v and d.

3.2 Design of Experiment

3.2.1 Factorial Experiment

Design of Experiment is defined as the procedure for selecting the number of trials and relevant conditions essential and sufficient for solving the problem that has been set at the required precision. The output parameter, k, can be mathematically represented as

$$k = \emptyset (v, d) \qquad\qquad (3.1)$$

where $\emptyset$ is the response function and v and d are input parameters known as factors. Each factor can take several values, called levels, in any trial which can be obtained by treatment combination of factors. The selection of the experimental region of factor space is connected with a priori information. The variations of v and d in fine grinding are usually in the ranges of 5 to 15 m/min, and 4 to 12 μ (micron), respectively. The response surface of k or d_c is shown in Figure 3.1. The region of determination of the factors v and d can be estimated by taking a section of the response surface parallel to the plane (d o v) and projecting lines, thus obtained on to that plane (Figure 3.2). An experiment in which all the possible combinations of the factor levels are realised is called a factorial experiment. As the factors, in our study are two, we have a 2 x 2 factorial experiment.

3.2.2 Repetition of Trials

The running of repetitions of trials never gives coincident results since some experimental error (error of reproducibility) is always present. This error is estimated by repeating the trials. The variance of k in i'th trial, $s_{i'}^2$, (k) consisting of n_1 repeated observations is calculated using the formula

$$s_{i'}^2 (k) = \frac{1}{n_1 - 1} \sum_{u=1}^{n_1} (k_{iju} - \bar{k}_{ij})^2 \qquad (3.2)$$

for $i' = 1, \ldots, N_1$. Hence i' denotes the trial having treatment combination of ith level of one factor and jth level of other factor, N_1 is the total number of such trials, and $\bar{k}_{ij}$ is the mean value of k obtained in repeated trails given by

$$\bar{k}_{ij} = \frac{1}{n_1} \sum_{u=1}^{n_1} k_{iju} \qquad (3.3)$$

where k_{iju} is the value observed at uth observation for the i'th trial. The variance of reproducibility, $s_{rep}^2 (k)$ of the parameter, k, can now be obtained from

$$s_{rep}^2 (k) = \frac{1}{N_1 (n_1 - 1)} \sum_{i'=1}^{N_1} \sum_{u=1}^{n_1} (k_{iju} - \bar{k}_{ij})^2 \qquad (3.4)$$

for equality of the number of repetition at all the trials, otherwise, from

$$S^2_{rep}(k) = \sum_{i'=1}^{N_1} f_{i'} \, S^2_{i'}(k) \Big/ \sum_{i=1}^{N_1} f_{i'} \qquad (3.5)$$

where $f_{i'}$ is the number of degrees of freedom in i'th trial, i.e.,

$$f_{i'} = n_1 - 1 \qquad (3.6)$$

3.2.3 Homogeneity of Variance

One of the requirements of regression analysis is the homogeneity of variance which means that there are no variances among the ones being summated that considerably exceeds the remaining one. As $S^2_{rep}(k)$ and $S^2_{i'}(k)$ are of the same order, homogeneity of variance can be assumed [65]. When it is thought that the population variances are not equal but more or less randomly scattered, the test most often used is the Bartlett's test [65]. The test statistic

$$B = \frac{1}{c_2} \left[f \log S^2_{rep}(k) - \sum_{i'=1}^{N_1} f_{i'} \log S^2_{i'}(k) \right] \qquad (3.7)$$

when

$$c_2 = 0.4343 \left[1 + \frac{1}{3(N_1 - 1)} \left(\sum_{i'=1}^{N_1} \frac{1}{f_{i'}} - \frac{1}{\sum_{i'=1}^{N_1} f_{i'}} \right) \right] \qquad (3.8)$$

and
$$f = \sum_{i'=1}^{N_1} f_{i'}$$

c_2 approximately obeys a chi-square distribution with $(N_1 - 1)$ degrees of freedom. For ensuring homogeneity of variances, the value $\chi_{\alpha_c}^2$ $(N_1 - 1)$ obtained from statistical table with $(N_1 - 1)$ degrees of freedom for α_c % significance level, must be less than B.

3.2.4 Analysis of Variance

Through analysis of variance, relating to the sum of squares identity, several sources of variations can be isolated, estimated and tested. The least square estimates of k, for the randomised 2 x 2 factorial experiments have been given in Table 6.3. The values of d_e obtained from the experimental profile (Figure 3.3 a to d) are listed in Table 6.1. The analysis of variance table for k or d_e can be prepared with the following identities and their corresponding degrees of freedom [66].

The identities and degrees of freedom are

SSd = Sum of squares for factor, d
$$= \frac{1}{r_1 n_1} \sum_{i=1}^{c_1} T_{i..}^2 - \frac{T^2}{c_1 r_1 n_1} \tag{3.9}$$

SSI = Sum of squares for interaction
$$= SS\ Tr - SSd - SSv \tag{3.10}$$

SSv = Sum of squares for factor v

$$= \frac{1}{c_1 \, n_1} \sum_{j=1}^{r_1} T_{.j.}^2 - \frac{T^2}{c_1 \, r_1 \, n_1} \tag{3.11}$$

SSS = Within sum of squares

$$= SST - SS\,Tr \tag{3.12}$$

SST = Total sum of squares

$$= \sum_{i=1}^{c_1} \sum_{j=1}^{r_1} \sum_{u=1}^{n_1} k_{iju}^2 - \frac{T^2}{c_1 \, r_1 \, n_1} \tag{3.13}$$

$SS\,Tr$ = Treatments sum of squares

$$= \frac{1}{n_1} \sum_{i=1}^{c_1} \sum_{j=1}^{r_1} T_{ij.}^2 - \frac{T^2}{c_1 \, r_1 \, n_1} \tag{3.14}$$

f_d = Degrees of freedom for d

$$= c_1 - 1 \tag{3.15}$$

f_I = Degrees of freedom for interaction

$$= (c_1 - 1)(r_1 - 1) \tag{3.16}$$

f_S = Degrees of freedom for within

$$= c_1 \, r_1 \, (n_1 - 1) \tag{3.17}$$

f_T = Degrees of freedom for total

$$= c_1 \, r_1 \, n_1 - 1 \tag{3.18}$$

f_{Tr} = Degrees of freedom for treatment combination

$$= f_d + f_v + f_I \tag{3.19}$$

f_v = Degrees of freedom for v

$$= r_1 - 1 \tag{3.20}$$

In the above equations

$$T_{ij.} = \sum_{u=1}^{n_1} k_{iju} \qquad (3.21)$$

$$T_{i..} = \sum_{j=1}^{r_1} \sum_{u=1}^{n_1} k_{iju} \qquad (3.22)$$

$$T_{.j.} = \sum_{i=1}^{c_1} \sum_{u=1}^{n_1} k_{iju} \qquad (3.23)$$

and

$$T = \sum_{i=1}^{c_1} \sum_{j=1}^{r_1} \sum_{u=1}^{n_1} k_{iju} \qquad (3.24)$$

The values of the above identities for d_e and k are given in Tables 6.2 and 6.4, respectively. From Table 6.4, it can be seen that the computed F - ratio for d to "within" is larger than the value obtained from statistical table, for the upper 5% level of the value of F distribution with the f_d and f_S. The statistic F - ratio for d is given by

$$\text{F - ratio} = \frac{SSd}{f_d} \Big/ \frac{SSS}{f_S} \qquad (3.25)$$

Thus, it can be concluded that the effect of depth of cut on the radial distribution parameter, k, is non-zero. Similarly, the effect of table speed on k can be obtained and which is also found to be non-zero, but the effect of interaction of d and v on k is negligibly small as the computed F ratio is very much less than the value obtained from statistical table. Proceeding in the same

manner, the sum of square identities can be obtained and hence the analysis of variance table for d_e (Table 6.2) can be prepared. It can be seen that all the computed values of F-ratio are much smaller than the theoretical values obtained from the statistical table. The effect of d, v, and their interaction on the effective profile depth, d_e, can therefore be assumed to be negligible and hence d_e can be taken as the mean of all the values obtained experimentally.

3.2.5 Least Square Estimation of k.

The least square estimates of k can be obtained from the factorial experiment at the minimum sum of squares, SSk, by giving iterative values of k [62] from the following equations

$$SSk = Min \sum_{k_1=0}^{m_1-1} (\hat{G}(fq, \xi) - \hat{G}(fq, \xi, k))^2 \quad (3.26)$$

at different frequency, fq, equal to $\dfrac{k_1 \, fc}{m_1}$ where it is assumed that

$$\hat{G}(fq, \xi) = \hat{G}(fq, \xi, k) + \mathcal{E}(fq) \quad (3.27)$$

In the above equations, $\mathcal{E}(fq)$ is uncorrelated error at frequency, fq, ξ represents kinematic and operating parameters (v, d and Sg), $\hat{G}(fq, \xi)$ is the smoothed spectral density of the actual profile at the frequency, fq, for grinding condition, ξ, $\hat{G}(fq, \xi, k)$ is the

smoothed spectral estimates of the theoretical profile

simulated at the grinding condition, $\bar{\xi}$, assuming some

known values of k and the number of spectral estimates

over a frequency range of 0 to cut-off frequency, fc,

is taken equal to m_1, the maximum lag number.

3.3 Spectral Analyses

3.3.1 Power Spectral Density

A single time or space history representing a
random phenomenon is called a sample function (or a sample
record when observed over a finite time or space interval).
The collection of all possible sample functions which the
random phenomenon might have produced is called a random
process or stochastic process. Hence a sample record of
data may be thought of as one physical realisation of a
random process. The workpiece profile produced by the
grinding wheel is a sample realisation of the random grind-
ing process. Power spectral density function measurements
of physical data establish the frequency composition of
the data which, in turn, bears important relationship to
the basic characteristics of the physical system involved.
The mean square value of a sample time (or space) history
record in a frequency range between fq and fq + Δfq may
be obtained by filtering the sample record, z (1), with
a band pass filter having sharp cut-off characteristics,

and computing the average of the squared output from the
filter. This average squared value will approach an
exact mean square value as the observation time, T', or
length, L, approaches infinity [67]. Mathematically,
this can be expressed as

$$\psi^2_z \left[fq, \ fq + \triangle fq \right] = \lim_{L \to \infty} \frac{1}{L} \int_0^L z^2 \ (l, \ fq, \ \triangle fq) \ dl$$

$$(3.28)$$

where $z \ (l, \ fq, \ \angle fq)$ is the portion of $z \ (l)$ in the
frequency range fq and $fq + \triangle fq$ and $\psi^2_z \left[fq, \ fq + \triangle fq \right]$
is the mean square value of the power spectral density
from fq to $fq + \triangle fq$.

For small $\triangle fq$, a power spectral density,
$G_z \ (fq)$, can be defined such that

$$\psi^2_z \left[fq, \ fq + \triangle fq \right] \approx G_z \ (fq) \triangle fq \qquad (3.29)$$

Therefore,

$$G_z \ (fq) = \lim_{\triangle fq \to 0} \frac{\psi^2_z \left[fq, \ fq + \triangle fq \right]}{\triangle fq}$$

$$= \lim_{\triangle fq \to 0} \lim_{L \to \infty} \frac{1}{(\triangle fq) \ L} \int_0^L z^2 \ (l, \ fq, \triangle fq) dl$$

$$(3.30)$$

For stationary process, the power spectral den-
sity is related to the autocorrelation function, $R_z \ (\tau)$,
of the process by a Fourier transformation as follows

$$G_z(fq) = 2 \int_{-\infty}^{\infty} R_z(\tau) e^{-j 2\pi fq \tau} d\tau$$

$$= 4 \int_{0}^{\infty} R_z(\tau) \cos 2\pi fq \tau \, d\tau \qquad (3.31)$$

$G_z(fq)$ is always a real valued, non-negative function as $R_z(\tau)$ is real and even function.

3.3.2 Autocorrelation Function

The autocorrelation function for random data describes the general dependence of the values of the data at one point on the values at other point. An estimate for the autocorrelation of z (1) at any length 1 and $1 + \tau$ may be obtained by taking the product of the two values and averaging over the observation length L. The resulting average product will approach an exact auto-correlation product as L approaches infinity. The auto-correlation function, defined as $R_z(\tau)$, is given by

$$R_z(\tau) = \lim_{L \to \infty} \frac{1}{L} \int_{0}^{L} z(1) z(1 + \tau) \, d1 \qquad (3.32)$$

$R_z(\tau)$ is always a real valued even function with maximum at $\tau = 0$ and may be either negative or positive, i.e.,

$$R_z(\tau) = R_z(-\tau) \qquad (3.33)$$

and

$$R_z(0) \geq |R_z(\tau)| \qquad (3.34)$$

for all τ.

The mean value of the process, μ_z, can be expressed in terms of autocorrelation functions as

$$\mu_z = \sqrt{R_z(\infty)} \qquad (3.35)$$

Similarly, the mean square value, ψ^2, can be given by

$$\psi^2 = R_z(0) \qquad (3.36)$$

i.e., mean square value is equal to autocorrelation at zero displacement lag.

3.4 Multiple Linear Regression Analysis

If the criteria for homogeneity of variances at different observation in any trial is satisfied and the levels of the factors are non-random and uncorrelated, the multiple linear regression analysis can be applied to estimate the regression coefficient. In this analysis, the random response of k is assumed to be linearly dependent on d, and v because the effect of the factor d and v are different from zero as discussed under analysis of variances (Table 6.4). It is further assumed that each observation, k_i, in any trial, is randomly drawn from a normal population with mean, η_i, where η_i denotes the true regression of k_i on d and v and given by

$$\eta_i = \alpha_1 + \beta_1 d_i + \beta_2 v_i \qquad (3.37)$$

for i = 1, ..., N_2 and variance σ^2. α_1, β_1, β_2 are

variable parameters, d_i and v_i are wheel depth of cut and table speed, respectively for ith observation and N_2 is the total number of observations. Estimators a_1, b_1 and b_2 of α_1, β_1, and β_2 are found so as to minimise the square identity, Q, given by

$$Q = \sum_{i=1}^{N_2} (k_i - a_1 - b_1 d_i - b_2 v_i)^2 \qquad (3.38)$$

Setting the partial derivatives of Q with respect to a_1, b_1, and b_2 equal to zero, we get the normal equations

$$N_2 a_1 + (\sum_{i=1}^{N_2} d_i) b_1 + (\sum_{i=1}^{N_2} v_i) b_2 = \sum_{i=1}^{N_2} k_i \qquad (3.39)$$

$$(\sum_{i=1}^{N_2} d_i) a_1 + (\sum_{i=1}^{N_2} d_i^2) b_1 + (\sum_{i=1}^{N_2} d_i v_i) b_2 = \sum_{i=1}^{N_2} d_i k_i \qquad (3.40)$$

$$(\sum_{i=1}^{N_2} v_i) a_1 + (\sum_{i=1}^{N_2} d_i v_i) b_1 + (\sum_{i=1}^{N_2} v_i^2) b_2 = \sum_{i=1}^{N_2} v_i k_i \qquad (3.41)$$

The solution of the above equations gives the unbiased estimators of the parameter α_1, β_1 and β_2. The estimated regression, $\widehat{k_i}$ of k_i on d_i and v_i will be

$$\widehat{k_i} = a_1 + b_1 d_i + b_2 v_i \qquad (3.42)$$

The unbiased estimators of σ^2 can be shown to be

$$s^2_{k/d,v} = \frac{1}{N_2 - 3} \sum_{i=1}^{N_2} (k_i - \widehat{k})^2 \qquad (3.43)$$

where,

$$\hat{k} = \frac{1}{N_2} \sum_{i=1}^{N_2} \hat{k_i} \qquad (3.44)$$

Using

$$\bar{d} = \frac{1}{N_2} \sum_{i=1}^{N_2} d_i, \qquad (3.45 \text{ a})$$

$$\bar{v} = \frac{1}{N_2} \sum_{i=1}^{N_2} v_i, \qquad (3.45 \text{ b})$$

and

$$\bar{k} = \frac{1}{N_2} \sum_{i=1}^{N_2} k_i, \qquad (3.45 \text{ c})$$

the normal equations (3.39), (3.40) and (3.41) can be further simplified to the form

$$a_{11} b_1 + a_{12} b_2 = g_1, \qquad (3.46)$$

$$a_{21} b_1 + a_{22} b_2 = g_2, \qquad (3.47)$$

and

$$a_1 = \bar{k} - \bar{d} b_1 - \bar{v} b_2 \qquad (3.48)$$

where

$$a_{11} = \sum_{i=1}^{N_2} (d_i - \bar{d})^2, \qquad (3.49)$$

$$a_{22} = \sum_{i=1}^{N_2} (v_i - \bar{v})^2, \qquad (3.50)$$

$$a_{12} = a_{21} = \sum_{i=1}^{N_2} (d_i - \bar{d})(v_i - \bar{v}), \qquad (3.51)$$

$$g_1 = \sum_{i=1}^{N_2} (d_i - \bar{d})(k_i - \bar{k}) \qquad (3.52)$$

and

$$g_2 = \sum_{i=1}^{N_2} (v_i - \bar{v})(k_i - \bar{k}) \qquad (3.53)$$

Solving the equations (3.46), (3.47) and (3.48), the values of a_1, b_1 and b_2 can be obtained and the regression of k_i and d_i and v_i can be obtained from equation (3.42) after substituting the values of a_1, b_1 and b_2.

The unbiased estimator of σ^2 in equation (3.43) can be simplified as

$$S^2_{k/d,v} = \frac{SSk - \sum_{i=1}^{2} g_i b_i}{N_2 - 3} \qquad (3.54)$$

where,

$$SSk = \sum_{j=1}^{N_2} k_j^2 - \frac{(\sum k_j)^2}{N_2} \qquad (3.55)$$

Since k_i's are independent, the variance of b_i, $\sigma^2_{b_i}$, can be expressed as

$$\sigma^2_{b_i} = c_{ii}\, \sigma^2 \qquad (3.56)$$

where c_{ii} can be obtained from the matrix $[c_{ij}]$ which is the inverse of the coefficient matrix a_{ij}, obtained from equations (3.46) and (3.47). Using the unbiased estimator of σ^2 given by equations (3.55) and (3.56), it can be shown that the statistic ($\dfrac{b_i - \beta_i}{S^2_{k/d,v}\sqrt{c_{ii}}}$) has student-t distribution with ($N_2 - 3$) degrees of freedom. The statistic can be used to test any hypothesis of the form

β_i = constant. The $(100 - \alpha_c)$ percent symmetric confidence interval of β_i is given by

$$\left[b_i - t_{\alpha_c/2} \, (N_2 - 3) \, s^2_{k/d,v} \sqrt{c_{ii}} \right] < \beta_i$$

$$< \left[b_i + t_{\alpha_c/2} \, (N_2 - 3) \, s^2_{k/d,v} \sqrt{c_{ii}} \right] \qquad (3.57)$$

for $i = 1, 2$, where α_c can be obtained from the confidence interval. From equation (3.57), 95% confidence interval for β_1 and β_2 can be obtained.
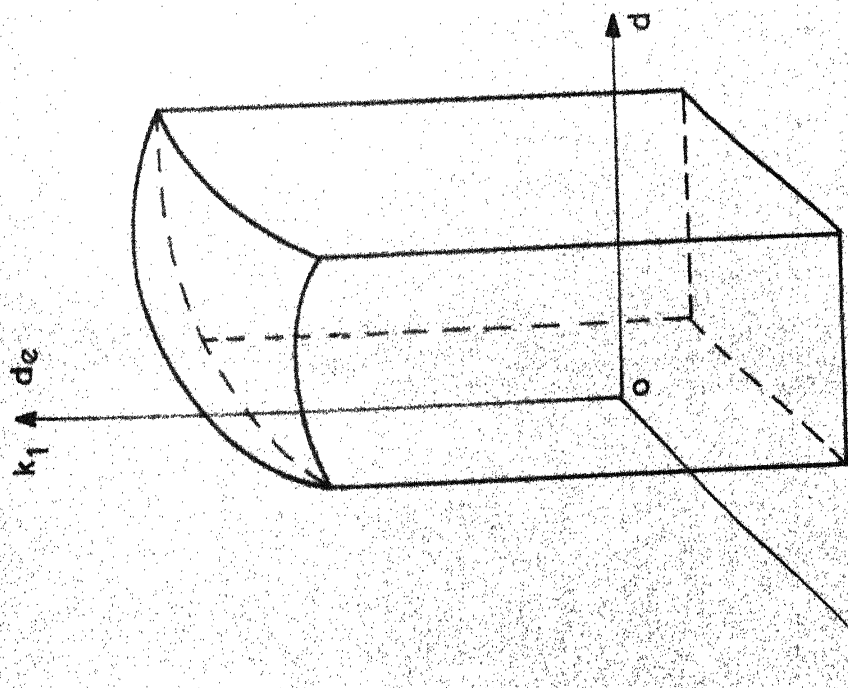
FIG. 3.2

FIG. 3.1

FIGURE 3.1 RESPONSE SURFACE OF k OR d_e WITH DEPTH OF CUT, d, AND FEED SPEED, v.
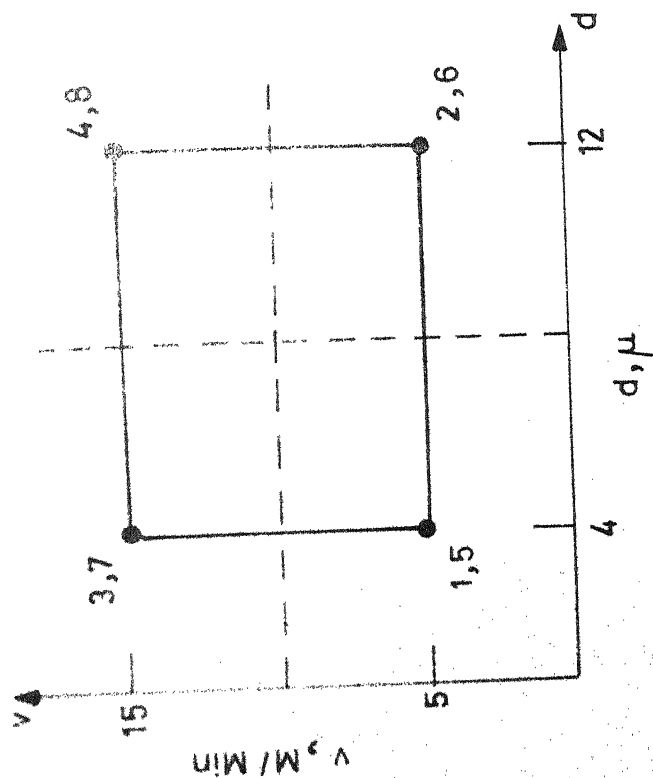
FIGURE 3.2 REGION OF DETERMINATION OF FACTOR AND TRIAL NUMBERS
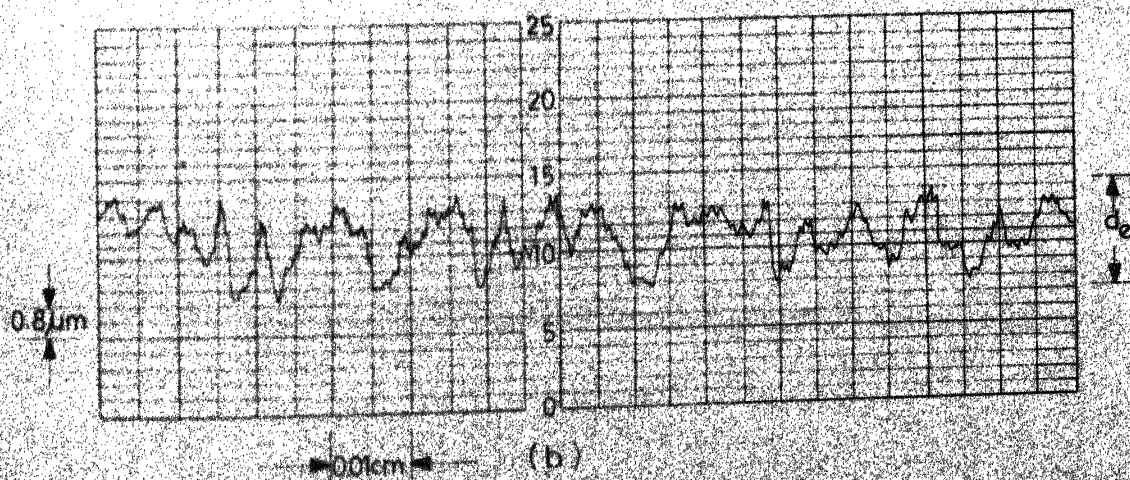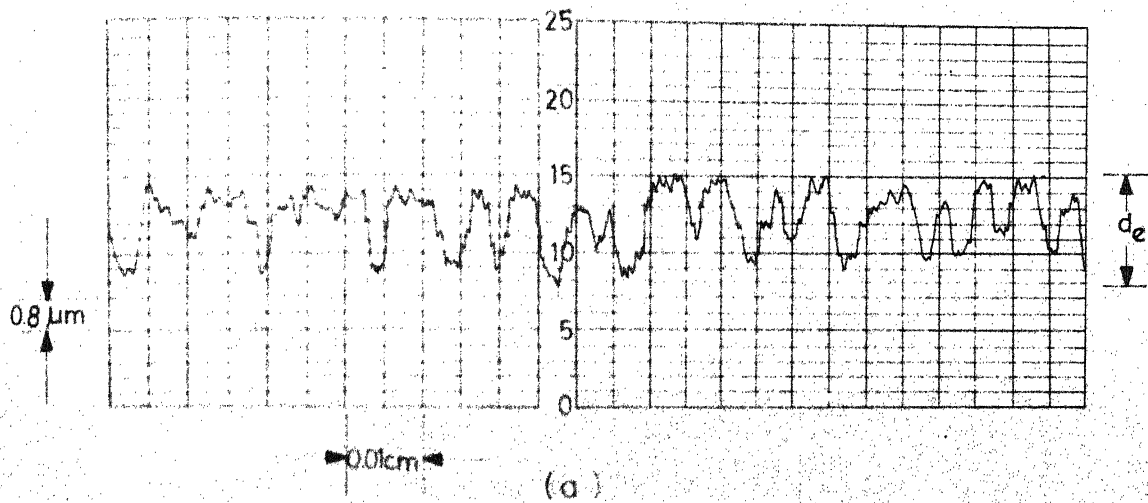
FIGURE 3.3 TALYSURF TRACES OF EXPERIMENTAL PROFILE FOR THE
GRINDING CONDITION :
(a) v: 3 m/min, d: 4 MICRON, WHEEL SPEED: 1500 rpm.
(b) v: 5 m/min, d:12 MICRON, WHEEL SPEED: 1500 rpm.
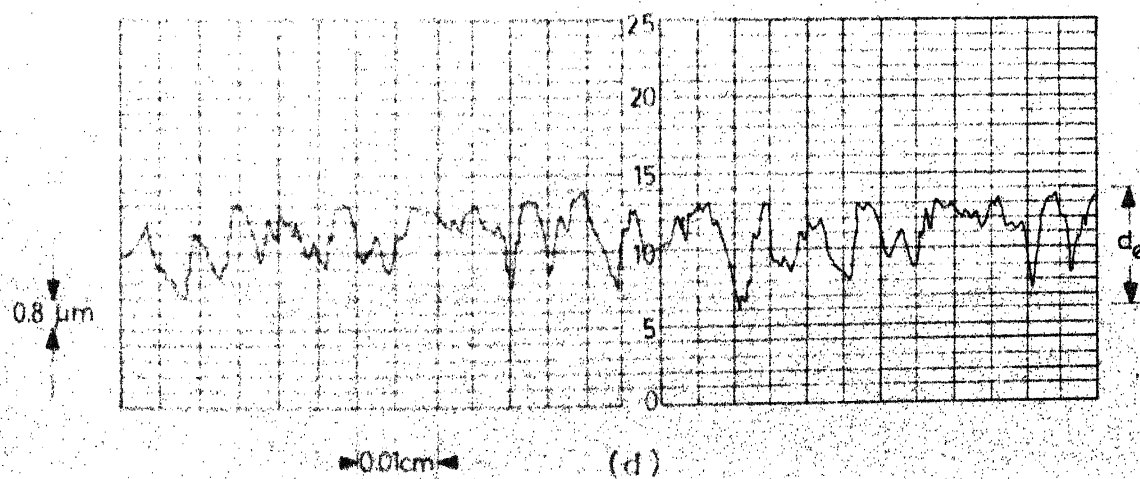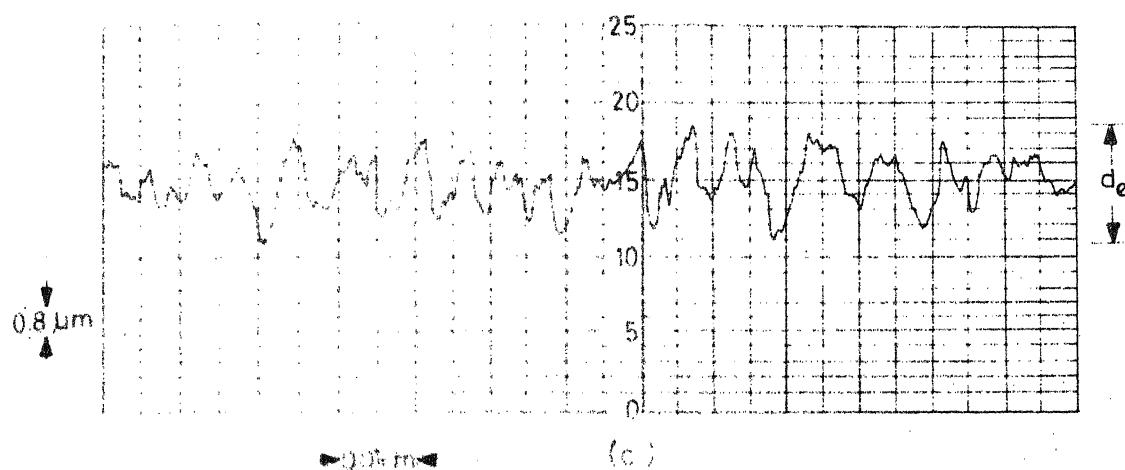
(c) v: 15 m/min, d: 4 MICRON, WHEEL SPEED: 1500 rpm.
(1) v: 15 m/min, d:12 MICRON, WHEEL SPEED: 1500 rpm.

NUMERICAL SOLUTION TECHNIQUE

4.1 Introduction

The processing of random data such as the surface height of workpiece profile requires digital technique. Discrete representation of continuous data involve problems of digitization, replacement of integrals with sum and relating record lengths and frequency band widths to corresponding digital parameter. All these techniques must ensure the least loss of information. The experimental surface profile is a continuous record which needs sampling and digital processing.

In order to compare the experimental results with the theoretical part, simulated profile must be generated from the known probability densities and statistical parameters by numerical techniques.

4.2 Digitization of Continuous Data

The process of digitizing consists of converting continuous data into discrete numbers. These involve two main parts, one is sampling and the other is quantization. The sampling is defined as selection of the points at which the data are observed. If the sampled values are seperated too far apart, sampled values would represent either too

low or too high frequencies in the original data. This
property is called aliasing [67] . If the space interval
is $\triangle 1$ between samples, then the sampling rate is $\frac{1}{\triangle 1}$
samples per interval. The useful data will be from 0 to
$\frac{1}{2 \triangle 1}$ cycles/interval (c/interval), since the frequency
in the data which are higher than $\frac{1}{2 \triangle 1}$ c/interval will be
folded into the lower frequency range from 0 to $\frac{1}{2 \triangle 1}$ and
confused with data in lower frequency range. The cut-off
frequency

$$fc = \frac{1}{2 \triangle 1} \tag{4.1}$$

is known as Nyquist frequency [67]. One of the practical
methods is to select fc to be few times greater than the
maximum frequency of interest.which can be determined from
the continuous record of the data. This process will lead
to choose $\triangle 1$ small. If $\triangle 1$ is too small, then samp-
ling will yield correlated and highly redundant data. For
proper quantization, it has been shown [67] that the sample
points should be greater than 256. Our values of sample
points satisfy this criterion.

4.3 Autocorrelation Functions and Power Spectral Density

4.3.1 Autocorrelation Functions

The autocorrelation function can be obtained
through the numerical calculation in Steps 1 to 6.

Step 1: Digitization of data and selection of sample size.

Let $z(l_{n'})$ be the values of any sample record $z(l)$ at discrete points

$$l_{n'} = l_0 + n' \Delta l \tag{4.2}$$

then $z(l_{n'})$ will be

$$z(l_{n'}) = z(l_0 + n' \Delta l) \tag{4.3}$$

for $n' = 1, \ldots, N_S$, where N_S is the sample size such that

$$N_S = \frac{l_r}{\Delta l} \tag{4.4}$$

and l_r is the minimum record length.

Step 2: Choice of correlation lag values.

As a thumb rule, the maximum number of correlation lag, n_l, is taken to be less than one-tenth of the sample size, N_S. Therefore the maximum displacement

$$\tau_{max} = n_l \Delta l \tag{4.5}$$

Step 3: Calculation of the mean value.

The sample mean, $\bar{z}$, is estimated from

$$\bar{z} = \frac{1}{N_S} \sum_{n'=1}^{N_S} z(l_{n'}) \tag{4.6}$$

Step 4: Transformation of data to zero mean value.

Define a new stress history record u (l) where

$$u (l) = z (l) - \bar{z} \tag{4.7}$$

u (l) will have sample values u $(l_{n'})$ given by

$$u (l_{n'}) = u (l_0 + n' \triangle l)$$

$$= z (l_{n'}) - \bar{z} \tag{4.8}$$

Step 5: Calculation of the mean square value.

The sample mean square is given by

$$\bar{u^2} = \frac{1}{N_S} \sum_{n'=1}^{N_S} u (l_{n'})^2 \tag{4.9}$$

The quantity $\bar{u^2}$ is a biased estimator of the true mean square value $\sqrt{\bar{u^2}}$. The sample standard deviation σ_u, is given by

$$\sigma_u = \left[\frac{1}{N_S - 1} \sum_{n=1}^{N_S} u (l_n)^2 \right]^{1/2} \tag{4.10}$$

Step 6. Calculation of autocorrelation function.

For N_S data values u $(l_{n'})$, n' = 1, ..., N_S from the transformed record, u (l), which is stationary with mean, $\bar{u} = 0$, the autocorrelation function is estimated by the formula

$$R_r = R_u (r \triangle l) = \frac{1}{N_S - r} \sum_{n'=1}^{N_S - r} u (l_{n'}) u (l_{n'+r}) \tag{4.11}$$

for r = 0, 1, ..., m_1.

4.3.2 Power Spectral Density

For a stationary random process, the power spectral density being the Fourier transform of the autocorrelation function of the sample record, the raw estimate, $\widetilde{G}_z(fq)$, of a true spectral density, $G_z(fq)$, can be obtained from the digital values of autocorrelation function for an arbitrary frequency fq in the range $0 \leqslant fq \leqslant fc$ [67] from

$$\widetilde{G}_z(fq) = 2 \Delta 1 \left[\widehat{R}_o + 2 \sum_{r=1}^{m_1-1} \widehat{R}_r \cos\left(\frac{\pi r \, fq}{fc}\right) \right.$$

$$\left. + \widehat{R}_{m_1} \cos\left(\frac{\pi m_1 \, fq}{fc}\right) \right] \tag{4.12}$$

The values of the function $\widetilde{G}_z(fq)$ need to be calculated only at the $m_1 + 1$ spatial discrete frequencies where

$$fq = \frac{k_1 \, fc}{m_1} \tag{4.13}$$

for $k_1 = 0, 1, 2, \ldots, m_1$. The spectral estimates at points less than $\frac{2 \, fc}{m_1}$ apart will be correlated.

Step 7 : Raw estimate of power spectral density at harmonic k_1.

The raw estimate of the power spectral density function, $\widetilde{G}_{k_1}$, at harmonic, k_1, corresponding to frequency $fq = \frac{k_1 \, fc}{m_1}$ can be obtained from [67]

$$\cdots \quad \cdots \quad \left(\frac{k_1 \; \hat{c}}{m_1}\right)$$

$$\cdots \cdots \Delta 1 \left[\hat{R}_0 + 2 \sum_{r=1}^{m_1-1} \hat{R}_r \cos\left(\frac{\pi \, r \, k_1}{m_1}\right) + (-1)^{k_1} \hat{R}_{m_1} \right] \qquad (4.14)$$

<u>Step</u>. ..... of raw estimate of power spectral density.

It is recommended to check the previous calculations for the relation given by [67]

$$\hat{R}_{..} (\cdot\cdot) = \frac{1}{2 \, \Delta 1 \; m_1} \left[\frac{1}{2}\hat{C}_0 + \sum_{k_1=1}^{m_1-1} \hat{G}_{k_1} + \frac{1}{2}\hat{G}_{m_1} \right]$$
$$(4.15)$$

<u>Step</u> 2: Prewhitening of input data.

The process of prewhitening, sometimes recommended in spectral analysis, amounts to applying a special filter (digital recursive) to the data which will result in the following data having a flat spectrum. This process can be achieved by the following moving linear combinations

$$u \; (n'') = (z \; (1_{n'+1}) - \bar{z}) - c_4 \; (z \; (1_{n'}) - \bar{z})$$
$$(4.16)$$

for $n'' = 1, \ldots, (n' - 1)$, where c_4 is a constant to be supplied and its value is

$$|c_4| < 1.0. \qquad (4.17)$$

77

While applying the prewhitening process (4.17), Step 9 is to be calculated along with Step 3 and all the numerical Steps from 5 to 8 with u (n") in place of u (1_n,)

<u>Step 10</u>:   Smoothing of the raw estimate of power spectral density.

Smoothing of the raw estimate of power spectral density can be done by Hamming [68]. The smoothed power spectral density $\widehat{G}_{k_1}$ will be given by the following equations:

$$\widehat{G}_0 = 0.54\,\widetilde{G}_0 + 0.46\,\widetilde{G}_1, \tag{4.18}$$

$$\widehat{G}_{k_1} = 0.23\,\widetilde{G}_{k_1-1} + 0.54\,\widetilde{G}_{k_1} + 0.23\,\widetilde{G}_{k_1+1} \tag{4.19}$$

for $0 < k_1 < m_1$, and

$$\widehat{G}_{m_1} = 0.54\,\widetilde{G}_{m_1} + 0.46\,\widetilde{G}_{m_1-1}. \tag{4.20}$$

The variability of the estimates of the true spectral density does not decrease with increased record length. This characteristic can be achieved by smoothing.

<u>Step 11</u>:   Compensating or recolouring of the smoothed spectrum (if prewhitening is applied).

The smoothed power spectrum, if prewhitening is applied, is compensated as

$$\widehat{G}(k_1) = \widehat{G}_{k_1} / (1 + c_4^2 - 2\,c_4 \cos(\frac{\pi k_1}{m_1})) \tag{4.21}$$

for $k_1 = 0, 1, \ldots, m_1$.

4.4 Longitudinal and Transverse Surface Profile

Once two values of k are estimated at different grinding conditions, the longitudinal and transverse surface profiles can be generated theoretically through the numerical simulation of the following steps.

Step 1: Generation of three sets of random numbers uniformly distributed between 0 and 1.

Uniformly distributed random numbers lying between 0 and 1 can be generated by pseudo-random number generation method or with the help of built-in-subroutine programmes RANDY1(X), RANDY2(X), RANDY3(X), available in IBM 7044 Computer.

Step 2: Calculation of L, N_c, M, $\bar{\lambda}$, $\bar{\lambda}_t$, and k

For any speed ratio, q, grinding condition, ξ, effective profile depth, d_c, obtained from experimental profiles, and simulated grinding width, $\mathcal{X}$, of grinding wheel of diameter D, having grain size, Sg, nominal grain density, C, the value of L, N_c, M, $\bar{\lambda}$, $\bar{\lambda}_t$, and k are calculated from the equations (2.12), (2.20), (2.21), (2.32) and (3.42) respectively.

Step 3: Generation of random positions of lowest grain tips in any groove along cutting direction.

Using the equations (2.34), (2.35), (2.36) and the random numbers generated in Step 1, the random positions of lowest grain tips in any groove along cutting direction are generated.

Step 4: Determination of longitudinal surface profile
height at different columns.

The successive positions of grain tips at any
sample point $l_{n'}$ in any jth column is calculated from
the equation

$$z_j^i (l_{n'}) = z_j^i + \frac{(l_{n'} - y_j^i)^2}{2 (R - z_j^i)} \qquad (4.22)$$

where, $l_{n'}$ is given by equation (4.2), and $\triangle l$ is equal
to workpiece traversed in one pass divided by sample size
N_s. The surface profile height at the sample point
$z_j (l_{n'})$ will be the minimum of d_o and all the values of
$z_j^i (l_{n'})$ obtained for $i = 1, \ldots, M$. This is continued
for all sample points for $n' = 1, \ldots, N_s$ and for all the
columns, $j = 1, \ldots, N_c$. Therefore the longitudinal pro-
file height at different columns can be obtained.

Step 5: Generation of transverse profile at any section BB
along transverse direction at a distance y_o.

Longitudinal profile heights at all the columns
at a distance y_o is calculated from Step 4 substituting
$l_{n'}$ equal to y_o. The z coordinates of any groove with its
midpoint at $z_j (y_o)$ at the sample point $l_{n''}$ is obtained
from the equation

$$z_j (l_{n''}) = z_j (y_o) + \frac{(l_{n''} - x_j)^2}{g} \qquad (4.23)$$

where,

$$l_{n''} = l_{o''} + n'' \triangle l'' \qquad (4.24)$$

and l'' is the increment equal to the simulated width α, of the grinding wheel divided by sample size, N_s, $l_{o''}$ is an arbitrary initial value. The transverse profile height at the sample point, $z (l_{n''})$, will be the minimum of d_e and all the values of $z_j (l_{n''})$ obtained for $j = 1$, ..., N_c. This iscontinued for all the sample points $n'' = 1$, ..., N_s and thus the transverse profile height can be obtained.

Step 6 : Calculation of average number of active grains responsible for surface generation.

After the Step 3, the coordinates of B (i, j) in any i'th column is obtained from equations (2.37) and (2.38) for $i = 1$, and $j = i + 1$, to M. If the minimum of all the values $z (i, j)$ is $z (1, k)$, then the count of the number of grains responsible for surface generation upto $y (1, k)$ is 2. Changing $i = k$, and $j = i + 1$, ..., M, the above procedure is continued and total count of the number of grains responsible for longitudinal surface generation, $N_3 (i')$, in i'th column can be obtained. Following the same procedure for $i' = 1$, ..., N_c, the average value

of the number of active grains responsible for surface
generation in any column can be obtained from the equation

$$\overline{N}_3 = \frac{1}{N_c} \sum_{i'=1}^{N_c} N_3 (i'). \tag{4.25}$$

The longitudinal profile heights along different
groove mid-positions at a distance $y_{n'}$ are obtained after
executing the Step 4 replacing $l_{n'}$ by $y_{n'}$. For this trans-
verse section lying at a distance $y_{n'}$, the intersection of
ith groove with jth groove is obtained using equations
(2.42) and (2.43). This process is repeated for $i = 1$ and
$j = i + 1$ to N_c. If the minimum of these values of $z_{1,j}$ is
$z_{1,m}$, then the count of the number of grooves responsible
for transverse surface generation is 2. Changing $i = m$
and $j = m + 1$ to N_c and repeating the above process, the
number of columns responsible for transverse surface gene-
ration, $N_4 (y_{n'})$ will be the cumulative sum of all the
previous counts. Taking more number of sections, the
average value of the active number of columns will be

$$\overline{N}_4 = \frac{1}{N_5} \sum_{n'=1}^{N_5} N_4 (y_{n'}) \tag{4.26}$$

where, N_5 is the number of transverse sections.

Therefore the average value of the number of
active grain density responsible for surface generation
will be

$$C_1 = \frac{\overline{N}_3 \, \overline{N}_4}{\pi \, D \alpha} \qquad\qquad (4.27)$$

Flow Chart

The computer flow charts for the above steps are shown in Figures 4.1 and 4.2.

COMPUTER FLOW CHART

START

READ INPUT DATA
D, d, v, V, S_9, d_e
α, Y_o, N_c, M, N_5

IS K KNOWN

YES

NO

ASSUME
INITIAL
VALUE, δ_i

2

7

UNIFORM RANDOM
NUMBER GENERATOR

COMPUTE AXIAL
POSITIONS OF
ALL COLUMNS

3

COMPUTE LOWEST
POSITION OF ALL
M GRAIN TIPS IN
jTH COLUMN

4

COMPUTE HEI-
GHT OF ALL
GROOVES AT
sample pOINT
l_n''

COMPUTE TRANSFORMED
HEIGHT OF M GRAIN TIPS
IN jTH COLUMN AT Y_o

COMPUTE TRANS-
VERSE PROFILE
HEIGHT AT l_n''

COMPUTE SURFACE
PROFILE HEIGHT IN
jTH COLUMN AT Y_o

$j = j + 1$

YES

$j > N_c$

NO

$n'' > N_s$

IS K ESTIMATED VALUE

YES

NO

5

COMPUTE CLA,
RMS VALUES

6

continued......

⑦

DIGITIZE THE
CONTINUOUS RECORD OF
EXPERIMENTAL PROFILE

TRANSFORM DATA TO
ZERO MEAN VALUE

PREWHITEN THE DATA

COMPUTE AUTOCO-
RRELATION FUNCTION
AT LAG NUMBERS
$v = 0, 1, \ldots, m_1$

COMPUTE RAW POWER
SPECTRAL DENSITY
AT HARMONIC NUMBERS
$k_1 = 0, 1, \ldots, m_1$

COMPUTE SMOOTH
POWER SPECTRAL DSTY.

PRINT POWER SPECT-
RAL DENSITY

⑥

TRANSFORM DISCRETE
PROFILE HEIGHT TO
ZERO MEAN VALUE

PREWHITEN THE DATA

COMPUTE AUTOCORRELATION
FUNCTION AT LAG NUMBER
$r = 0, 1, \ldots, m_1$

COMPUTE RAW POWER
SPECTRAL DENSITY AT
HARMONIC NUMBERS
$k_1 = 0, 1, \ldots, m_1$

COMPUTE SMOOTH POWER
SPECTRAL DENSITY

IS K ESTIMATED VALUE   YES

NO

COMPUTE SUM OF THE
SQUARE OF DIFFERENCE OF
THEORETICAL AND EXPERI-
MENTAL PROFILES AT
DISCRETED FREQUENCIES
$k_1 = 0, 1, \ldots, m_1 - 1$

PRINT CLA,
RMS, POWER
SPECTRAL
DENSITY

STOP

PRINT SQUARE ERROR, K

⑧

FIGURE 4.1 ESTIMATION OF K ASSOCIATED WITH
TRANSVERSE SURFACE GENERATION
$(\delta_1 \leqslant k \leqslant \delta_2)$

START

READ INPUT DATA
$D, d, v, V, \alpha,$
d_e, N_s, Y_0, k

COMPUTE
N_c, M

UNIFORM RANDOM
NUMBER GENERATION

COMPUTE X_j,
Y_j^i, z_j^i, for

$j = 1, \ldots, N_c$
$i = 1, \ldots, M$

ISUM = 0

②

COMPUTE $z_j^i(0)$

COMPUTE MINIMUM
OF $z_j^i(0)$ FOR
$i = 1, \ldots, M$

MINIMUM = $z_j^{k1}(0)$

ICOUNT = 1

COMPUTE $z(k1, j1)$
FOR $j1 = k1+1, \ldots, M$

COMPUTE MINIMUM
OF $z(k1, j1)$
FOR $j1 = k1+1, \ldots, M$

MINIMUM = $z(k1, k2)$

$k2 = M$

YES

NO

$k1 = k2$

ICOUNT = COUNT + 1

ISUM = ISUM + ICOUNT

$J = j + 1$

② ——No—— $j > N_c$

YES

COMPUTE N_3
N3 = ISUM/N_c

③

continued.....
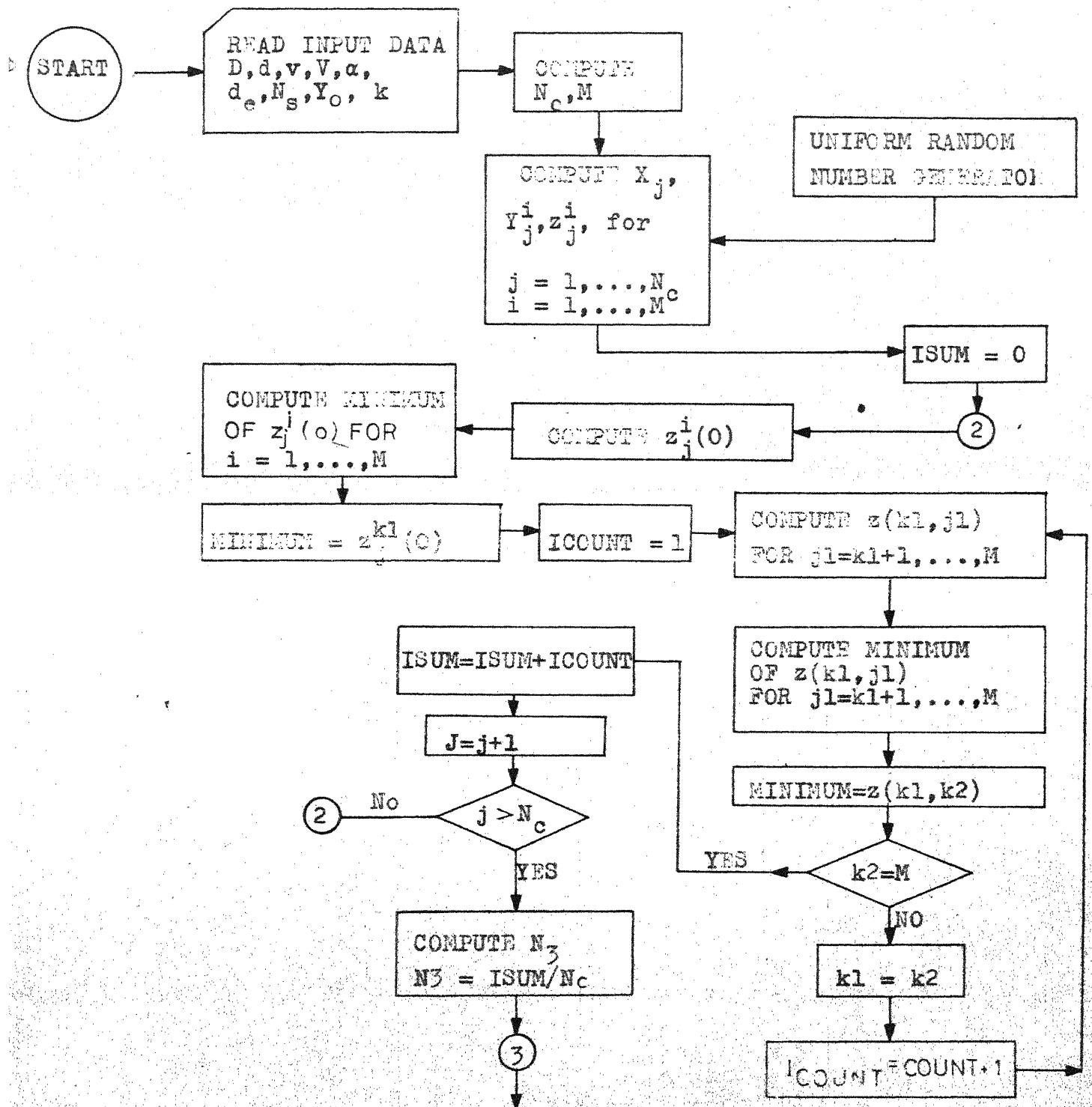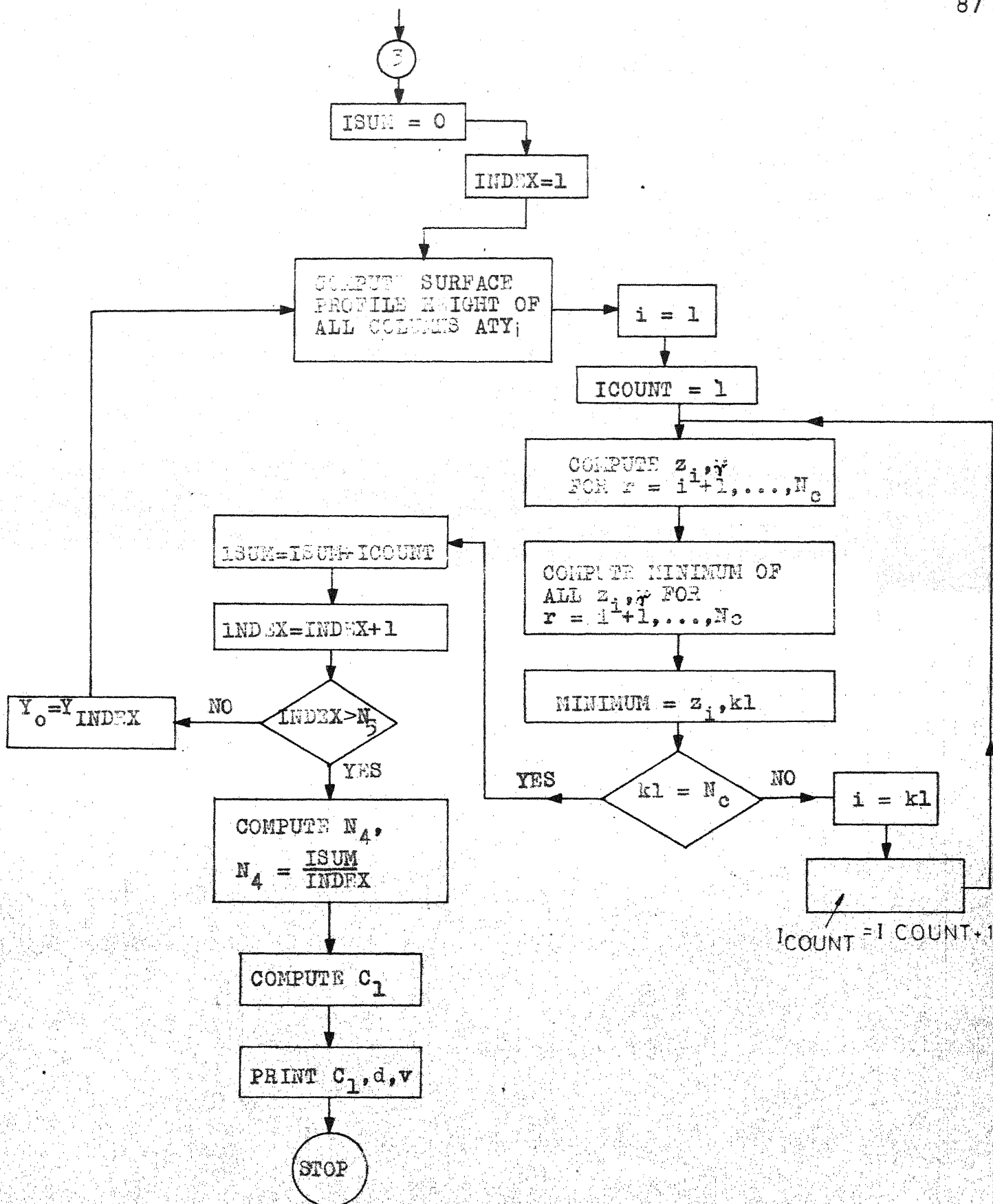
FIGURE 4.2 COMPUTER FLOW CHART FOR : CALCULATION OF ACTIVE GRAIN DENSITY RESPONSIBLE FOR SURFACE GENERATION.

CHAPTER V

APPROXIMATE ANALYSIS

5.1 Introduction

It has been shown earlier that the radial distribution parameter, k, and effective profile depth, d_e, describes the distribution of grain on the wheel surface. In the simulated study of the grinding process d_e was evaluated from the experimental profiles where it was assumed that the effective profile depth, d_e, is equal to the maximum peak to valley height of the work surface. When interest lies in determining the values of surface roughness produced in fine grinding, a simplified model can be proposed.

5.2 Determination of Peak to Valley Height

The surface produced on a stable grinding machine consists of scallops left on the workpiece due to finite spacing of successive grains. If all grains are assumed to be at the same radial distance and equally spaced, the plan view of the finished surface will consist of array of slender shaped scratches as shown in Figure 5.1. Assuming the mid-point of the scratch to be the deepest point located at a distance h, defined as idealised mean peak to valley height [28], h can be evaluated from

$$h = \frac{v}{2 \, V \, C \sqrt{2 \, \rho \, D}} \qquad (5.1)$$

The value of C in the above equation corresponds to $z' = h$ (Figure 1.4) and equation (5.1) can be solved for h by iteration. As the grains are randomly distributed, the assumption that the active grains extend the same distance from the wheel surface is a crude approximation. Figure 5.2 shows that the peak to valley height depends on the coarsest and finest spacings h_1 and h_u respectively and upon the scallop height h_s at $z = h_u$ [33]. From this figure, it is evident that the grains producing grooves lie within h_u and generate the transverse profile. For any grain to be active, the grain depth of cut should be positive i.e., the grain must contact the workpiece [63]. Under these conditions, the limiting value of the radial zone within which grains contribute cutting is approximately equal to

$$h_u = 2 \, \bar{\lambda}_2 \, \frac{v}{V} \sqrt{\frac{d}{D}} \qquad (5.2)$$

where $\bar{\lambda}_2$ is the average linear grain spacing. Therefore, the maximum peak to valley height of the surface can be taken to be equal to the maximum value of the undeformed chip thickness. If C_2' is the active grain density then

$$c'_{\chi} = \frac{1}{\lambda_2 \, b} \tag{5.3}$$

where b is the average width of the groove produced by a grain and can be obtained from [28].

$$\rho = \frac{d}{2} + \frac{b^2}{8 \, d} \tag{5.4}$$

Therefore, from equations (5.2) and (5.3), we get

$$h_u = \frac{v}{V \, c'_{\chi} \sqrt{2\rho - d} \, \sqrt{D}} \tag{5.5}$$

The probability density function $f_H (h)$ of having a grain tip at any level h can be ~~obtained from equation (2.28)~~ shown to be given by [10,11], ~~by substituting h in place of z" since z" = h. Thus,~~

$$f_H (h) = \frac{(k + 1) (h + d_e)^k}{(2^{k+1} - 1) \, d_e^{k+1}} ; \quad 0 < h \leqslant d_e \tag{5.6}$$

If M' is the total number of grains lying below h_u, then,

$$M' = M'' \, \text{Prob} \, (h \leqslant h_u) \tag{5.7}$$

where M" is the total number of grains lying below d_e for an average width of cut b. For a nominal grain density, C, M" is given by

$$M'' = \pi D \, b \, C \tag{5.8}$$

Thus,

$$M' = M'' \int_0^{h_u} f_H (h) \, d h \tag{5.9}$$

On simplification, we get

$$M' = \frac{M'' \left((h_u + d_e)^{k+1} - d_e^{k+1} \right)}{(2^{k+1} - 1) \, d_e^{k+1}} \qquad (5.10)$$

Also,

$$\lambda_z = \frac{\pi D}{M'}$$

$$= \frac{(2^{k+1} - 1) \, d_e^{k+1}}{C \, b \left((h_u + d_e)^{k+1} - d_e^{k+1} \right)} \qquad (5.11)$$

Substituting the values of λ_z in equation (5.3), we obtain

$$c'_z = \frac{C \left((h_u + d_e)^{k+1} - d_e^{k+1} \right)}{(2^{k+1} - 1) \, d_e^{k+1}} \qquad (5.12)$$

Using equations (5.5) and (5.12), we get

$$h_u = \left(\frac{v}{V} \right) \left(\frac{1}{\sqrt{2f - D}} \right) \left(\frac{1}{\sqrt{D}} \right) \frac{(2^{k+1} - 1) \, d_e^{k+1}}{C \left((h_u + d_e)^{k+1} - d_e^{k+1} \right)} \qquad (5.13)$$

Direct evaluation of h_u from the above equation is difficult, due to implicitness of the functions. Therefore, iterative method is used to solve equation (5.13) in order to evaluate h_u for known values of k and d_e. Once h_u is known for any cutting condition, c'_z can be determined from equation (5.12).

5.3 Surface Roughness

Farmer, Brecker and Shaw [70] conducted tests
under various grinding conditions and their experimental
values of maximum peak to valley height are shown in
Figure 5.3. It is observed that the maximum peak to
valley height lie between the two dotted lines such that
$4\bar{h} < h < 6\bar{h}$, where $\bar{h}$ is the centre line average value
of the surface. Hence to a fairly good approximation, it
can be assumed that

$$\bar{h} \simeq \frac{1}{5} h. \tag{5.14}$$
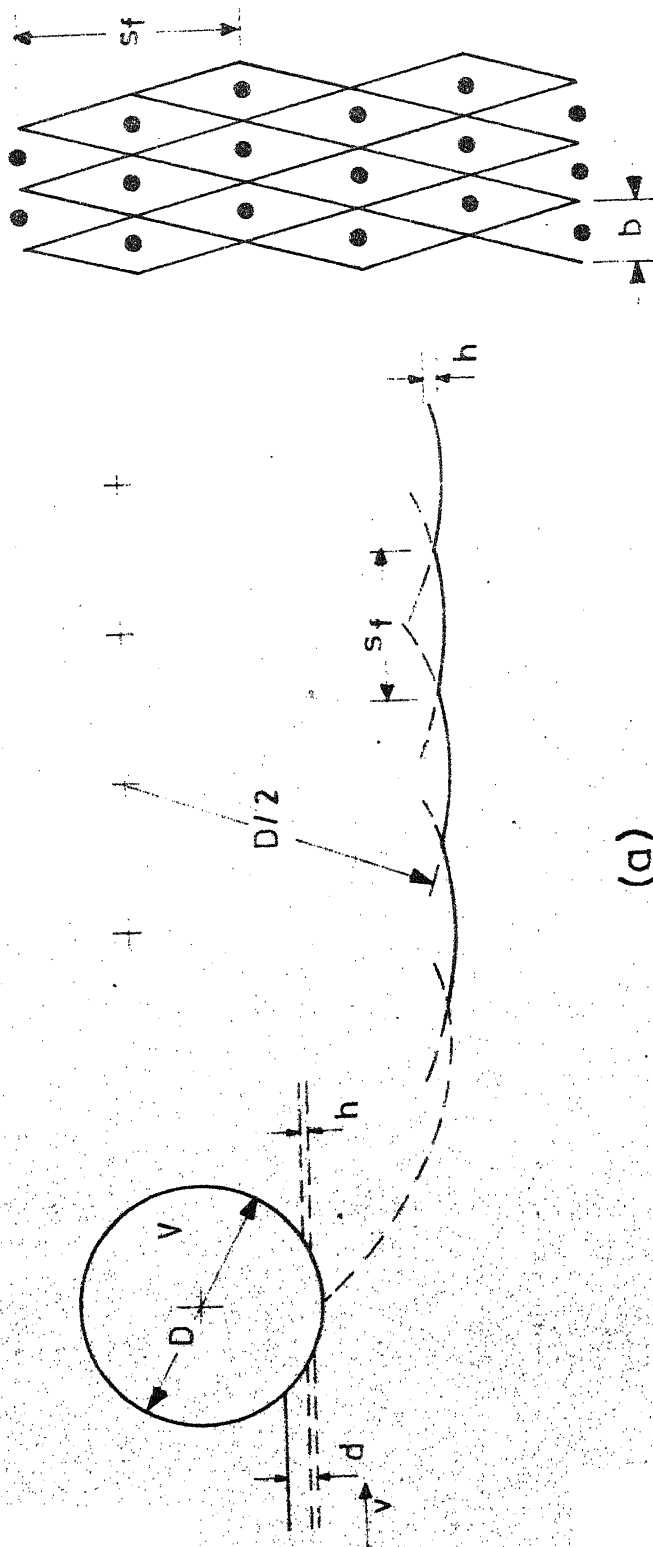
(a)

(b)

FIGURE 5.1 (a) SOURCE OF SCALLOPS H LGHL h, ON GROUND SURFAC

(b) PLAN VIEW OF SCALLOPS LEFT ON GROUND SURFACE BY
WHEEL HAVING UNIFORMLY SPACED ACTIVE GRAINS
[AFTER LAL AND SHAW [26]]
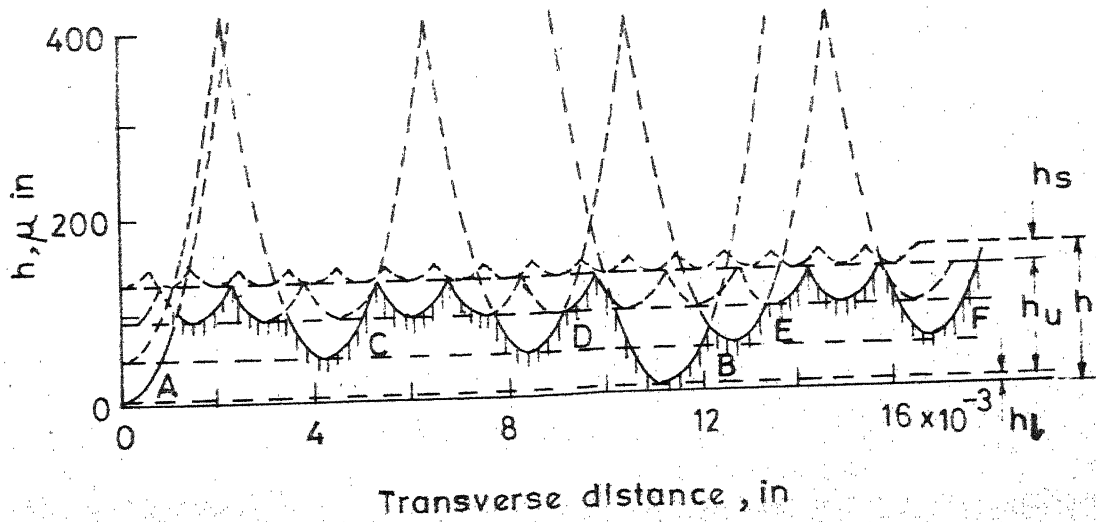
FIGURE 5.2 CONSTRUCTION OF TRANSVERSE PROFILE OF GROUND SURFACE.
[AFTER NAKAYAMA AND SHAW [33]]
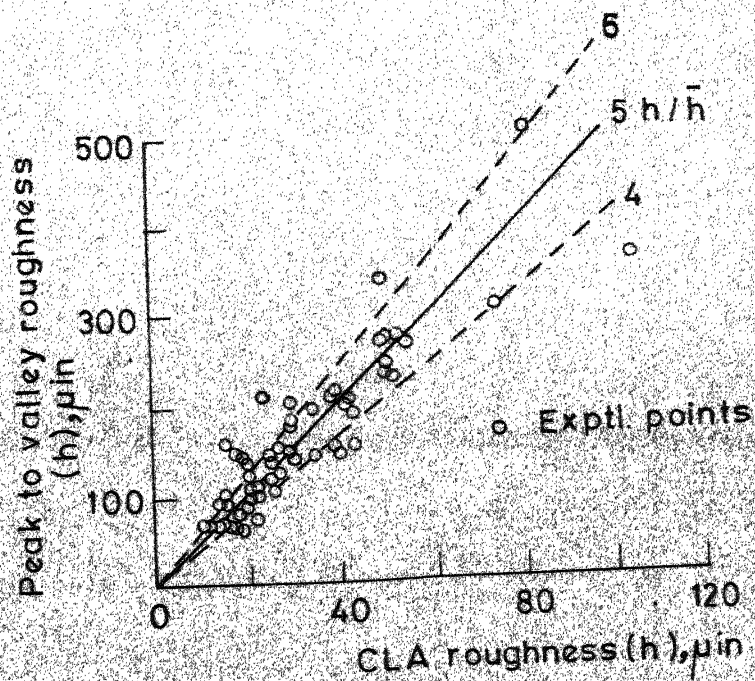
FIGURE 5.3 CORRELATION PLOT FOR RELATION BETWEEN PEAK TO
VALLEY ROUGHNESS, h AND AVERAGE ROUGHNESS, h̄
[AFTER FARMER, BRECKER, ET AL, [70]]

CHAPTER VI

RESULTS, DISCUSSION AND CONCLUSIONS

6.1 Introduction

The system parameters k and d_e which control
the probabilistic distribution of grains on the grinding
wheel are the sources of variation for the random output
of the grinding system (ground surface profile). There-
fore, k and d_e have to be estimated so that the simu-
lated and experimental profiles match. The techniques
adopted for evaluating these parameters are shown schema-
tically in the block diagram (Figure 6.1). The values of
d_e for various grinding conditions obtained from the
experimental profiles are fed to the variance analyser
block. It is found (discussed later) that d_e is practi-
cally independent of the cutting conditions in the fine
grinding range. With this value of d_e and a given
value of k, the theoretical surface profile is simulated
and fed to the comparator through correlator and spectral
density analyser. The experimental surface profile is
also fed to the comparator after being passed through
correlator and spectral density analyser block. In the
comparator block, the theoretical and experimental
spectral estimates at different frequencies for various
values of k are compared. The outputs from the

comparator block are then fed to the least square estimator where the values of k for any cutting condition is estimated such that the comparator output is a minimum. This process is repeated for all cutting conditions. The least square estimates of k are then passed on to the variance analyser where the effect of d and v on k is evaluated. The regression estimates of k for its functional dependence on d and v are obtained in the regression analyser, the input for which are the least square estimates. The values of k, thus obtained, are then fed to the grinding system and the theoretical profile is generated which simulates the actual profile. The CLA value of the simulated surface profiles, can thus be calculated and compared with the experimental results.

6.2 Experimental Details

To obtain the experimental profiles, experiments have been carried out on a Hindustan Machine Tools Ltd., Horizontal Spindle Surface Grinding Machine. The specifications of this machine are given in Appendix C. The following grinding conditions have been used:

1. Wheel : A 46 - J 5 - V 10.

2. Workpiece: Mild Steel, length : 4 cm; width: 2 cm; height: 1 cm; hardness: R_B 60.

3. Wheel diameter : 30 cm

4. Wheel depth of cut: 4 to 12 (microns)

5. Table speed: 5 to 15 m/min.

6. Wheel speed: 1500 r.p.m.

7. Grinding fluid: dry

8. Wheel dressing: (i) 2 passes at 12 microns and

   1 m/min cross-feed.

   (ii) 2 passes at 6 microns and

   1 m/min cross-feed

   (iii) spark out

9. Nominal grain density: 160 cm^{-2}

10. Simulated width : 0.25 cm.

All tests have been carried out under plunge cut conditions. The workpiece surface was mirror-finished and before performing each test ten passes were given with the dressed wheel on a seperate workpiece in order to eliminate the effect of "dulling" produced during dressing. This process was repeated for each test. The workpiece surface profile produced on the mirror-finished testpiece after a single pass was recorded on a Talysurf-4 Surface Measuring Instrument. As discussed in Chapter III, Sec. 3.2.1, a suitable 2 x 2 factorial experiment was adopted. A few representative traces of the experimental profiles are shown in Figures 3.3.

6.3 Simulated Results

6.3.1 Evaluation of d_e

To evaluate d_e and its possible dependence on
d and v, the peak to valley height of the traces of
the factorial experimental profiles were obtained. The
values, thus obtained, are given in Table 6.1.

TABLE 6.1

Data for 2 x 2 factorial experiment for evaluating

d_e (μ)

Level of factor, d		4 μ		12 μ	
Level of factor, v		5 m/min	15 m/min	5 m/min	15 m/min
Repetition	1	2.8	3.0	2.8	3.0
	2	3.0	2.9	3.0	3.2
Total		5.8	5.9	5.8	6.2
Grand Total			23.7		

With the help of square identities and associated degrees
of freedom, discussed in Chapter III, Sec. 3.2.4, the ana-
lysis of variance table is prepared (Table 6.2).

TABLE 6.2

Analysis of variance Table for d_e

Source of Variation	Sum of Squares	Degree of Freedom	Mean Squares	Computed F-ratio
Treatment combination (Tr)	0.054	3	-	-
Factor, d	0.0115	1	0.0115	0.707
Factor, v	0.0315	1	0.0315	1.877
Interaction (I)	0.011	1	0.011	0.677
Within (S)	0.065	4	0.01625	-
Total (T)	0.119	7	-	-

From this table, it is observed that the computed F-ratio for d and v and their interactions are less than 7.71, the value obtained from statistical table for 'F' distribution for upper 5% significance level. Therefore it can be concluded that the effect of d and v on d_e is negligibly small. Thus, the value of d_e can be taken to be equal to the mean of all values obtained from experimental profiles. Therefore,

$$d_e = \frac{23.7}{8} = 3.0 \; \mu.$$

6.3.2 Evaluation of k

Once the value of d_e is estimated, the following numerical values are calculated as

N_c = Number of columns within the simulated width

$\quad = 124$,

M = Number of grains per column $= 34$,

and the sample size, N_s and maximum lag number, m_1, are taken as 500 and 50, respectively.

As shown in the block diagram representing the scheme of the solution technique (Figure 6.1), the theoretical transverse surface profile is generated using known values of k and the random grain positions (equations (2.34) to (2.36)) following the computer flow charts (Figures 4.1 and 2). The output of the comparator block in terms of SSk (Chapter III, sec. 3.2.5)for iterative values of k is compared in the least square analyser for any grinding condition. The least square estimate of k is that value for which SSk is a minimum. This process is repeated for all cutting conditions. The comparison of spectral densities of theoretical profiles generated with the least square estimated values of k and experimental profiles for some representative cases are shown in Figures 6.2. The least square estimates of k for the 2 x 2 factorial experiments are presented in Table 6.3.

TABLE 6.3

Data for 2 x 2 factorial experiment for evaluating k

Level of factor, d		4 μ		12 μ	
Level of factor, v		5 m/min	15 m/min	5 m/min	15 m/min
Repetition	1	5.0	9.5	8.0	12.5
	2	5.5	8.5	8.8	13.0
Total		10.5	18.0	16.8	25.5
Grand Total			70.8		

The results of the analysis of variance are shown in
Table 6.4. The procedure adopted was the same as that
for evaluating d_e.

TABLE 6.4

Analysis of variance table for k

Source of Variation	Sum of Squares	Degrees of Freedom	Mean Squares	Computed F-ratio
Treatment Combination (Tr)	56.79	3	–	–
Factor, d	23.805	1	23.805	88.98
Factor, v	32.805	1	32.805	122.70
Interaction (I)	0.180	1	0.180	0.67
Within (S)	1.07	4	0.2675	–
Total (T)	57.86	7	–	–

This table shows that the computed F-ratio for d and v are much larger than 7.71, the value obtained from statistical table for 'F' distribution for upper 5% significance level, where as for interaction effect on k, the computed F-ratio is very small compared to the statistical value. Therefore, it can be concluded that the variation of k is due to the effect of d and v but not due to their interaction. The functional dependence of k and d and v can be estimated by regression analysis.

One of the requirements of the regression analysis, is the homogeneity of the variances in each trial. As discussed in Chapter III, Sec. 3.2.3, the variance of reproducibility of parameter, k is obtained and presented in Table 6.5.

TABLE 6.5

Calculation of variance of reproducibility

Trial No.	k_1	Repeated Trial No.	k_2	$\bar{k}$	S_i^2, (k)
1	5.0	5	5.5	5.25	0.125
3	9.5	7	8.5	9.0	0.50
2	8.0	6	8.8	8.4	0.32
4	12.5	8	13.0	12.75	0.125

S_{rep}^2 (k) = 0.535

Since there is no variance, $s_{i'}^2(k)$ that considerably exceeds the remaining ones, and $s_{rep}^2(k)$, and $s_{i'}^2(k)$ are of the same order, homogeneity of variances, can be assumed. However, to apply Bartlett test [65], the value of c_2 is calculated from equation (3.8) as

$$c_2 = 0.6182$$

substituting the values of c_2 in Bartlett's test statistic, B, given by equation (3.7), we get

$$B = 0.131 < \chi^2 (= 7.81) \text{ for } 5\% \text{ significance}$$

level and three degrees of freedom. Hence we can conclude that the variances are homogeneous assuring the reproducibility of the values of k.

Assuming multiple linear regression analysis, the equations (3.39), (3.40) and (3.41) given in Chapter III, Sec. 3.4, are solved for a_1, b_1 and b_2. The estimated regression of k on d and v is given by

$$k_{i'} = 1.35 + 0.4125 \, d + 0.42 \, v \qquad (5.1)$$

where, a_1, b_1 and b_2 are 1.35, 0.4125 and 0.42, respectively. Solving equation (3.59), 95% confidence interval for β_1 and β_2 are $0.3087 < \beta_1 < 0.5163$ and $0.35 < \beta_2 < 0.618$, respectively.

6.3.3 Determination of Surface Roughness and C_1

Using equation (6.1) for various grinding conditions, the theoretical profile is generated and their spectral density curves are shown in Figures 6.3. From these theoretical profiles, the centre line average value (CLA) of the surface roughness are calculated. The CLA values, thus obtained, for various cutting conditions for both theoretical and experimental profiles are shown in Figures 6.4 and 6.5. Using the computer flow charts, the active number of grain density responsible for surface generation are numerically obtained and plotted in Figures 6.6 for various grinding conditions.

6.4 Results of Approximate Analysis

Equation (5.13) of Chapter V, Sec. 5.2, is solved iteratively with an initial value of h_u as 0.5μ with convergence criterion 0.001μ. The values of centre-line average (CLA) of the surface roughness are calculated by using equation (5.14). The number of active grain density, C_3, can be obtained from equation (5.12). The variation of surface roughness with d and v are shown in Figures 6.7 while the variation of active grain density with h_u is shown in Figures 6.8

6.5 Discussion

As the surface generated is the sample realisation of grains on the wheel surface, the surface profile produced during the wheel work interaction will be random in nature. It has been shown through statistical analysis that d_e is independent of the cutting condition, therefore, this randomness is primarily due to the effect of radial distribution parameter. The number of cutting points on the wheel surface though varies with the radial distance from the outermost grain, it quickly gets saturated as the radial depth is increased. Therefore, it is quite reasonable that the effective profile depth remains more or less constant for a particular wheel and a large part of fluctuations in the experimental data may be due to chance variation.

When the wheel is stationary, the depth of cut and the table speed are zero and the value of k is a_1 which shows the static distribution of the grains on wheel surface. Earlier analysis [61] gave the value of k under the above circumstance as zero which does not have any physical bearing. The dynamic influence of table speed and depth of cut on radial distribution parameter is functionally expressed by equation (6.1).

Actual ground surface is distorted from an ideal profile by various causes, some of which are probabilistic

and others are systematic. Comparison of real surface
with ideal one will provide information about the real
system if the ideal one is properly simulated to satisfy
the spectrum characteristics associated with the real
surface. In earlier analyses, 57, 61, it was observed
that the power spectra of the actually ground surface is
very much amplified in low frequency range having peaks
at very small frequency and with increasing values of d
and v, the profile variances increased. In the results
shown in Figures 6.2 the above criterion is observed for
the experimental profiles, having high spectral density
in low frequency range (less than 0.15 c/$\triangle$) with peaks
concentrated around 0.02 c/$\triangle$. The power spectral den-
sity of the simulated profile shows amplification in the
low frequency range (less than 0.15 c/$\triangle$) but no peaks
are observed (Figures 6.3).

A possible explanation for this, lies in the fact
that the sample experimental surface, even though mirror
finished, to start with, will have some irregularities
and is not ideally flat as considered for the theoretical
analysis. The effect of vibration during grinding and
individual grain deflection will have contribution to the
above effect. Therefore, the error involved in estimation
of the power spectral density of the real system in terms
of the theoretical spectral density will be

$$\xi(fq) = \hat{G}(fq, \xi) - \hat{G}(fq, \xi, k) \qquad (6.2)$$

Our aim is to obtain a sound theoretical model, so that this error is very small. However, one might want, for example, to minimise the probability

$$\text{Prob} \left\{ \left| \hat{G}(fq, \xi) - \hat{G}(fq, \xi, k) \right| > a \right\}, \quad a \ll 1 \qquad (6.3)$$

Such a requirement, though very realistic, is difficult to handle analytically. In the model, this criterion is reasonably solved by the minimisation of the mean square error, e, [62] given by

$$e = E\left[\left| \hat{G}(fq, \xi) - \hat{G}(fq, \xi, k) \right|^2 \right] \qquad (6.4)$$

where it was assumed that $\xi(fq)$ is uncorrelated. Least square estimate of k is obtained from the above equation.

As the depth of cut, d and v are increased, the profile variances represented by the area under the curve increases (Figures 6.3). The power spectral density also increases. As the root mean square value of the profile is equal to the area under the spectral density curve, the increase in profile variance indicates relatively rough surface with increasing d and v.

The effect of grinding conditions on surface roughness is shown in Figures 6.4 and 6.5. It is seen that with the increase in the value of d and v, surface finish deteriorates. The two important parameters that

will have significant effect on surface roughness are the undeformed chip thickness and active grain density. With increasing values of chip thickness, the peak to valley height of surface profile will increase while the increase in grain density will tend to decrease it. It appears that the chip thickness has more pronounced effect causing a deterioration of surface finish. This aspect is indicated by both theoretical and experimental results shown in the above figures. Further, there appears to be a reasonably close agreement between the experimental and simulated results.

The effect of grinding conditions on active grain density is shown in Figures 6.6a and 6.6b. These figures clearly indicate that both d and v affect the number of cutting points responsible for surface generation. An individual grain will only see the undeformed chip thickness and this value will increase with increasing values of d and v. As the chip thickness increases, more and more grains will get involved in cutting. This, however, will not increase infinitely but will tend to saturate beyond a certain value. This aspect is clearly seen in the above figures and the trend of the result agrees with those published earlier [61].

Once the dependence of k on d and v are known, it is possible to develop an approximate analysis for

evaluating the undeformed chip thickness, t. In deriving
this expression for t, it has been assumed that there
exists an average linear grain spacing, $\widehat{\Lambda}$. However, the
radial positions of grain have been assumed to be distri-
buted randomly between 0 and t. The upper limit for t
has been taken to be that value where C gets saturated.
Thus, the effective profile depth has been assumed to be
the limiting value of t for the approximate analysis.
In previous analyses [33, 28, 29] , an average linear
grain spacing has been taken while all grains have been
assumed to be at the same radial height from the wheel
surface. In addition, it was also assumed that the actual
grain density C remains constant and independent of t.

Results of the approximate analysis(Figures 6.7)
show that the surface finish deteriorates as the depth of
cut and table speed are increased. Comparison with expe-
rimental results also show reasonable agreement. The
plot of C versus t (Figure 6.8)clearly indicates that
the active grain density increases with increasing value
of t and agrees with the trend of the experimental curve
obtained by Nakayama and Shaw [33]. Such a curve is
valid only in the fine grinding range since the active
grain density can not rise infinitely but must saturate
at some value of t. Therefore, the approximate analysis
suggested is valid only in the fine grinding range.

6.6 Conclusions

A probabilistic approach seems to be natural for forming an analytical basis for the grinding process which involves several complex random parameters.

The analysis shows that the process can be described in terms of two fundamental parameters, the radial distribution parameter and the effective profile depth. Results show that the radial distribution parameter k is a linear function of the wheel depth of cut and table speed, while the effective profile depth is statistically independent of cutting conditions. The computer simulated surface profiles show close agreement with the experimental profiles in terms of stochastic characteristic such as spectral density functions. Results also indicate that surface finish deteriorates with increasing values of wheel depth of cut and table speed and agrees with the experimental results.

Once the dependence of radial distribution parameter on cutting conditions is established, the approximate analysis proposed can be used to predict the values of chip thickness, and surface finish. Comparison of theoretical and experimental results show reasonable agreement.

In the simulated analysis, only single pass plunge cut conditions have been considered and also the workpiece has been assumed to be a perfectly smooth

surface. This analysis can be extended to include the effect of original workpiece roughness, on the surface generated. In single pass operations the wear of abrasive grains can be neglected but in multipass operations this effect must be incorporated. In all fine grinding operations, spark out condition are used during the last few passes. The work can be further extended to include these effects.

The mechanics of chip formation with single grains is still not clearly understood. It is believed that there are three regimes, rubbing, ploughing, and cutting, during cutting with single abrasive grains depending upon the depth of cut. In the present analysis, it has been assumed that every interference between the grain and the workpiece removes material in the form of a chip without side pile-up. Once this mechanism is clearly understood, this aspect can also be incorporated in the analysis.
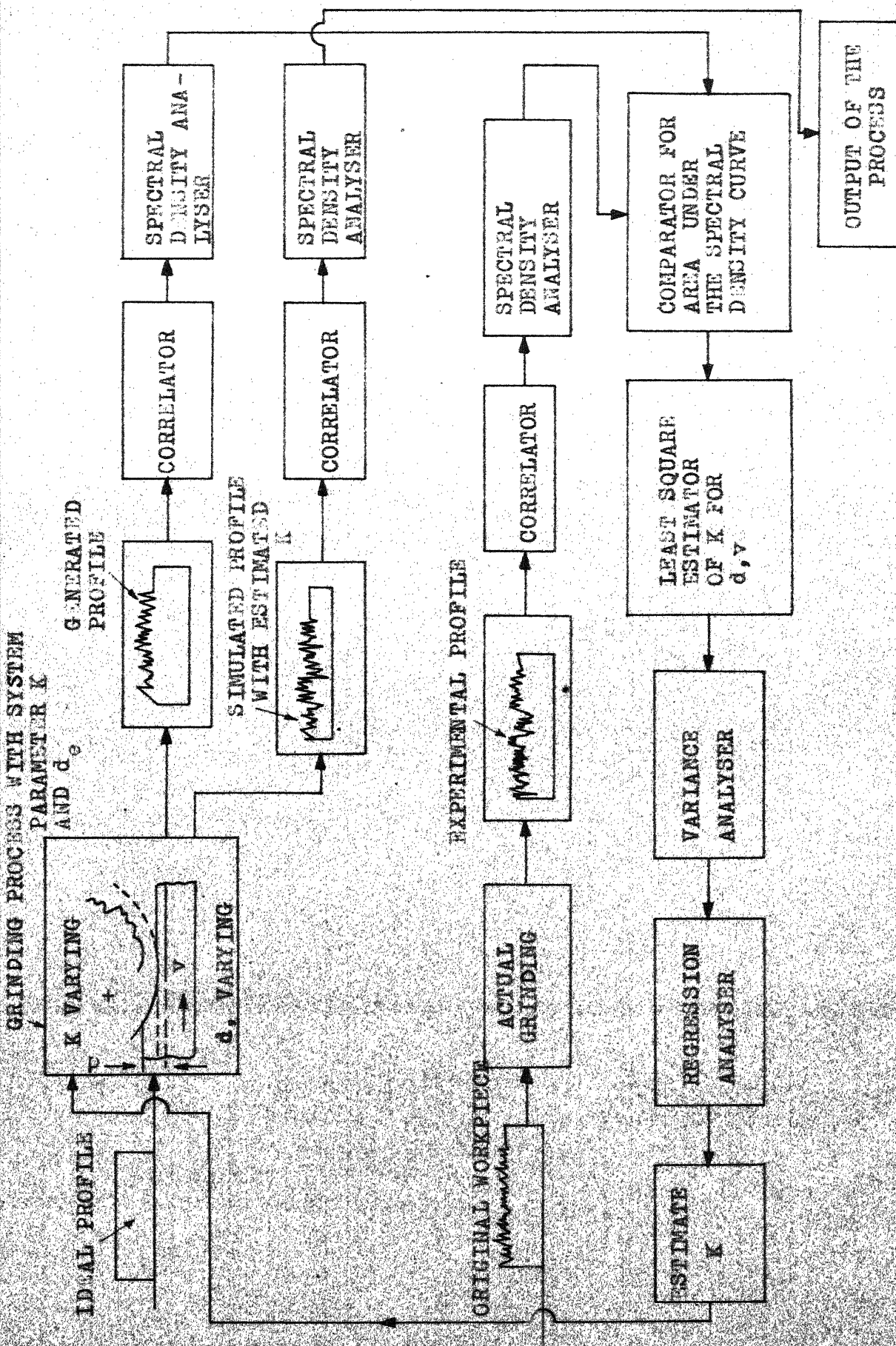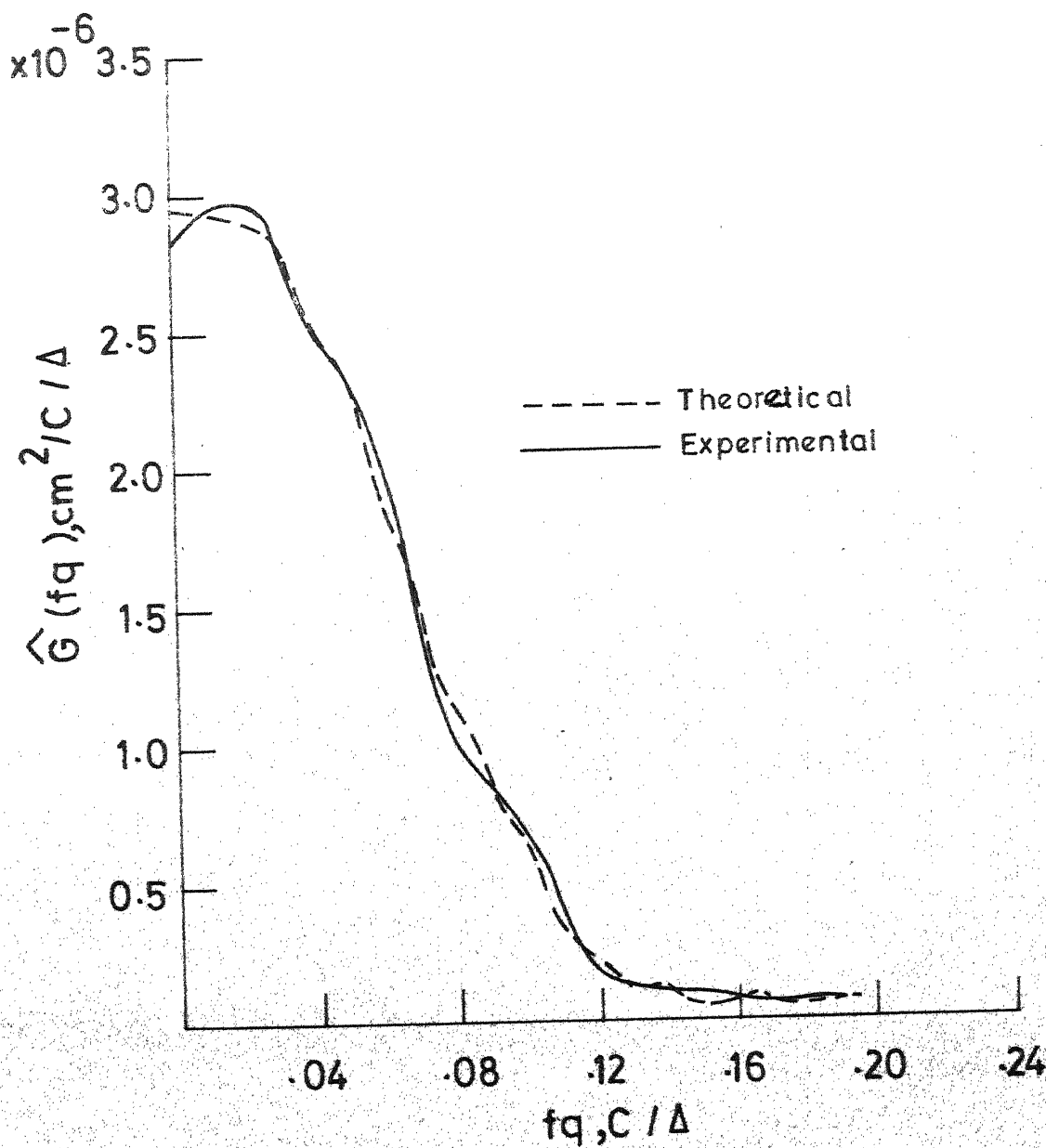
FIGURE 6.1 SCHEME OF SOLUTION TECHNIQUE

(a)

FIGURE 6.2 COMPARISON OF SPECTRAL DENSITIES OF THEORETICAL AND
EXPERIMENTAL PROFILES FOR :
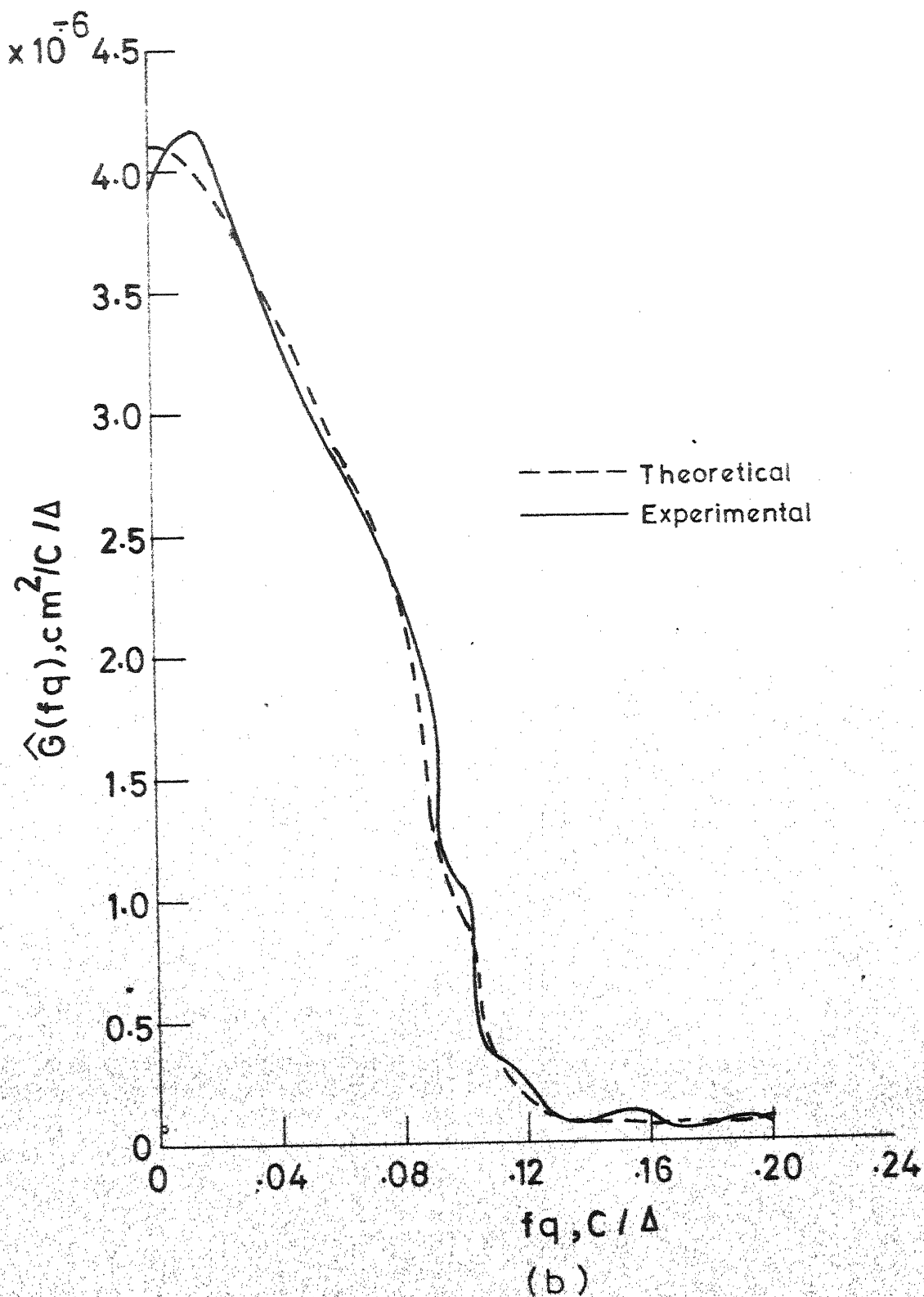(a) LEAST SQUARE ESTIMATE, K : 5.0, v : 5 m/min,
d : 7 MICRON, WHEEL SPEED : 1500 rpm

FIGURE 6.2 (CONTINUED)
(b) LEAST SQUARE ESTIMATE, K : 9.7; v : 15 m/min;
d : 4 MICRON; WHEEL SPEED; 1500 rpm
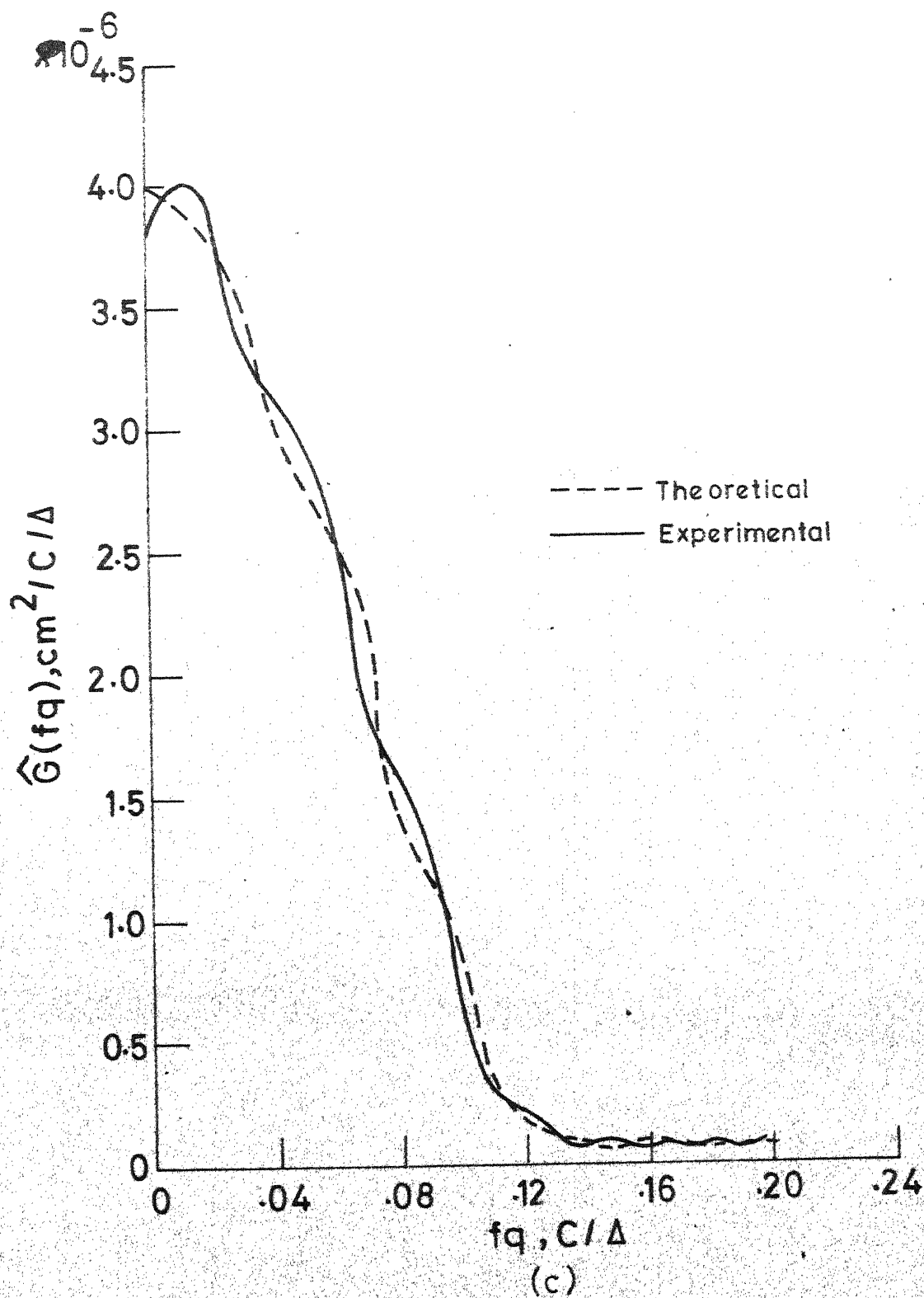
FIGURE 6.2 (c) LEAST SQUARE ESTIMATE k : 8.0, v : 5 m/min,
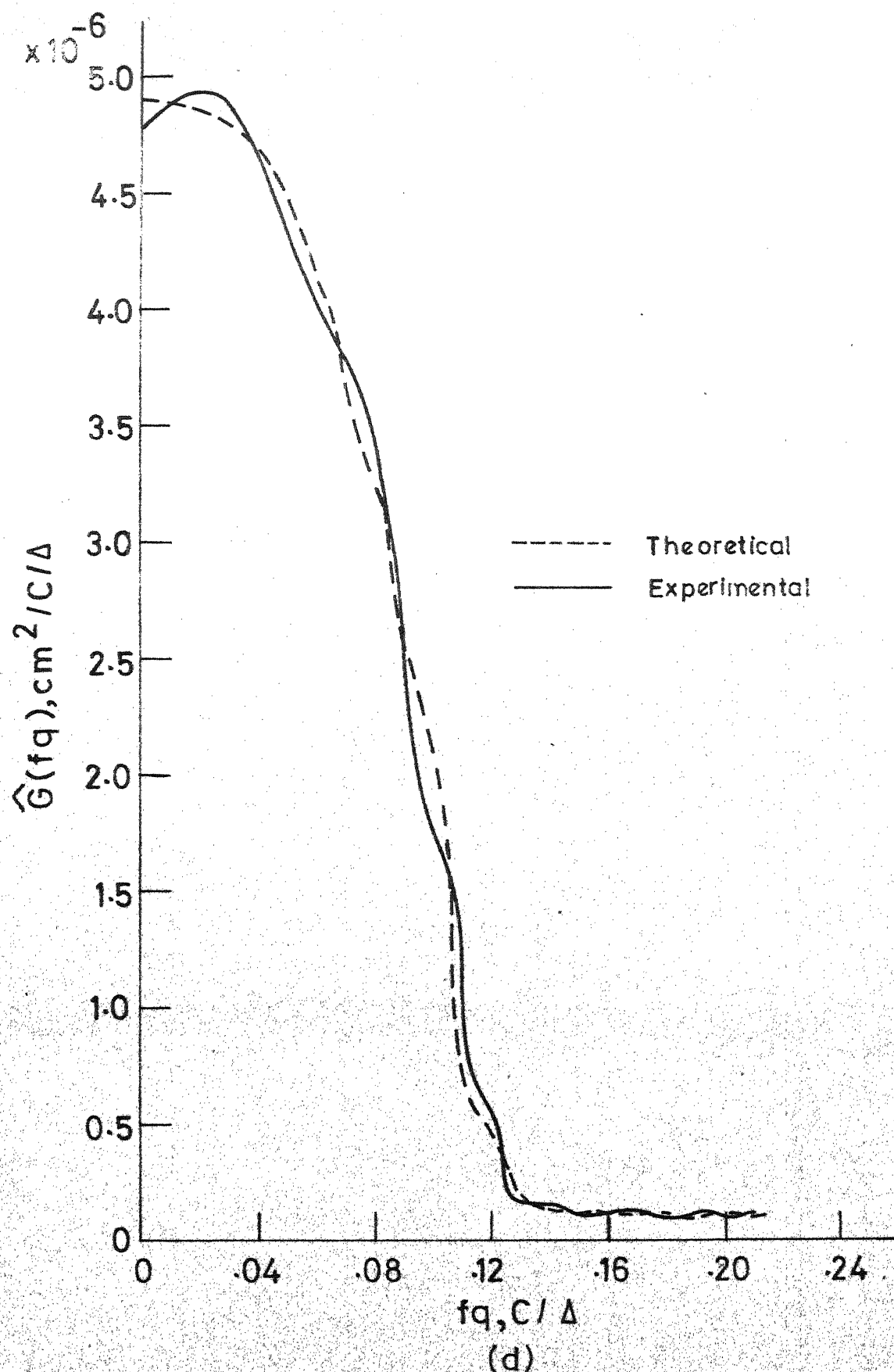d : 12 MICRON, WHEEL SPEED : 1500 rpm

FIGURE 6.2 LEAST SQUARE ESTIMATE, k: 12.5, v: 15 m/min,
(d) d: 12 MICRON, WHEEL SPEED, 1500 rpm.

(a) d: 4 μ; v: 5 m/min
(b) d: 12 μ; v: 5 m/min
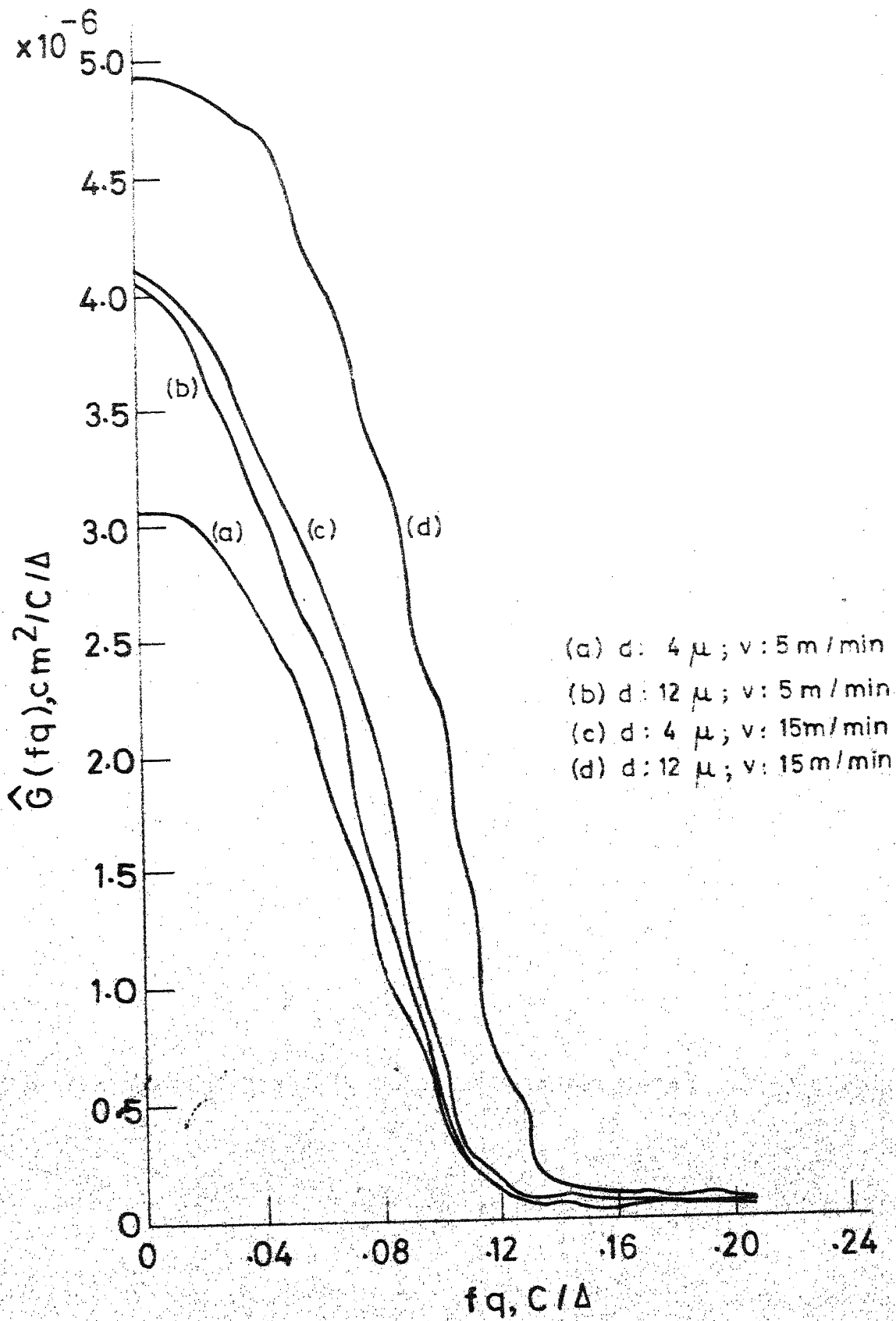(c) d: 4 μ; v: 15 m/min
(d) d: 12 μ; v: 15 m/min

FIGURE 6.3 COMPARISON OF SPECTRAL DENSITIES OF SIMULATED
PROFILES FOR VARIOUS CUTTING CONDITIONS
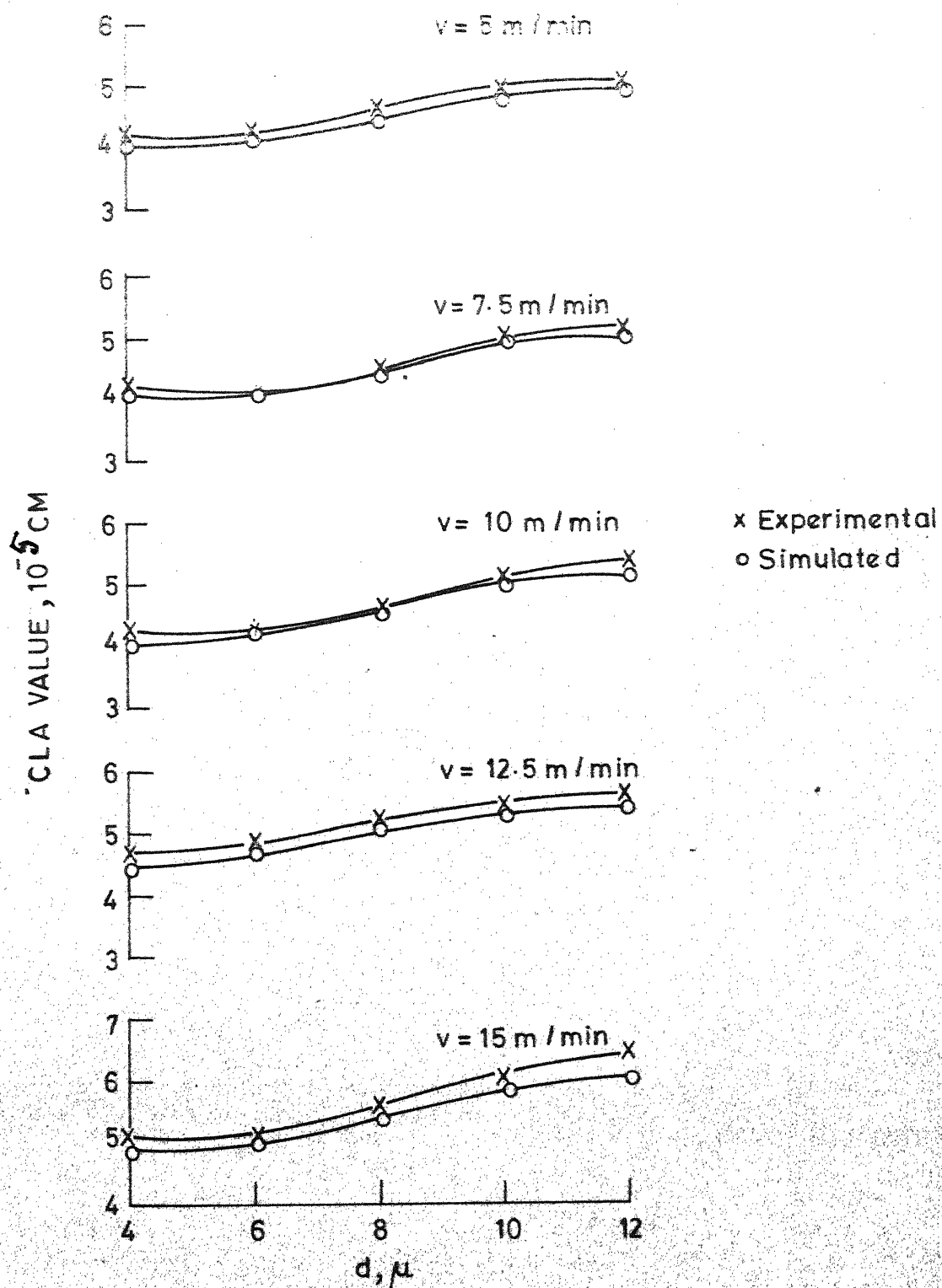
FIGURE 6.4 COMPARISON OF SURFACE ROUGHNESS OF SIMULATED AND EXPERIMENTAL PROFILE WITH DEPTH OF CUT FOR VARIOUS TABLE SPEED
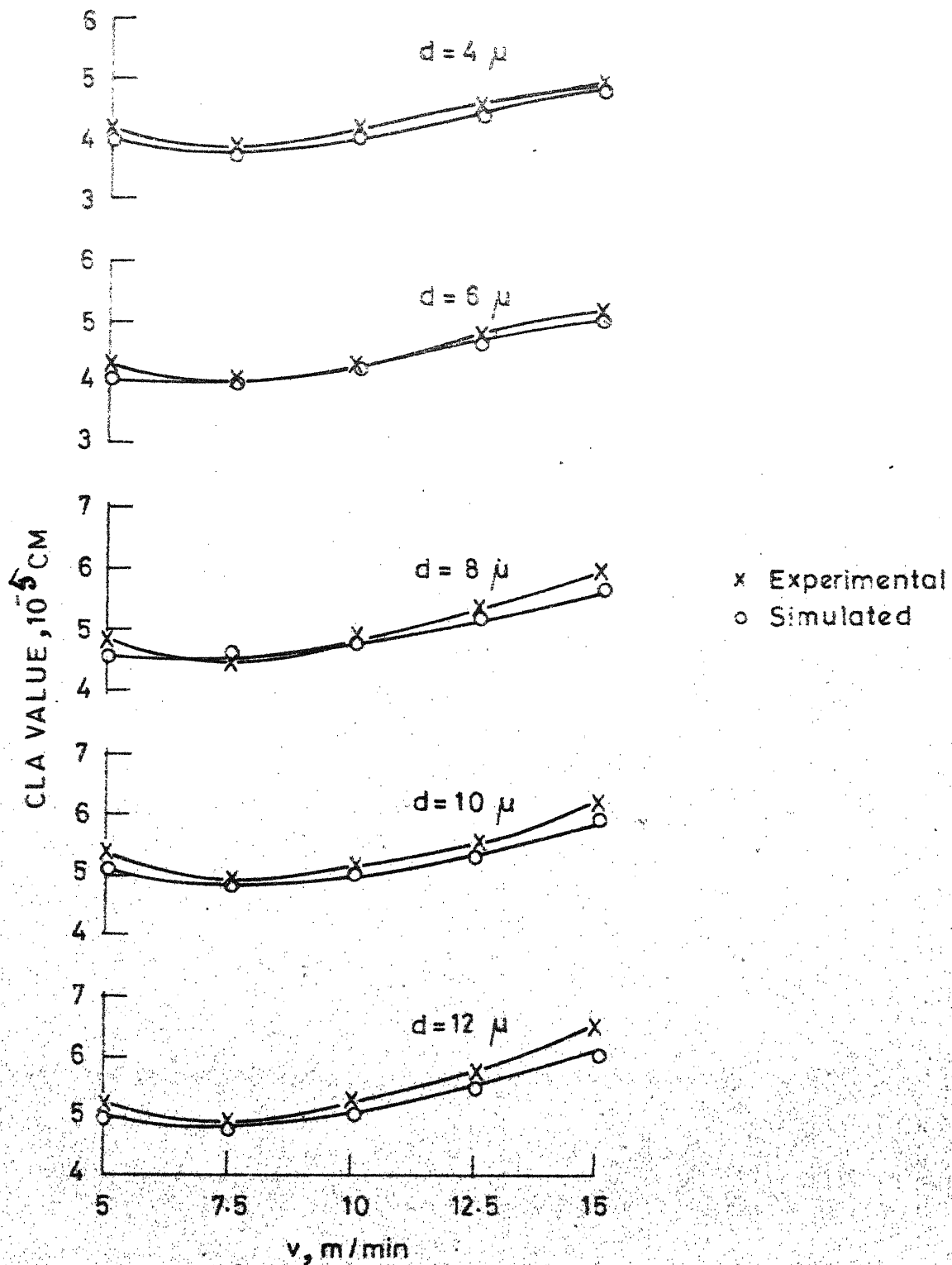
FIGURE 6.5 COMPARISON OF SURFACE ROUGHNESS OF SIMULATED AND
EXPERIMENTAL PROFILES WITH TABLE SPEED FOR
VARIOUS DEPTH OF CUT

(a)

(b)
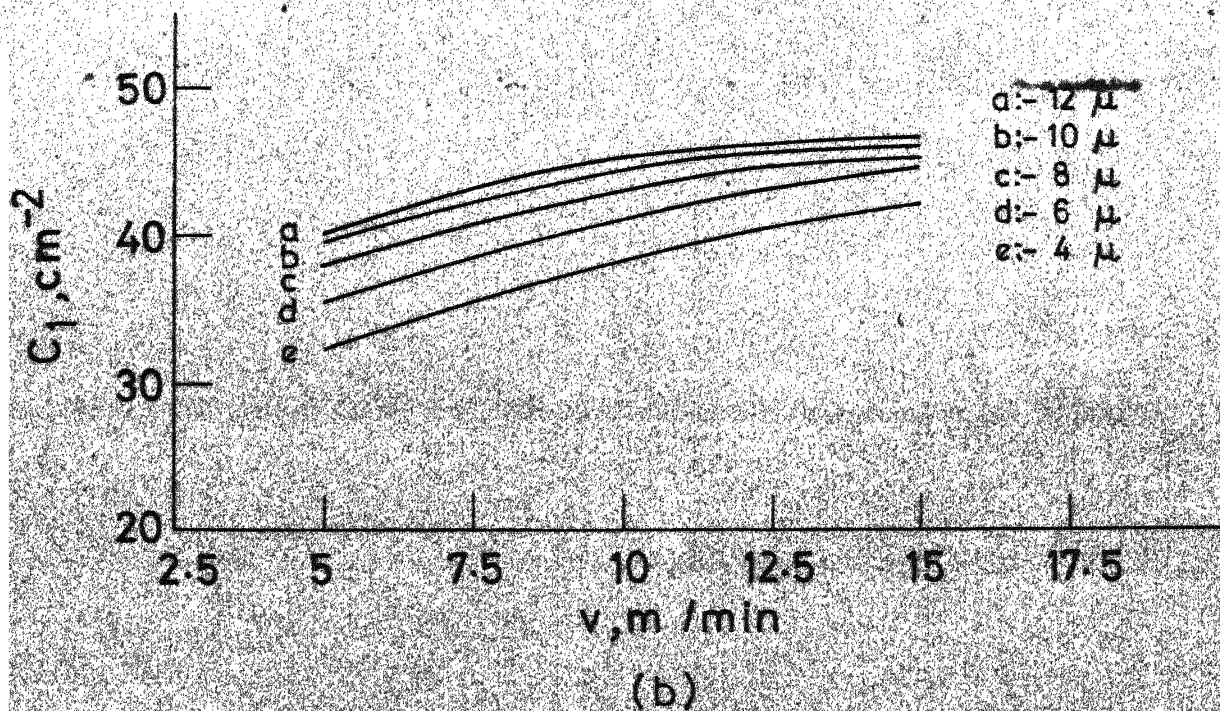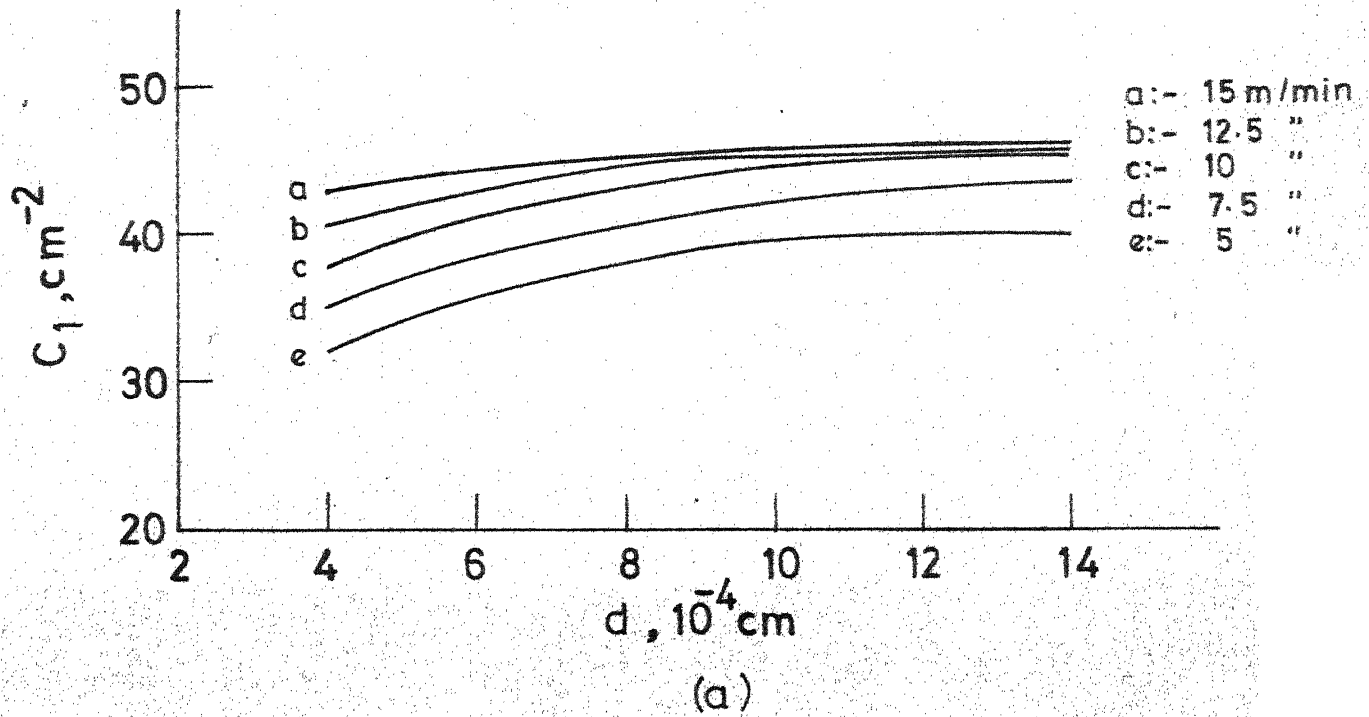
FIGURE 6.6 VARIATION OF ACTIVE GRAIN DENSITY, C_1 OBTAINED FROM
SIMULATE PROFILE:

(a) WITH DEPTH OF CUT FOR VARIOUS TABLE SPEEDS

(b) WITH TABLE SPEED FOR VARIOUS DEPTH OF CUT

x Experimental
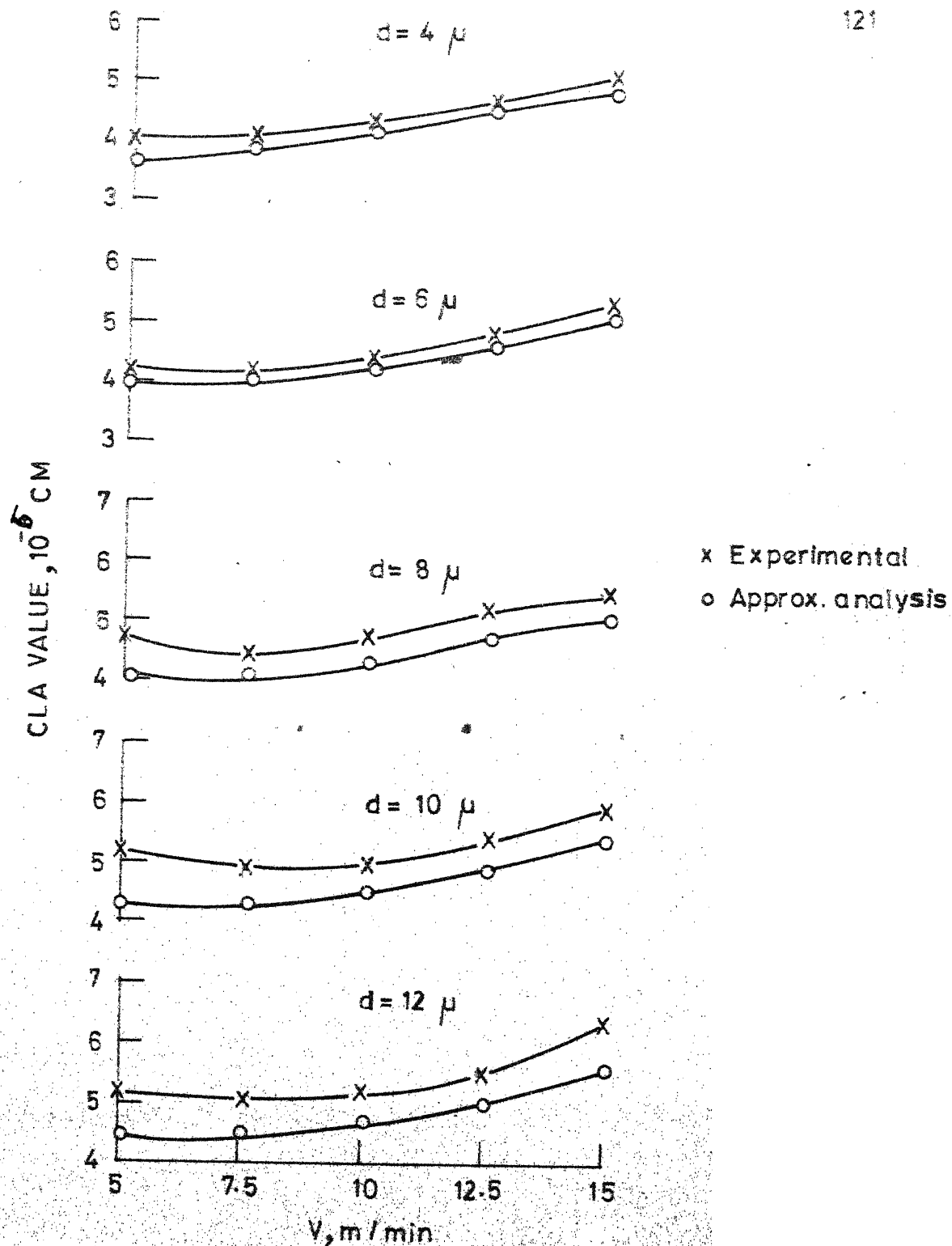
o Approx. analysis

FIGURE 6.7   COMPARISON OF EXPERIMENTAL AND THEORETICAL
             (APPROXIMATE ANALYSIS) SURFACE ROUGHNESS;
             (a) WITH TABLE SPEED FOR VARIOUS DEPTH OF CUT,

FIGURE 6.7 (b) WITH DEPTH OF CUT FOR VARIOUS
TABLE SPEED.

FIGURE 6.8 VARIATION OF ACTIVE GRAIN DENSITY C₃ WITH
UNDEFORMED CHIP THICKNESS

BIBLIOGRAPHY

1. H.F.G. Ueltz, "Abrasive Grains-Past, Present and Future", Prod. Int. Grinding Conf., Carnegie-Mellon University, Pittsburgh, U.S.A., 1972, pp. 1-53.

2. "Guide to Grinding Wheel Selection", Carborundum Universal Ltd., Madras, India, 1975.

3. K. Takazawa, R. Honda and K. Nishikawa, "Fracture Strength and Fragment Size of Abrasive Grains", Memoirs of the Faculty of Technology, Kanazawa University, Japan, Vol. 4, 1965, pp. 56-57.

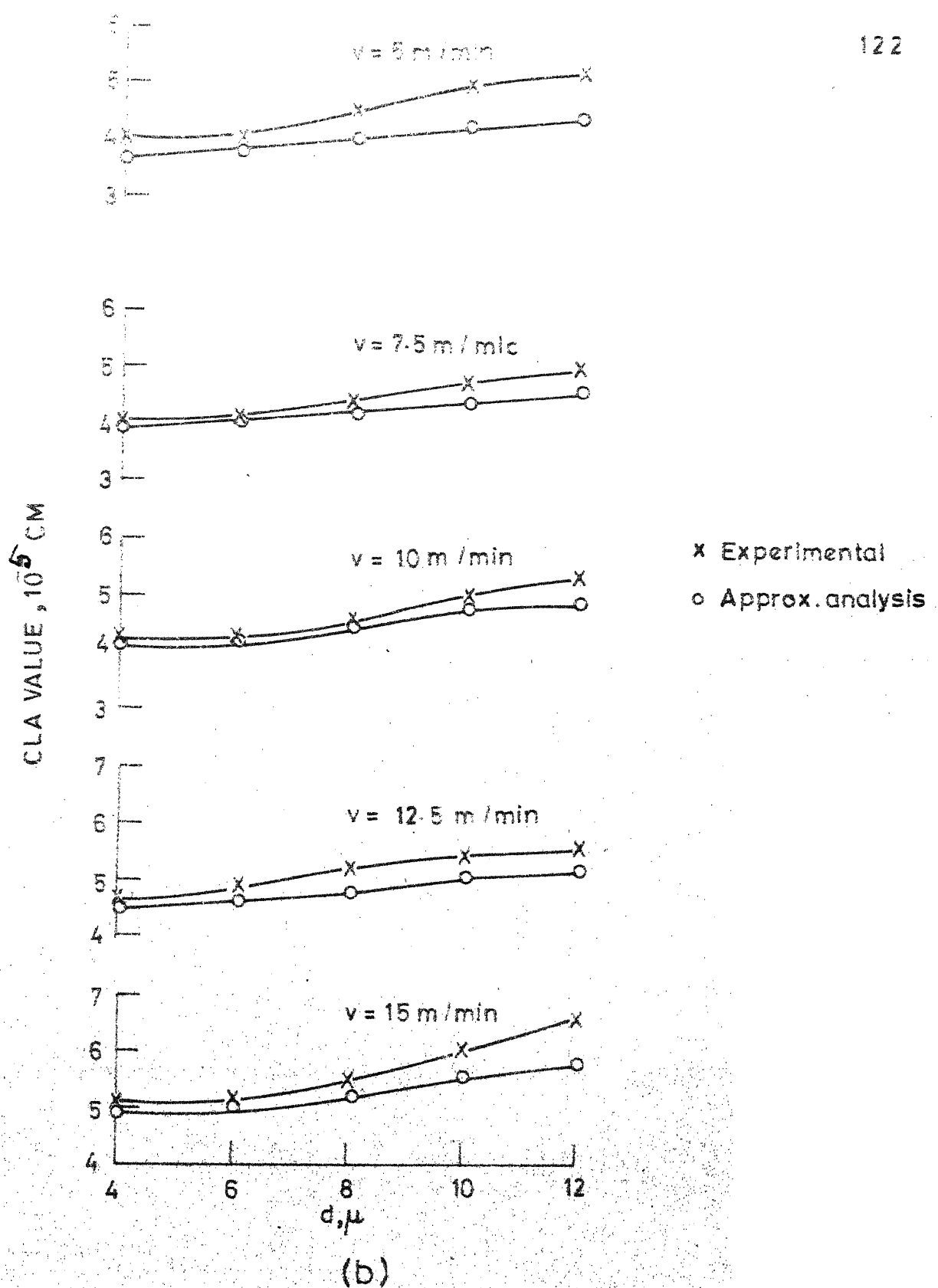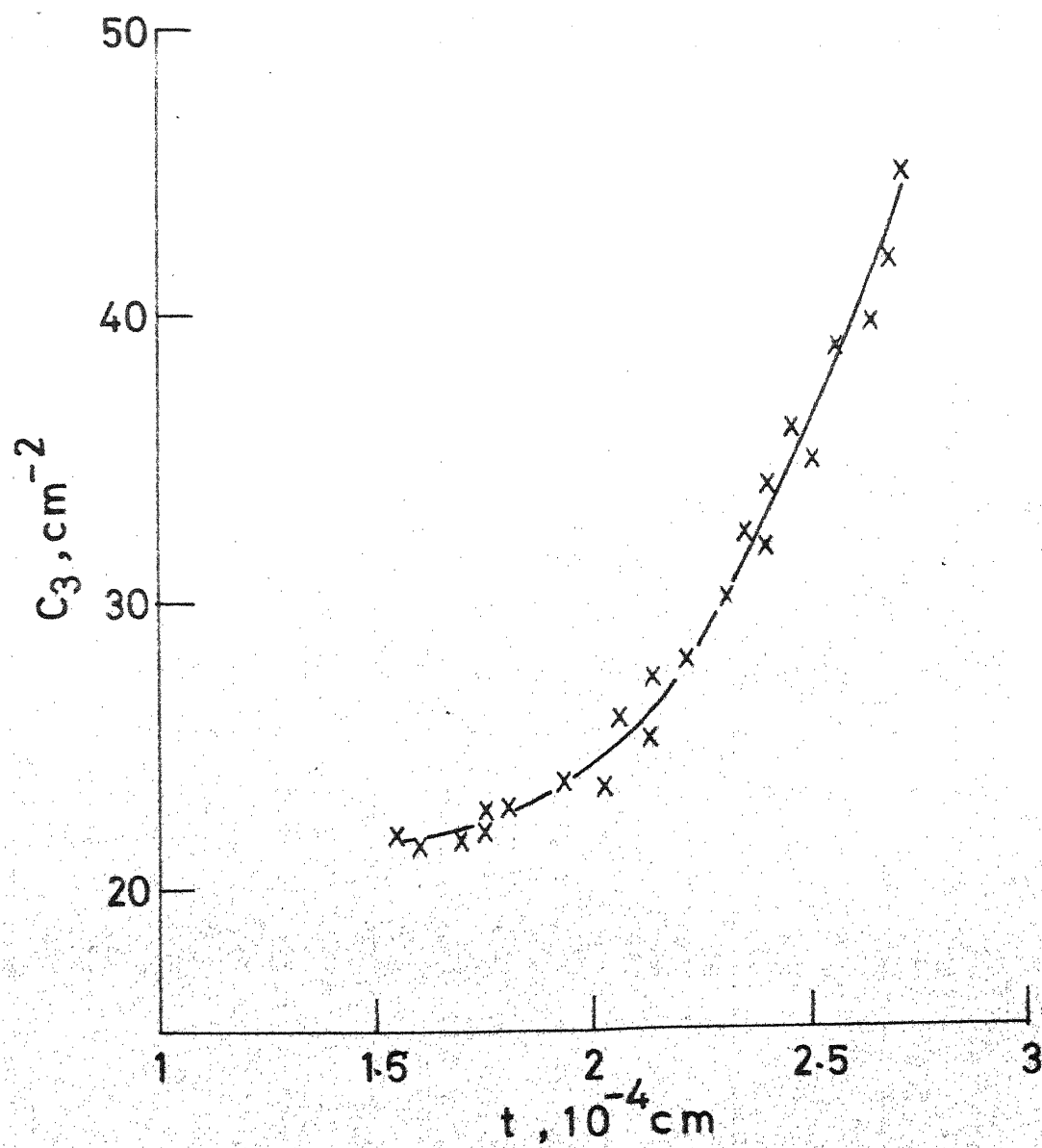4. T. Matsuo and M.C. Shaw, "Study of Compatability of Abrasive Grains With Various Work Materials", J. Japan Soc. of Prec. Eng., Vol. 36, 1970, pp. 278-284.

5. J.C. McMullen, "A Review of Patents in Silicon Carbide Furnacing", J. Electro-Chem. Soc., Vol. 104, 1957, pp. 462-465.

6. W.E. Kuhn, Ed., "The Formation of Silicon Carbide in the Electric Arc in Ultrafine Particles", John Willey, New York, 1963.

7. E.D. Whitney, "Thermodynamic Properties of Abrasive Materials", Proc. Int. Grinding Conf., Carnegie-Mellon University, Pittsburgh, U.S.A., 1972, pp. 53-73.

8. T.R. O'connor and J. Smilters, Ed., "Silicon Carbide", Pergamon Press, New York, 1960.

9. K.B. Lewis, Ed., "The Grinding Wheel", The Grinding Wheel Inst., U.S.A., 1957, pp. 13-15.

10. H.W. Wagner, "New Concepts of Abrasive Properties as Affecting Grinding Performance", Mech. Eng., Vol. 72, 1960, pp. 225-226.

11. J.N. Plendl and P.J. Gielisse, "Hardness of Non-metalic Solids on Atomic Basis", Phys. Rev., Vol. 125, 1962, pp. 828-832.

12. C.E. Woddell, "Method of Comparing the Hardness of Electric Furnace Products and Natural Abrasives", Trans. Electro-chem. Soc., Vol. 68, 1935, pp. 111-130.

13. F.A. Cottn, Ed., "Progress in Inorganic Chemistry", Interscience Publishers, New York, 1966.

14. J. Peklenik, "Grinding Fundamentals-II", Proc. Int. Prod. Res. Conf., Carnegie-Mellon University, Pittsburgh, U.S.A., 1963, pp. 201-208.

15. M.C. Shaw, "The Grinding of Metals", Proc. Conf. on Tech. of Eng. Mfg., I. Mech. E., London, 1958, pp. 443-439.

16. R.S. Hahn, "On the Nature of Grinding Process", Proc. 3rd Int. MTDR Conf., Birmingham, U.K., 1962, pp. 136-139.

17. Olov Svahn, "Efficiency in Grinding Related to Grinding Mechanics", Proc. Int. Grinding Conf., Carnegie-Mellon University, Pittsburgh, U.S.A., 1972, pp. 332-326.

18. K. Okamura and M.C. Shaw, "Study of the Cutting Mechanism of Abrasive Grain (2nd Report)", J. Japan Soc. of Prec. Eng., Vol. 32, 1966, pp. 551-557.

19. K. Sato, "Progress of Researches on Grinding Mechanics in Japan", Bull. Japan Soc. of Prec. Engrs., Vol. 5, 1965, pp. 1-25.

20. R.S. Hahn and R.P. Lindsey, "Some Factors Affecting Surface Finish in Grinding", Annals CIRP, Vol. 14, 1966, pp. 47-52.

21. R.S. Hahn, "Relation Between Grinding Conditions and Thermal Damage in the Workpiece", Trans. ASME, Vol. 78, 1956, pp. 807-812.

22. E. Marshall and M.C. Shaw, "Forces in Dry Surface Grinding", Trans. ASME, Vol. 74, 1952, pp. 51-58.

23. R. Snoeys, J. Peters and A. Decneut, "The Significance of Chip Thickness in Grinding", Annals CIRP, Vol. 23, 1974, pp. 227-237.

24. W.R. Backer, E.R. Marshal and M.C. Shaw, "The Size Effect in Metal Cutting", Trans. ASME, Vol. 74, 1952, pp. 61-72.

25. G.S. Reichenbach, J.E. Mayer, S. Kalpakcioglu and M.C. Shaw, "The Role of Chip Thickness in Grinding", Trans. ASME, Vol. 58, 1956, pp. 847-859.

26. W.R. Backer and M.E. Merchant, "On the Basic Mechanics of Grinding Process", Trans. ASME, Vol. 80, 1958, pp. 141-148.

27. L.P. Tarasov, "Grinding Fundamental I", Proc. Int. Prod. Res. Conf., Carnegie-Mellon University, Pittsburgh, U.S.A., 1963, pp. 196-200.

28. G.K. Lal and M.C. Shaw, "The Role of Grain Tip Radius in Fine Grinding", Trans. ASME, J. Eng. for Ind., Vol. 97, 1975, pp. 1119-1125.

29. M.C. Shaw, "Fundamentals of Grinding", Proc. Int. Grinding Conf., Carnegie-Mellon University, Pittsburgh, U.S.A., 1972, pp. 220-256.

30. S. Malkin and N.H. Cook, "The Wear of Grinding Wheels", Trans. ASME, J. Engg. for Ind., Vol. 93, 1971, pp. 1120-1126.

31. S.G. Red'ko and A.V. Korolev, "Distribution of Abrasive Grains on Grinding Wheel Faces", Machines and Tooling, Vol. 41, 1970, pp. 64-65.

32. G.H. Grisbrook, "Cutting Points on the Surface of a Grinding Wheel and Chip Produced", Advances in MTDR, Pergamon Press, London, 1963, pp. 155-161.

33. K. Nakayama and M.C. Shaw, "Study of the Finish Produced in Surface Grinding - Part 2", Proc. I. Mech. E., London, Vol. 182, 1967-68, pp. 179-194.

34. J.N. Brecker, et. al., "Grinding Fundamentals", Unpublished Report, Carnegie-Mellon University, Pittsburgh, U.S.A., 1971.

35. S. Malkin and R.B. Anderson, "Active Grains and Dressing Particles in Grinding", Proc. Int. Grinding Conf., Carnegie-Mellon University, Pittsburgh, U.S.A., 1972, pp. 161-175.

36. T. Sasaki and K. Okamura, "The Cutting Mechanism of Abrasive Grain", Bull. Japan Soc. of Mech. Engrs. Vol. 3, 1960, pp. 547-550.

37. A.J. Sedriks and T.O. Mulhearn, "Mechanics of Cutting and Rubbing in Simulated Abrasive Process", Wear, Vol. 6, 1963, pp. 457-466.

38. J. Goddard and H. Williams, "A Theory of Friction and Wear During the Abrasion of Metals", Wear, Vol. 5, 1962, pp. 114-135.

39. N.S. Eiss, "Fracture of Abrasive Grain in Grinding", Trans. ASME, J. Eng. for Ind., Vol. 89, 1967, pp. 463-470.

40. F.P. Bowden and T.H.C. Childs, "The Friction and Deformation of Clean Metal at Very Low Temperature", Proc. Roy. Soc., Vol. 312, 1969, pp. 451-456.

41. T.H.C. Childs, "The Sliding of Rigid Cones Over Metals in High Adhesion Conditions", Int. J. Mech. Sci., Vol. 12, 1970, pp. 393-408.

42. R.F. Scrutton, N. Yusef and L.R. Bell, "The Scraping Action of Conical Tools", Wear, Vol. 14, 1969, pp. 415-422.

43. R.F. Scrutton and N. Yusef, "The Action of Build-up When Scraping with Rough Conical Tools", Wear, Vol. 15, 1970, pp. 411-421.

44. G.K. Lal and R.F. Scrutton, "The Simulation of the Action of Single Abrasive Grits Using Spherical and Conical Tools", Proc. 5th All India MTDR Conf., University of Roorkee, India, 1972, pp. 215-222.

45. K. Sato, "Grinding Temperatures", Bull. Japan Soc. of Grinding Engrs", Vol. 1, 1961, pp. 31-36.

46. N. Takenaka, "A Study of the Grinding Action by Single Grit", Annals CIRP, Vol. 13, 1966, pp. 183-190.

47. M.C. Shaw, "A New Theory of Grinding", Harold Armstrong Conf. on Prod. Sci. in Industry, Monash University, Melbourne, Australia, 1971.

48. G.K. Lal and M.C. Shaw, "Wear of Single Abrasive Grain in Fine Grinding", Proc. Int. Grinding Conf., Carnegie-Mellon University, Pittsburgh, U.S.A., 1972, pp. 107-126.

49. M.C. Shaw, et. al., "Grinding Fundamentals", Unpublished Report, Carnegie-Mellon University, Pittsburgh, U.S.A., 1971.

50. Y.K. Lin, "Probabilistic Theory of Structural Dynamics", McGraw Hill, New York, 1967.

51. I.M. Sobol, "The Monte Carlo Method", Mir Publishers, Moscow, 1975.

52. W. Feller, "An Introduction to Probability Theory and Its Application, Vol.-1", Wiley Eastern (Pvt.) Ltd., New Delhi, 1972.

53. C.T. Yang and M.C. Shaw, "The Grinding of Titanium Alloys", Trans. ASME, Vol. 77, 1955, pp. 645-651.

54. T. Orioka, "Probabilistic Treatment of the Grinding Geometry", Bull. Japan Soc. of Grinding Engrs., Vol. 1, 1961, pp. 27-29.

55. H. Opitz, W. Konig, and G. Werner, "Kinematics and Mechanics in Grinding With Regard to the Machining Process", Proc. Int. Grinding Conf., Carnegie-Mellon University, Pittsburgh, U.S.A., 1972, pp. 259-275.

56. R.M. Baul, "Mechanics of Metal Grinding With Particular Reference to Monte-Carlo Simulation", Proc. 8th Int. MTDR Conf., University of Manchester, U.K., 1967, pp. 923-946.

57. H.T. McAdams, "Markov Chain Models of Grinding Profiles", Trans. ASME, J. Engg. for Ind., Vol. 86, 1964, pp. 383-387.

58. H. Yoshikawa and T. Sata, "Simulated Grinding Process by Monte Carlo Method", Annals CIRP, Vol. 16, 1968, pp. 297-302.

59. J. Peklenik, "Contribution to the Correlation Theory for the Grinding Process", Trans. ASME, J. Eng. for Ind., Vol. 86, 1964, pp. 85-94.

60. S.J. Deutsch and S.M. Wu, "Selection of Sampling Parameters for Modelling Grinding Wheels", Trans. ASME, J. Eng. for Ind., Vol. 92, 1970, pp. 667-677.

61. S.S. Law and S.M. Wu, "Simulation Study of Grinding Process", Trans. ASME., J. of Eng. for Ind., Vol. 93, 1973, pp. 972-978.

62. A. Papoulis, "Probability, Random Variables, and Stochastic Process", McGraw-Hill Kogakusha Ltd., New Delhi, 1965.

63. K. Nakayama, "Grinding Wheel Geometry", Proc. Int. Grinding Conf., Carnegie-Mellon University, Pittsburgh, U.S.A., 1972, pp. 197-211.

64. K. Nakayama, J. Brecker and M.C. Shaw, "Grinding Wheel Elasticity", Trans. ASME, J. of Eng. for Ind., Vol. 93, 1971, pp. 609-614.

65. Yu.P. Adler, E.V. Markova and Yu.V. Granovsky, "The Design of Experiments to Find Optimal Conditions", Mir Publishers, Moscow, 1975.

66. R.L. Wine, "Statistics for Scientists and Engineers", Prentice-Hall, New Delhi, India, 1966.

67. J.S. Bendat and A.G. Piersol, "Measurement and Analysis of Random Data", John Willey, New York, 1966.

68. W.J. Dixon, Ed., "Biomedical Computer Programmes", University of California Press, London, 1970.

69. A.B. Pritsker and P.J. Niviat, "Simulation With GASP II", Prentice-Hall, New York, 1969.

70. D.A. Farmer, J.N. Brecker and M.C. Shaw, "Study of the Finish Produced in Surface Grinding - Part 1", Proc. I. Mech. E., London, Vol. 182, 1967-68, pp. 171-179.

APPENDIX A

The random variables p_1, p_2, ..., etc. are constructed with the density function given by equation (2.9). Assuming that the random variables are independent, the distribution function of p is obtained from

$$F_p(p) = \int_0^p \frac{2}{L^2}(L - p)\, dp \qquad (A.1)$$

where L is the maximum width of cut. If, R_{u_j}, is a random number, uniformly distributed between 0 and 1, we have [69]

$$R_{u_j} = F_p(p)$$

$$= \frac{2}{L} p - \frac{p^2}{L^2} \qquad (A.2)$$

Solving the equation (A.2), we get

$$p = L(1 \pm \sqrt{1 - R_{u_j}}) \qquad (A.3)$$

As the maximum value of axial pitch will be less than or equal to L,

$$p = L(1 - \sqrt{1 - R_{u_j}}) \qquad (A.4)$$

Hence, by definition of axial pitch,

$$x_j = x_{j-1} + L(1 - \sqrt{1 - R_{u_j}}) \qquad (A.5)$$

The distribution function, $F_Y(\triangle y)$, can be obtained from equation (2.31). Starting from an arbitrary point $y^{i-1} = 0$, we form the points

$$y^i = \triangle y^i$$

$$y^{i+1} = \triangle y^i + \triangle y^{i+1} \tag{A.6}$$

$$\cdots \qquad \cdots \qquad \cdots$$

$$y^M = \triangle y^i + \triangle y^{i+1} + \ldots + \triangle y^M$$

These points are Poisson distributed with parameter, λ_1. Therefore, the random number, R_u, will be

$$R_u = \frac{1}{\lambda_1} \int_0^{\triangle y^i} e^{-\frac{\triangle y}{\lambda_1}} \, dy$$

$$= (1 - e^{-\triangle y^i/\lambda_1}) \tag{A.7}$$

or

$$+ e^{-\triangle y^i/\lambda_1} = 1 - R_u \tag{A.8}$$

Taking natural lograthm on both sides, we get

$$\triangle y^i = -\lambda_1 \log_e (1 - R_u)$$

$$= -\lambda_1 \log_e (R_{u_{i-1}}) \tag{A.9}$$

where,

$$R_{u_{i-1}} = 1 - R_u \tag{A.10}$$

is also random number uniformly distributed between 0 and 1. Hence, the random point given by equation (A.6) can

be obtained using equation (A.10) as

$$y^i = y^{i-1} - \hat{\lambda}_1 \log_e(R_{u_{i-1}}) \qquad (A.11)$$

All other points can be similarly obtained. Using the same principle, the random points, z^i, z^{i+1}, ..., z^M can be generated from the equation

$$R_{u_i} = \int_0^{z^i} f_Z(z^i) \, dz \qquad (A.12)$$

which on simplification gives

$$z^i = d_e \left((2^{k+1} - 1) R_{u_i} + 1 \right)^{1/(k+1)} - d_e \qquad (A.13)$$

for $i = 1, ..., M$.

In Figure B.1, E (i, j) is the intersection of the path traced by ith and jth grain in any column. The coordinates of the lowest point of ith grain in its path is given by (y^i, z^i) in the plane along the cutting direction. Similarly, the coordinates of the lowest point of jth grain in its path will be (y^j, z^j). As shown in Figure B.1, A1 and A2 represent the radii of the locus of paths of ith and jth grain respectively. Therefore

$$A1^2 - y1^2 = A2^2 - y2^2 \qquad (B.1)$$

or

$$y2^2 - y1^2 = A2^2 - A1^2 \qquad (B.2)$$

where,

$$A1 = R - z^i \qquad (B.3)$$

and

$$A2 = R - z^j, \qquad (B.4)$$

and

$$y1 + y2 = y^j - y^i \qquad (B.5)$$

Solving equations (B.2) and (B.5), we get

$$y1 = \frac{1}{2} \left[(y^j - y^i) - \frac{(A2^2 - A1^2)}{y^j - y^i} \right] \qquad (B.6)$$

Again,

$$A2^2 - A1^2 = (R - z^j)^2 - (R - z^i)^2$$

$$= -2R(z^j - z^i) + (z^{j2} - z^{i2}) \qquad (B.7)$$

Neglecting the higher order term $(z^{j^2} - z^{i^2})$ in equation (B.7), we get

$$A2^2 - A1^2 \approx - 2R \ (z^j - z^i) \qquad (B.8)$$

Therefore,

$$y1 = \frac{1}{2} \left[\frac{2R \ (z^j - z^i)}{(y^j - y^i)} + (y^j - y^i) \right] \qquad (B.9)$$

and the y coordinate of the intersection point in the (y, z) plane will be

$$y \ (i, j) = y^i + \frac{1}{2} \left[\frac{2R \ (z^j - z^i)}{(y^j - y^i)} + (y^j - y^i) \right] \qquad (B.10)$$

The vertical height of the intersection point will be

$$z \ (i, j) = z^i + A3 \qquad (B.11)$$

where A3 can be obtained from equation

$$(R - z^i - A3)^2 + y1^2 = (R - z^i)^2 \qquad (B.12)$$

which on simplification reduces to

$$A3 \approx \frac{y1^2}{2 \ (R - z^i)} \qquad (B.13)$$

Therefore,

$$z \ (i, j) = z^i + \frac{(y \ (i,j) - y^i)^2}{2 \ (R - z^i)} \qquad (B.14)$$

Using the same procedure, the coordinates of the intersection of grooves in transverse section at any distance y_o can be obtained, where the circular shaped grooves of

radius ρ are superimposed with its mid point at the lowest point of the groove in any column. Therefore, it can be shown that

$$x_{i,j} = x_i + \frac{1}{2} \left[\frac{g \; (z_j \; (y_o) - z_i \; (y_o))}{(x_j - x_i)} + (x_j - x_i) \right]$$

(B.15)

and

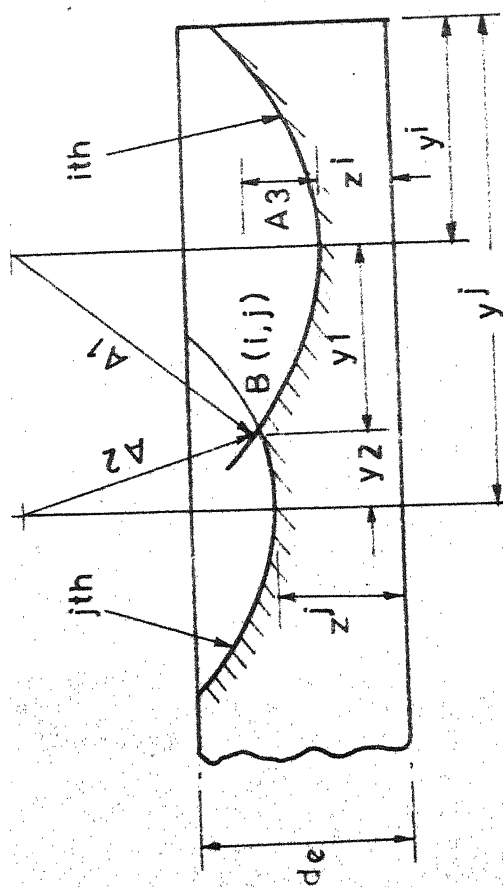$$z_{i,j} = z_i \; (y_o) + \frac{(x_{i,j} - x_i)^2}{g}$$

(B.16)

FIGURE B.1 AN ENLARGED SCHEMATIC VIEW OF THE PROCESS
SHOWING INTERSECTION POINT.

APPENDIX C

MACHINE SPECIFICATIONS

		Range Value	Units
1.	Working Surface	250 x 1000	mm
2.	Maximum Transverse Traverse of Grinding Wheel	320	mm
3.	Maximum Longitudinal Traverse of Table	1150	mm
4.	Maximum Grinding Length	1000	mm
5.	Maximum Grinding Height	400	mm
6.	Infinitely Variable Table Speeds	2.5 - 25	m/min
7.	Automatic Continuous Traverse Feed of Grinding Wheel	0.3 - 3.5	m/min
8.	Automatic Intermittent Tranverse Feed of Grinding Wheel/ Table Stroke	1 - 32	mm
9.	Downfeed of Grinding Wheel 1 Graduation =	0.002	mm
10.	Rapid Vertical Speed of Grinding Wheel	0.6	m/min
11.	Grinding Wheel Speed	1440/2880	rpm
12.	Wheel Diameter Upto	300	mm
13.	Wheel Width Upto	63	mm
14.	Wheel Bore	76	mm
15.	H.P. of Grinding Motor	4/5.7	h.p.